ATOMIC FLUORESCENCE SPECTROSCOPY

by

KENNETH CLIVE THOMPSON, B.Sc., A.R.C.S.(Lond.)

A thesis submitted for the degree of

DOCTOR OF PHILOSOPHY

in the University of London

Department of Chemistry,
Imperial College of Science and Technology,
LONDON, S.W.7.

February, 1968

ABSTRACT

Three methods of flame spectroscopic analysis have been investigated - atomic-fluorescence, atomic-absorption and flame-emission spectroscopy.

The emphasis in the first part of this work has been on the development of the relatively new technique of atomic-fluorescence spectroscopy. This technique was found to be very sensitive and virtually free from all cation and anion interferences. The optimisation of the various operating parameters are described, and general methods for the measurement of atomic-fluorescence using commercially available sources are discussed.

The preparation and operation of microwave excited electrodeless discharge tubes as atomic spectral line sources, for use in atomic-fluorescence and atomic-absorption spectroscopy, are fully described. These sources were found to be superior to commercially available atomic spectral line sources.

Using electrodeless discharge tube sources, the fluorescence and absorption characteristics of 5 elements, in a variety of flames, have been determined. Sensitive methods of analysis for each of the 5 elements have also been developed.

The second part of this work deals with new developments in flame-emission spectroscopy. The analysis of sulphur and phosphorus using the emission from unstable molecular species in a new type of 'cool flame' is described.

The spectroscopic properties of the high temperature, low-background nitrous oxide-hydrogen flame are also investigated.

ACKNOWLEDGEMENTS

The work described in this thesis was carried out in the Chemistry Department of Imperial College of Science and Technology between October, 1965, and February, 1968. It is entirely original except where due reference is made and no part has been previously submitted for any other degree.

I wish to express my gratitude to my supervisors, Professor T. S. West and Dr. R. M. Dagnall, for their unfailing assistance and encouragement given throughout this project, and to the other members of the Analytical Research team for many helpful discussions and suggestions.

I am also grateful to the Science Research Council for the provision of a Research Studentship.

Thanks are also due to I.C.I. Ltd. for the provision of a grant for the purchase of the Unicam SP900A spectrophotometer used in this research, and to Mrs. S.A. Thomas for so expertly typing this thesis.

Finally, I would like to thank my future wife, Elizabeth, for her help in the proof reading of this thesis.

CONTENTS

FOREWORD

Recently there has been a steadily growing interest in the development of flame spectroscopy for the determination of trace amounts of various elements. Flame spectroscopy is, in this instance, a general term encompassing atomic-absorption, atomic-fluorescence and flame-emission spectroscopy.

Atomic-absorption spectroscopy (A.A.S.) is a selective and sensitive technique which at present is capable of determining over 60 elements with little or no sample pretreatment. Atomic-fluorescence spectroscopy (A.F.S.) is a selective and an even more sensitive technique than A.A.S., which up to the present time has been used to determine ca 25 elements and should prove eventually to be as versatile as A.A.S. Flame-emission spectroscopy is also a very sensitive technique, but it is not as selective as either A.A.S. or A.F.S.

Methods for the determination of several elements have been developed using these three techniques, and other spectroscopic emission methods have been examined during the course of this work. This thesis has been divided into two parts; the first deals with the techniques of atomic-absorption and atomic-fluorescence spectroscopy with emphasis on the latter, and the second with flame-emission spectroscopy. This division

was chosen because atomic-absorption and atomic-fluorescence spectroscopy require an external source whilst flame-emission spectroscopy does not.

Included in the first part is a discussion of the principles and theory of A.A.S. and A.F.S., the preparation and uses of electrodeless discharge tubes, the use of various types of flame in A.F.S. and A.A.S. and brief mention is made of other applications of electrodeless discharge tubes and microwave excitation techniques. Part two consists of atomic and molecular emission studies in a variety of flames.

INTRODUCTION

HISTORY

Flame Emission Spectroscopy

The beginnings of flame emission spectroscopy extend back to the middle of the eighteenth century (e.g. Geoffray 1732, Melvill 1752 and Marggraf 1758). These chemists observed the colour imparted to the alcohol and candle flames by metallic salts and Marggraf even used this coloration to some extent for distinguishing different materials. Talbot (1826 and 1836) showed a remarkable insight for his time; the method of qualitative flame emission revealed in his publications was basically sound, but was unfortunately very briefly described. These early workers were limited by their use of luminous diffusion flames and it was not until the work of Kirchhoff and Bunsen[1,2] that brought the decisive turning point. Just prior to this in 1855 Bunsen developed the Bunsen burner with its colourless, premixed, hot flame which proved invaluable in his later studies. Together with Kirchhoff, Bunsen developed a spectroscope of remarkable efficiency for that time and they succeeded in demonstrating that the visible spectral lines were not due to compounds, but to the elements. This laid the foundations of the science of flame

emission and also resulted in the discovery of new elements (e.g. caesium, rubidium, thallium, indium and gallium).

The first quantitative flame emission method was the determination of sodium by Champion, Pellet and Grenier (1873). The method used two flames, one was saturated with sodium whilst the sample was drawn through the other flame on a platinum wire. A blue wedge was passed in front of the sodium saturated flame until the flames appeared equally bright.

Owing to the advent of arc and spark spectroscopy in the early twentieth century interest in flame emission spectroscopy almost ceased until 1928, when the Swedish agronomist Lundegårdh and his coworkers[3] demonstrated the merits of F.E.S. in a series of papers. These workers used a pneumatic atomiser and an air-acetylene flame. Commerically available instruments did not appear until the mid nineteen-forties and these were mainly for the determination of the alkali metals with their easily excited resonance lines. It is only comparatively recently (the last 10-15 years) that F.E.S. has been extended to encompass most of the periodic table.

Atomic--Absorption Spectroscopy

Atomic-absorption spectroscopy may simply be defined as the

absorption of radiation by discrete atoms. The basic principles underlying A.A.S. were established by Kirchhoff[1] as long ago as 1860, using the atomic absorption lines in the Fraunhofer spectrum to deduce the presence of certain elements in the solar atmosphere. The theory of A.A.S. was evolved in the early nineteen hundreds by physicists and astrophysicists. The work of these early researchers (summarised in the treatise by Mitchell and Zemansky[4]) was mainly performed at low pressures in enclosed vessels, and was not directed towards analytical purposes except for some astrophysical studies on the determination of the compositions of the solar and stellar atmospheres. A special case was the estimation of the contamination of air by mercury vapour, which is unique in having an appreciable vapour pressure at room temperature.

Whereas emission methods of analysis (arc, spark and flame) soon became firmly established, the potentialities of absorption methods were virtually overlooked until 1953 when Walsh[5] and later in 1955 Alkemade and Milatz[6] demonstrated the use of A.A.S. for general analytical purposes.

Atomic-Fluorescence Spectroscopy

Atomic-fluorescence spectroscopy may be defined as the measurement of radiation from discrete atoms that are being excited by the absorption

of radiation from a given source which is not seen by the detector. A.F.S. may be considered to be the analogue of molecular spectrofluorimetry and was first reported in 1905 when Wood[7] succeeded in exciting fluorescence of the D lines of sodium vapour. This was achieved by vaporising some sodium metal in an evacuated test tube and illuminating the test tube with the light from a gas flame containing sodium chloride and visually observing the yellow D lines. Wood called this fluorescence resonance radiation because it was predicted by the classical theory of a light wave vibrating with the same frequency as the dipole oscillations of the medium. Soon after this initial discovery, resonance radiation was observed for mercury, lithium, cadmium, zinc and many other elements. This work has been summarised by Mitchell and Zemansky[4]. Most of the early work on 'resonance radiation' was performed using mercury owing to its relatively high vapour pressure at room temperature and was generally of a theoretical nature. In addition to these studies, A.F.S., like A.A.S., found its primary use in astrophysical work for the determination of the composition of solar and stellar atmospheres.

These early studies utilised special quartz or glass cells for the confinement of the atomic vapour which was usually at a low pressure; thus most of the results obtained were not affected by collisional broadening

which is an important contribution in flames at atmospheric pressure. The fluorescence of atoms in flames was first reported by Nichol and Howes[8] in 1923 and then by Badger[9] and Mannkopff[10] who obtained weak fluorescence signals from barium, cadmium, calcium, lithium, magnesium, mercury, sodium, silver and strontium when present in a high concentration in a flame irradiated by light containing the resonance line of the appropriate metal.

More recently Robinson[11] observed weak fluorescence of the 2852 Å magnesium line in an oxy-hydrogen flame using a magnesium hollow cathode lamp. In 1962 Alkemade[12] used the atomic fluorescence of sodium to obtain mechanisms of excitation and deactivation of atoms in flames and to measure the quantum efficiency of the sodium 5890 Å line. He was also the first to point out the possible analytical applications of this technique. The first analytical method was developed by Winefordner and his co-workers in a series of four papers[13-16] published in 1964-65. A year later Dagnall, West and Young[17,18] utilised commercially available A.A.S. equipment for measuring atomic-fluorescence and the author has since greatly extended this application along similar lines.

THEORY

Flame-Emission Spectroscopy and Atomic-Absorption Spectroscopy

The underlying theory of A.A.S. is quite complex and because only a vastly oversimplified version is given in most texts on A.A.S., a more complete description is attempted here.

Consider a population of atoms at a given temperature in a uniform media (a flame supplied with a given species from a pneumatic nebuliser is a fair approximation to this). The ratio of the number of atoms in the excited state to the number in the ground state is given by the equation:

$$\frac{N_1}{N_o} = \frac{g_1}{g_o} \exp\left(\frac{-E_1}{kT}\right)$$

where g_o and g_1 = The statistical weights of the ground and excited states respectively

N_o = Number of atoms in the ground state

N_1 = Number of atoms in the excited state

k = Boltzmann Constant e.v./^oK.

T = Absolute Temperature ^oK.

E_1 = Energy of the excited state above the ground state e.v.

Except for easily excited elements (e.g. Caesium, Potassium and Calcium, etc.) at extremely high temperatures, the number of atoms in the lowest excited state is negligible in comparison to the number in the ground state (see Table 1).

TABLE 1

Ratio of Number of Atoms in the Excited State to Number in the Ground State[5]

Resonance Line (Å)	T = 2000	3000	4000	5000°K
Cs 8521	4.4×10^{-4}	7.2×10^{-3}	3×10^{-2}	6.8×10^{-2}
Na 5890	9.8×10^{-6}	5.9×10^{-4}	4.4×10^{-3}	1.5×10^{-2}
Ca 4227	1.2×10^{-7}	3.7×10^{-5}	6.0×10^{-4}	3.3×10^{-3}
Zn 2139	7.3×10^{-15}	5.6×10^{-10}	1.5×10^{-7}	4.3×10^{-6}

The ratio $\frac{N_1}{N_o}$ increases exponentially with temperature and wavelength. Although at 3000°K only 0.72% of the caesium atoms are in the excited state it is important to remember that at this temperature appreciable ionisation of the metal atoms will occur, thus seriously depleting the ground state population. This effect will be observed for all easily ionised atoms and is usually overcome by adding an excess of an easily ionisable element (e.g. potassium) to the flame thus suppressing the ionisation. Thus it can

be seen that, except for the easily ionisable elements, only a negligible proportion of the atoms exist in the excited state.

Since the number of excited atoms in the flame is very small, interelement effects can easily arise, e.g. deactivation by collision, preferential excitation of other species and energy transfer processes in general. These various effects do not of course affect the ground state population of atoms. Also a slight change in the flame temperature has a profound effect on the $\frac{N_1}{N_o}$ ratio because this varies exponentially with the absolute temperature (see Table 2).

TABLE 2

Effect of temperature on the $\frac{N_1}{N_o}$ ratio

Temp. °K	Wavelength Å 3000	3500	Enhancement (Times)
2000	10^{-10}	$10^{-8.6}$	30
3000	$10^{-6.7}$	$10^{-5.7}$	9
6000	$10^{-3.3}$	$10^{-3.0}$	2.3

Table 2 also shows that the $\frac{N_1}{N_o}$ ratio is much more sensitive to temperature at short wavelengths where many resonance lines lie. For a fuller description of the basic principles of F.E.S. the reader is referred to the second part of this thesis.

It can be proved that for a given absorption line the integrated absorption $\int_0^\infty k_\nu dV$ (at low values of N) is given by the equation[4]:

$$\int_0^\infty k_\nu dV = \frac{\pi e^2 N f}{mc} \qquad (1)$$

where k_ν = absorption coefficient at frequency V

e = electronic charge

m = electronic mass

c = velocity of light

N = number of atoms

f = oscillator strength.

Hence for a transition from the ground state the integrated absorption is proportional to the concentration of free atoms, is independent of temperature and is independent of whatever physical processes are responsible for the formation of the absorption line. There is, however, the problem of the measurement of the integrated absorption. At temperatures between 2000 and 3000°K the width of an absorption line is ca 2×10^{-2} Å and this mainly results from Doppler and collisional broadening as the natural absorption line width is ca 10^{-4} Å. The accurate measurement of the

profile of an absorption line would require a monochromator with a resolution of 500,000, which is beyond the capacity of most monochromators. By using a sharp-line source with a much smaller half-width than the absorption line, the absorption coefficient at the centre of the line can be determined.

Consider a parallel beam of radiation of intensity I_o from a line source passing through a pathlength 'L' of atomic vapour (see fig.1).

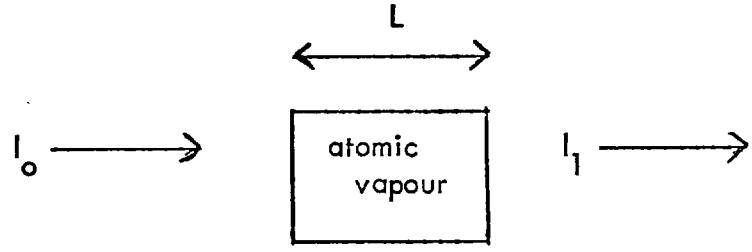

Fig.1

$$I_o = K \int_{\Delta V_s} J_v dV \qquad (2)$$

where K = instrument proportionality factor (constant)

J = intensity per unit of frequency

V_s = source line width.

The signal from the source after passing through the flame with the sample solution being aspirated is given by:

$$I_1 = K \int_{\Delta V_s} J_v \exp(-k_v L) dV \qquad (3)$$

where L = pathlength in the flame.

The absorption coefficient K_v is a complex function of frequency and is described by the following formulae[4]:

$$K_v = k_o \frac{a}{\pi} \int_{-\infty}^{\infty} \frac{e^{-y^2} dy}{a^2 + (w-y)^2} \qquad (4)$$

$$k_o = \frac{\sqrt{4\pi \ln 2}\ e^2 Nf}{mc\, \Delta V_D} \qquad (5)$$

$$w = \sqrt{4 \ln 2}\ \frac{V - V_o}{\Delta V_D} \qquad (6)$$

$$a = \frac{\Delta V_c}{\Delta V_D} \sqrt{\ln 2} = \text{the damping constant} \qquad (7)$$

$$y = \frac{2\delta}{\Delta V_D} \sqrt{\ln 2} \qquad (8)$$

$$\Delta V_D = \sqrt{\frac{8RT \ln 2}{M}} \frac{V_o}{c} \qquad (9)$$

where k_v = absorption coefficient at frequency V.

k_o = maximum absorption coefficient when only Doppler broadening is present

V_o = frequency at the line centre.

ΔV_D = Doppler half-width of the absorption line

ΔV_c = collisional half-width of the absorption line

M = atomic mass

T = absolute temperature

R = the gas constant

δ represents a small variable distance from a given point on the Doppler broadened absorption line.

(The derivation of K_v assumes that Doppler and collisional broadening are independent processes and K_v is obtained by considering every infinitesimal frequency band of the pure Doppler broadened absorption line to

be broadened by collisonal broadening. Suppose a frequency band at a distance $V - V_o$ from the centre of an absorption line showing only Doppler broadening is chosen. To represent the collisional broadening of this frequency band, a variable distance δ from the point $V - V_o$ is chosen. For further information the reader is referred to the treatise by Mitchell and Zemansky.[4])

If a very sharp line source is used, such that the absorption line half-width is much greater than that of the source, then k_v can be considered to be effectively constant over the source line width and equal to $\overline{K}_v = C' k_o$ [19] (where C' is a constant) in analytically used flames.

Hence from equation (2)

$$I_1 = K \int_{\Delta V_s} J_v \exp(-\overline{k}_v L) dV = K \exp(-\overline{k}_v L) \int_{\Delta V_s} J_v dV$$

$$= I_o \exp(-\overline{k}_v L) = I_o \exp(-C' k_o L) \qquad (10)$$

$$\text{Absorbance } A = \log_{10} \frac{I_o}{I} = 0.434\, C' k_o L =$$

$$\frac{0.434\, C' L (4\pi \ln 2)^{\frac{1}{2}} e^2 N f}{mc\, \Delta V_D} \qquad (11)$$

Thus a plot of the absorbance versus the concentration of an element in the flame should be linear and should extend over an extremely large concentration range. In fact up to that point where resonance broadening causes the damping constant to change, i.e. in the region of molar solutions[19]. In practice, however, the linear range of the working curve is restricted because in general the line width from a hollow-cathode lamp is not negligible with respect to the absorption line-width[20]. In this case K_v is not constant over the line width and will not increase linearly with concentration. The approximation of equation (10) is therefore no longer valid and the theory becomes very complex. It is often found in practice that the plot of absorbance versus concentration is linear at low absorbances (i.e. $\lesssim 0.5$) and slopes off towards the concentration axis at higher absorbances. This indicates (assuming no self-reversal of the source) that equation (10) is a good approximation at low absorbances (i.e. the average absorption coefficient $\bar{k}_v$ over the source line width is proportional to the concentration of the element at low absorbances). Figure 11 shows pictorially the ideal and more usual cases.

The half-intensity widths of absorption and emission lines is of considerable importance in F.E.S., A.A.S. and A.F.S. and it is worthwhile to include a brief summary of the broadening processes involved.

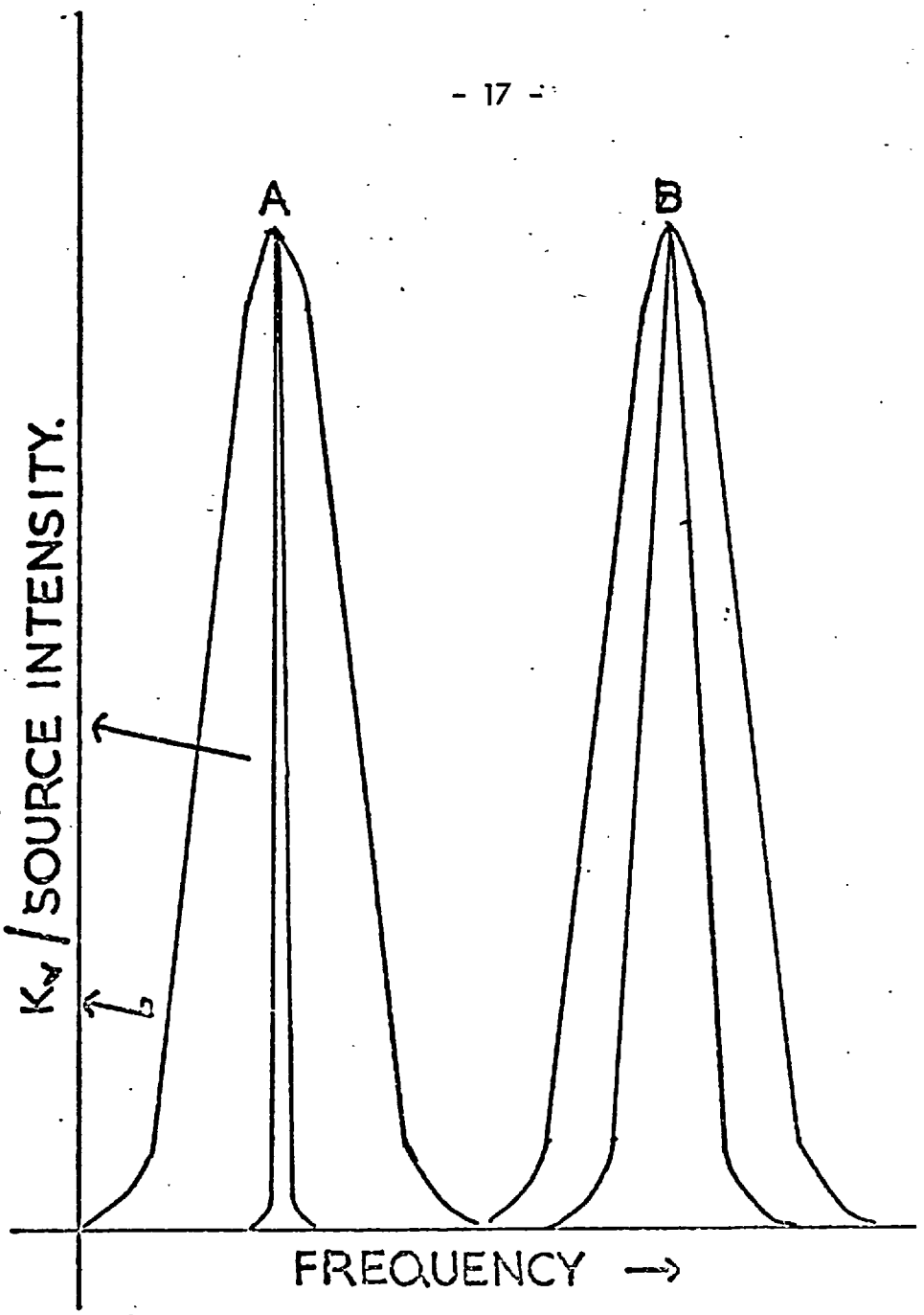

FIGURE II Absorption Line Profiles

A. Ideal Case

B More usual case

Broadening Processes of Atomic Spectral Lines

(1) Natural Broadening

Natural broadening is due to the finite lifetime of the atom in the excited state (i.e. Heisenberg's uncertainty principle). For resonance lines this natural width is of the order of 10^{-4} Å which is negligible compared with that due to other causes in analytically used flames.

(2) Doppler Broadening

Doppler broadening is caused by the absorbing or the emitting atoms having different component velocities along the line of observation.

(3) Collisional Broadening (also known as Pressure or Lorentz Broadening)

Collisional broadening is due to perturbation of the absorbing or emitting atom by foreign gas atoms. The effect of this type of broadening varies for different foreign gases and for different atomic states. Owing to these various factors the calculation of collisional half-intensity line widths is very difficult and the results obtained are not always consistent.

(4) Resonance Broadening

Resonance broadening is due to perturbation of the absorbing or emitting atom by atoms of the same type. This type of broadening is generally negligible in analytically used flames unless high concentrations

of a given element (ca. Molar solutions) are nebulised into the flame.

(5) Stark and Zeeman Broadening

Stark and Zeeman broadening are caused by electric and magnetic fields respectively. Although Stark broadening can cause lines to become diffuse in the arc, both these broadening effects are negligible in flames, but an important factor within hollow-cathode sources used in A.A.S.

(6) Hyperfine Structure

Hyperfine structure is due to nuclear spin and/or the presence of several isotopes and results in the fact that each line consists of a number of separate hyperfine components each behaving as an independent line. The total separation of the various components ranges from a few hundredths to a few tenths of a wavenumber[4]. For most spectral lines the influence of isotopes and the nuclear spin on the line width is negligible[21]. (Each hyperfine component will be broadened by the process described above, and that with regard to absorption, each component can be treated as an independent line.)

The total half-intensity line width ($\Delta\lambda_T$) is related to the half-intensity line widths of the natural broadening effect ($\Delta\lambda_N$), the Doppler broadening effect ($\Delta\lambda_D$), the resonance broadening effect ($\Delta\lambda_R$) and

the collisional broadening effect ($\Delta\lambda_c$) by the expression[21]:

$$\Delta\lambda_T = \left[(\Delta\lambda_D)^2 + (\Delta\lambda_c + \Delta\lambda_R + \Delta\lambda_N)^2 \right]^{\frac{1}{2}}$$

This expression can be simplified when applied to analytically used flames, as $\Delta\lambda_N$ and $\Delta\lambda_R$ are then negligible. Thus

$$\Delta\lambda_T = \left[(\Delta\lambda_D)^2 + (\Delta\lambda_c)^2 \right]^{\frac{1}{2}}$$

The measurement of absorption line widths is a complicated process and the results obtained are not always consistent, mainly owing to an uncertainty in the value of the collisional cross sections (σ_c) for most spectral lines in analytically used flames. Winefordner[21] has theoretically calculated some maximum and minimum values of the collisional half-intensity line widths ($\Delta\lambda_c$) for a series of elements in the air-acetylene flame and from these values calculated the maximum and minimum total half-intensity line widths ($\Delta\lambda_T$). Some of these values are shown in Table 3.

TABLE 3

Half-intensity line widths of some analytically important lines in a slightly fuel rich air-acetylene flame

Element	Line	Natural half-width	Doppler half-width	Collisional half-width		Total line half-width	
				max	min	max	min
	Å	Å	Å	Å	Å	Å	Å
Al	3093	0.000047	0.021	0.018	0.004	0.028	0.022
Bi	2231	0.000003	0.006	0.007	0.001	0.009	0.006
Cd	2288	0.00011	0.008	0.008	0.002	0.011	0.008
Hg	2537	0.000040	0.006	0.009	0.002	0.011	0.007
Na	5890	0.000042	0.044	0.068	0.014	0.081	0.046
Sb	2176	0.000016	0.007	0.007	0.001	0.010	0.007
Sn	2863	0.000077	0.009	0.012	0.002	0.015	0.010
Te	2143	0.000047	0.007	0.007	0.001	0.009	0.007
Tl	3776	0.000038	0.009	0.020	0.004	0.022	0.010
Zn	2139	0.000154	0.009	0.007	0.001	0.012	0.010
K	7665	0.000125	0.044	0.100	0.020	0.110	0.048

Thus it may be seen that the absorption line half-intensity widths are in general ca 0.01 Å and tend to increase at longer wavelengths.

Atomic-Fluorescence Spectroscopy

The basic experimental orrangement is as shown in Fig. III which consists of an intense source focussed on o flame cell containing otomic vopour of o given element.

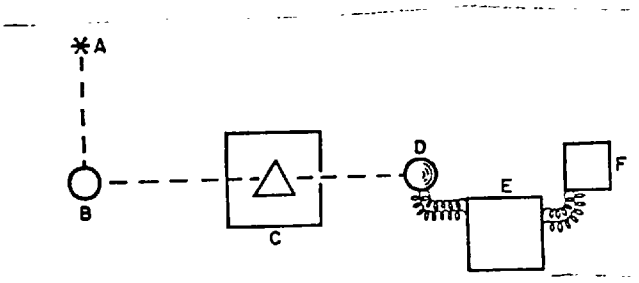

FIGURE III Experimental Arrangement for Atomic-Fluorescence Measurements.

A.	Source	B.	Flame
C.	Monochromator	D.	Photomultiplier
E.	Amplifier	F.	Recorder

The resulting fluorescence radiation is observed at right angles to the incident exciting radiation and the fluorescence radiation is focussed on the entrance slit of a monochromator (i.e. the detector does 'see' the source of excitation).

The source may be either a line source or a continuum and serves to excite atoms by absorption of radiation of the proper wavelength. The atoms are then deactivated partly by collisional quenching with flame gas molecules and partly by the emission of radiation of the same or of a longer wavelength. (In rare cases a shorter wavelength is emitted.) The wavelength of the emitted radiation is characteristic of the absorbing atoms and the intensity of emission may be used as a measure of their concentration.

There are five basic types of atomic-fluorescence: resonance fluorescence, direct-line fluorescence, stepwise-line fluorescence, sensitised fluorescence and thermally assisted direct-line fluorescence (see Fig. IV).

(1) Resonance Fluorescence

Resonance fluorescence occurs when an atom emits a spectral line of the same wavelength as that used for excitation of the atom.

(2) Direct-Line Fluorescence

Direct-line fluorescence occurs when an atom emits a spectral line

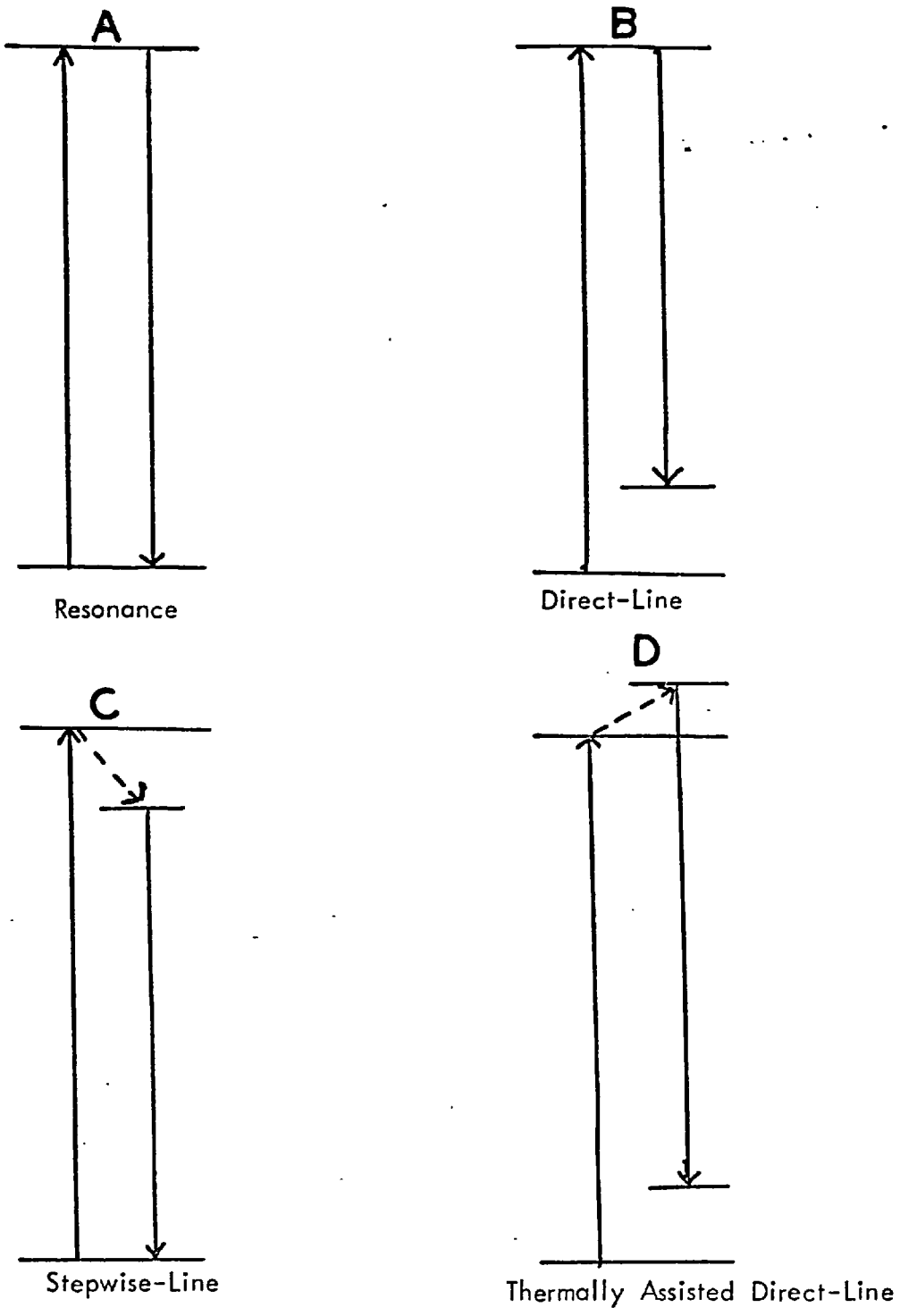

FIGURE IV Types of Atomic-Fluorescence

of longer wavelength than the spectral line used for excitation. (Both the exciting and the emitted lines originate from the same excited state.) Thus after the fluorescence emission occurs the atom is in a metastable state above the ground state.

e.g. emission of the 2386 Å tellurium line after excitation by the 2143 Å tellurium line.

(3) Stepwise-Line Fluorescence

Stepwise-line fluorescence occurs when an atom emits resonance radiation after excitation of the atoms to a higher energy state than the first resonance state and then radiationless deactivation to the first excited state.

e.g. emission of the 3068 Å bismuth line after excitation by the 2062 Å bismuth line.

(4) Sensitised Fluorescence

Sensitised fluorescence occurs when a given atom emits radiation after collisional activation by a foreign atom which has been previously excited by the absorption of resonance radiation.

For example, if a gas contains a high pressure of mercury and thallium vapour and the mercury atoms are excited by the absorption of the 2537 Å mercury line, (from a mercury vapour lamp) then the following

reactions, which result in the emission of the 3776 and 5350 Å thallium lines, will occur.

$$Hg^* + Tl \longrightarrow Tl^* + Hg$$

$$Tl^* \longrightarrow Tl + hV$$

This type of fluorescence from enclosed systems has often been reported in the literature[4,22], but has never been observed in flames. This is probably due to the low concentration of atoms in flames obtained, using conventional nebulisers, and also to the very low fluorescence intensities involved.

(5) Thermally Assisted Direct-Line Fluorescence

This type of fluorescence which was first observed in the present study occurs when an atom is raised to an excited state by absorption of a resonance line and then is further excited to a slightly higher energy excited state by energy from the flame (i.e. collisions with flame gas molecules). Fluorescence emission then occurs from this higher energy excited state either to the ground state or to a metastable state above the ground state. In the present study this type of fluorescence was found for the 2938 Å bismuth line after excitation by the 2062 Å bismuth line.

Derivation of the Relationship between the Fluorescence Intensity and Concentration

The relationship between the fluorescence intensity I_F and the concentration of a given element has been derived[13,24,25] and is now discussed.

The basic experimental arrangement is that shown in Fig.III. A simplified representation of the flame cell is shown in Fig.VB. (This figure is drawn such that the areas are equivalent to the true case shown in Fig.VA.)

The basic integrated atomic fluorescence intensity expression for an isolated spectral line is given by[24]:

$$I_F = I_A \frac{\phi_T}{4\pi} f_z \ W/cm^2 - ster \qquad (12)$$

where I_A is the intensity absorbed by the resonance line (W/cm^2)

4π is the number of steradians in a sphere

f_z is a factor (no units) to account for the decrease in the fluorescent intensity in region z of Fig.V by absorbing atoms

ϕ_T is the total power or energy efficiency for fluorescence[26].

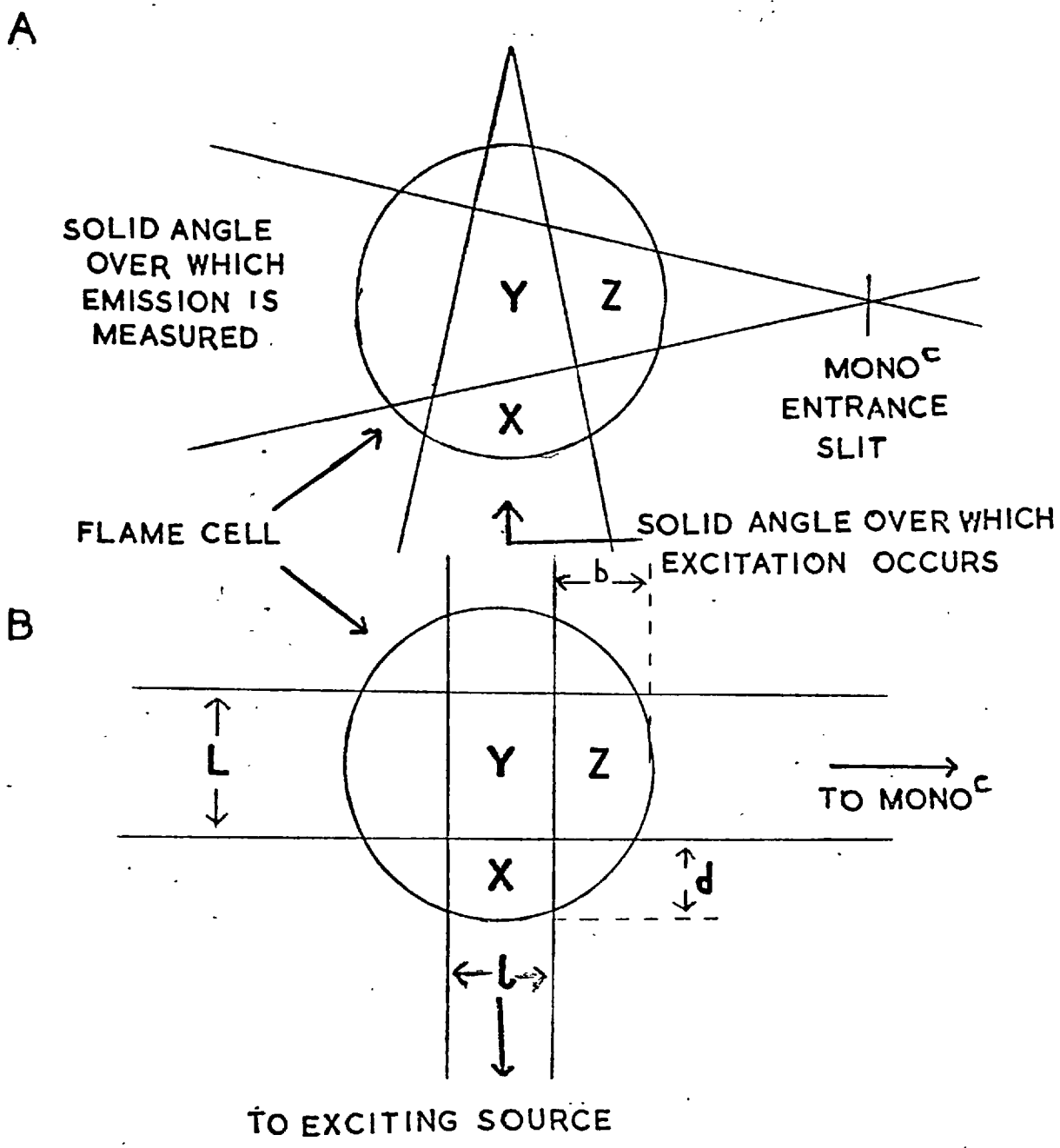
A
SOLID ANGLE OVER WHICH EMISSION IS MEASURED
Y
Z
X
MONOC ENTRANCE SLIT
FLAME CELL
SOLID ANGLE OVER WHICH EXCITATION OCCURS
b
B
L
Y
Z
TO MONOC
X
d
l
TO EXCITING SOURCE

FIG. V.

(i.e. The ratio of the power emitted to the power absorbed and is related to the quantum efficiency ϕ by the equation:

$$\phi_T = \frac{V_f}{V_a}\phi \qquad (13)$$

where V_f and V_a are the frequencies (sec^{-1}) of the fluorescence (f) and the absorbed (a) photons respectively.

$$\phi = \frac{\text{number of photons emitted per sec by fluorescence}}{\text{number of photons absorbed per sec.}} \qquad)$$

The intensity absorbed by a spectral line I_A is given by the equation:

$$I_A = I_o f_x \Omega_a A_T \quad W/cm^2 \qquad (14)$$

Where: f_x is a factor (no units to account for the decrease in the intensity of the exciting radiation in region X of Fig V by absorbing atoms.

Ω_a is the solid angle (no units) of incident radiation used for excitation of the atomic vapour.

I_o is the incident intensity of the exciting radiation from a continuous source (W-sec/cm^2-ster). This represents the radiant power per unit source area per unit solid angle per frequency interval.

If the exciting radiation is a narrow line I_o must be replaced by:

$$I_L \frac{2\sqrt{\ln 2}}{\sqrt{\pi}\,\Delta V_L} = I_o \qquad (14a)$$

where I_L is the intensity of the source line (W/cm^2-ster)

ΔV_L is the source line half-width in sec^{-1} for a line with a Gaussian contour. (The $\frac{2\sqrt{\ln 2}}{\sqrt{\pi}}$ factor is necessary to convert Gaussian half-widths to triangular half-widths; this simplifies the calculation of line areas.)

A_T is the total absorption factor (sec^{-1}) and represents the fraction of the incident radiation absorbed in region Y of the flame (see Fig. V) and is defined by the equation[4,24]:

$$A_T = \int_o^\infty \frac{I_{V_o} - I_{V_t}}{I_{V_o}}\, dV = \int_o^\infty \left[1 - \exp(-k_v L)\right] dV \ sec^{-1} \qquad (15)$$

where: I_{V_o} is the intensity of the exciting radiation as a function of frequency ($W\text{-}sec/cm^2$-ster)

I_{V_t} is the intensity transmitted through the flame of average width L at frequency V

K_V is the atomic absorption coefficient in cm^{-1} as a function of frequency V.

L is the average path length over which absorption occurs and the resulting atomic fluorescence is measured (see Fig.V).

f_x and f_z are both factors related to the distances over which absorption occurs and to the atomic absorption coefficient $\bar{k}$ averaged over all frequencies and all absorbing atoms. f_x and f_z both approach unity as the solid angle over which excitation occurs is increased to cover the entire flame cell and as the solid angle over which the fluorescence is measured is increased to include the entire flame cell.

General Intensity Expression for Resonance Fluorescence

For an isolated atomic resonance line excited by the same line, the intensity of fluorescence can be found by combining equations (12) and (14). Thus

$$I_F = I_o f_x \frac{\Omega a}{4\pi} A_T \phi_T f_z \quad W/cm^2\text{-ster} \qquad (16)$$

General Intensity Expression for Stepwise- and Direct-Line Fluorescence[4,24]

For an isolated fluorescence line produced by stepwise-line fluorescence, the intensity of fluorescence can be found by combining equations (12) and

(14), but then all the absorption lines (other than the resonance absorption) which are effective in exciting fluorescence energy level must be considered as well as the influence of re-absorption of the fluorescence radiation by atoms of the same kind within the region of observation (region Z of Fig.V). If there are j absorption lines (other than resonance absorption) resulting in excitation of an atom to the fluorescence energy level, then the intensity of fluorescence is given by

$$I_F = \frac{\Omega}{4\pi} f_z f_y \phi_T \sum_i I_{o_i} f_{x_i} A_{T_i} \quad W/cm^2\text{-ster} \qquad (17)$$

where f_y accounts for re-absorption of the fluorescence radiation produced by non-resonance absorption within region Y of Fig.V, by atoms of the same kind as the fluorescent ones. For the case of resonance fluorescence, re-absorption is inherently considered in the A_T factor and so f_y is unity for resonance fluorescence (ie. $f_y = \left(\frac{1 + \exp(-\bar{k} L)}{2}\right)^{24}$ where $\bar{k}$ is the average atomic absorption coefficient for absorption of radiation produced by means other than resonance absorption, thus for resonance fluorescence f_y is unity.

All the terms within the summation sign concern the absorption line which produces the fluorescence line, i.e. I_{o_j} is the intensity of the exciting radiation at the frequency of the absorption line j,

A_{T_j} is the total absorption for the absorption line j,

ϕ_T is the total power efficiency for the fluorescence line resulting from absorption of radiation[26].

Equation (17) is also a general expression for evaluating the intensity of atomic fluorescence for the case of direct-line fluorescence and so is a general expression whatever the mechanism of excitation and whatever emission transition is involved. For the case of direct-line fluorescence, there may still be j absorption routes of excitation, but the fluorescence transition does not involve the ground electronic state and thus f_y and f_z are unity (assuming no thermal population of the lower metastable state of the fluorescence transition). In many cases of direct-line fluorescence, only one absorption line is involved, this type of fluorescence may be termed simple direct-line fluorescence. For this type of fluorescence equation (17) reduces to equation (16) and f_z is then unity as the fluorescence emission line is a non-ground state line and will not suffer self-absorption.

For thermally excited direct-line fluorescence, usually only one absorption line is responsible for excitation[23,27] and I_F can be found using

equation (16) with an exponential term (exp $-\frac{\Delta E}{kT}$) included to account for the energy difference (ΔE) between the excited state (that the atom is initially raised to by absorption of resonance radiation) and the excited state from which fluarescence occurs.

If more than one fluorescence transition is involved, e.g. a multiplet of closely spaced lines, then a summation of expressions like equation (5) can be added together to give the total fluorescence intensity. Hyperfine splitting of spectral lines due to isotopes or nuclear spin effects can also be considered using equation (17).

Thus from equations (16) and (17) it can be seen that for a given set of flame conditions and a constant source intensity, (assuming that ϕ_T is independent of the concentration of a given element in the flame gases which at the concentrations used in analytical flames is a very good approximation); then for resonance or simple direct-line fluorescence:

$$I_F \propto f_x f_z A_T$$

and for stepwise- and/or direct-line fluorescence

$$I_F \propto f_z f_y \sum_i f_{x_i} A_{T_i} \qquad i \text{ absorption lines.}$$

At low concentrations and small values of the distances d and b, (see

Fig.V), f_x f_y and f_z are effectively constant and equal to unity. Thus I_F is directly proportional to the A_T factor (or the sum of the A_T factors).

Evaluation of the Total Absorption Factor, A_T

The value of the A_T factor depends upon the line-width of the absorption line compared to the line-width of the exciting radiation and upon the product of NL (the number of atoms in the ground state per cm^3 of the flame gases times the absorption path length of region Y of Fig.V).

The Absorption Line Half-Width is narrow compared to the Source Line Half-Width (e.g. a continuous source)

Low NL

In this case A_T is approximately given[4] by the equation:

$$A_T = \int_0^\infty \left[1 - \exp(-k_\nu L)\right] dV = \int_0^\infty k_\nu L dV (sec^{-1})$$

$$= \frac{\pi e^2 NfL}{mc} \qquad (18) \qquad \text{(derived from equation (1))}$$

For definition of the symbols used the reader is referred back to equation (1).

Thus it can be seen that at low concentrations A_T increases linearly with N, so that I_F will also increase linearly with N. This is shown pictorially in Fig. VI.

High NL

At high values of NL, A_T is given by the equation[24]:

$$A_T = \left[\frac{k_o L \Delta V_D^2 a \pi^{\frac{1}{2}}}{\ln 2}\right]^{\frac{1}{2}} = \left[\frac{2\pi e^2 f NL \Delta V_D a}{mc(\ln 2)^{\frac{1}{2}}}\right]^{\frac{1}{2}}$$

As from equation (5)

$$k_o = \frac{[4\pi \ln 2]^{\frac{1}{2}} e^2 Nf}{mc \Delta V_D}$$

Thus it can be seen that A_T (and I_F) will increase linearly with $\sqrt{N}$. This is shown pictorially in Fig. VI.

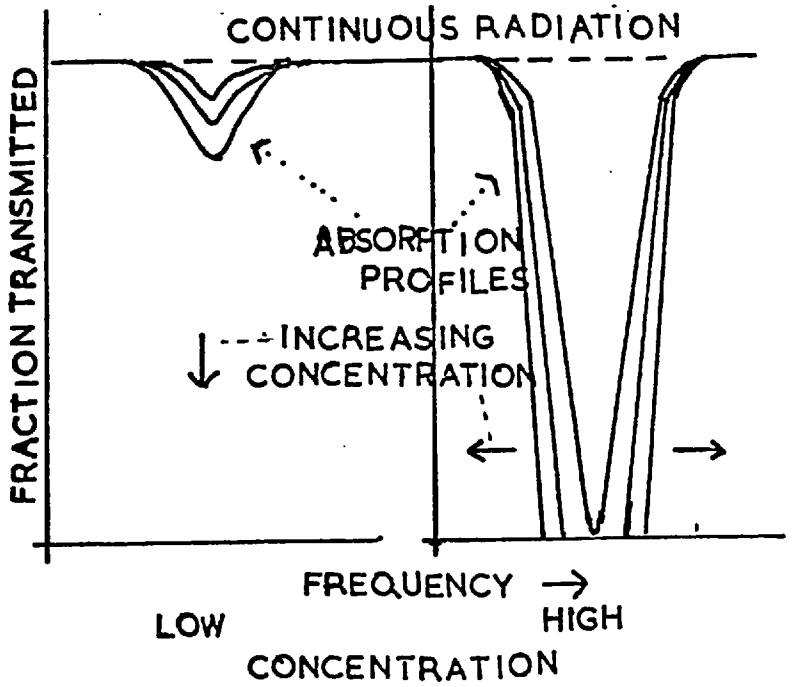

Variation of Total Absorption of Radiation from a Continuous Source with Atomic Concentration

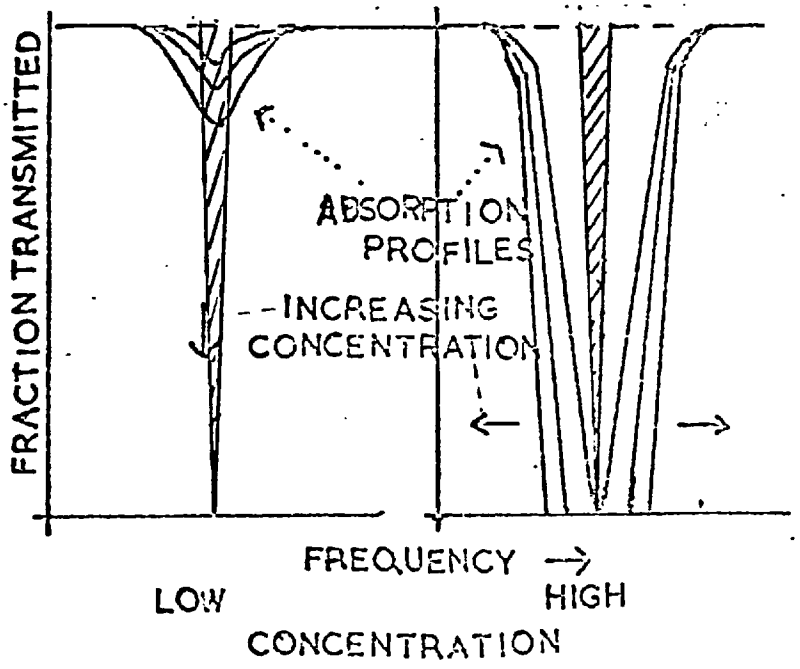

Variation of Total Absorption of Radiation from a Line Source with Atomic Concentration

FIGURE VI.

The Absorption Line Half-Width is large compared to the Source Line Half-Width (e.g. a sharp-line source)

Low NL

At low NL values, the value of A_T is given by:

$$A_T = \int_0^{\frac{\Delta V_L}{2}\left(\frac{\pi}{\ln 2}\right)^{\frac{1}{2}}} \left[1 - \exp(-k_v L)\right] dV$$

$$= \int_0^{\frac{\Delta V_L}{2}\left(\frac{\pi}{\ln 2}\right)^{\frac{1}{2}}} k_v L dV \qquad = \frac{k_o^{\ell} L \Delta V_L}{2}\left(\frac{\pi}{\ln 2}\right)^{\frac{1}{2}} \qquad (20)$$

where k_o^{ℓ} the peak atomic absorption coefficient at the centre of the line.

The integration limits are the source line half-width (triangular distribution) not the absorption line half-width. The integration in equation (20) is obtained by multiplying the peak atomic-absorption coefficient (k_o^{ℓ}) by the pathlength by the triangular half-width of the source line. (At low NL

values $k'_o \cong Kk_o$, where k_o is the maximum absorption coefficient when only Doppler broadening is present, and K is a constant.)

Now $$I_F \propto I_o A_T \qquad (21)$$

($I_o A_T$ is used instead of A_T because I_o for a line source is dependent on ΔV_L, the source-line half-width, and the use of $I_o A_T$ results in a simpler expression.)

Now from equation (14a)

$$I_o = \frac{2I_L}{\Delta V_L} \left(\frac{\ln 2}{\pi}\right)^{\frac{1}{2}}$$

Thus from equation (20)

$$I_o A_T = Kk_o L I_L = \frac{K \left[4\pi \ln 2\right]^{\frac{1}{2}} e^2 NLfI_L}{mc\ \Delta V_D} \qquad (22)$$

Thus I_F will increase linearly with N. This is shown pictorially in Fig.VI as N increases (assuming L to be constant) the area (A_T) under the emission line profile increases almost linearly with N.

High NL

At high NL values the value of A_T can be found by assuming essentially complete absorption of the source line occurs (i.e. $\exp(-k_v L) = 0$).

Thus:

$$A_T = \int_0^{\frac{\Delta V_L}{2}(\frac{\pi}{\ln 2})^{\frac{1}{2}}} \left[1 - \exp(-k_v L)\right] dV = \int_0^{\frac{\Delta V_L}{2}(\frac{\pi}{\ln 2})^{\frac{1}{2}}} dV$$

$$= \frac{\Delta V_L}{2}(\frac{\pi}{\ln 2})^{\frac{1}{2}} \qquad (23)$$

Hence using equation (21), $I_o A_T$ can be evaluated

$$I_F \propto I_o A_T = I_L \qquad (24)$$

Thus I_F is independent of N and only depends on I_L. This is shown pictorially in Fig. VI. Essentially complete absorption occurs over the entire source line profile and further absorption can only occur if the source-line half-width widens or intensity increases (i.e. I_F is constant as N increases). If the absorption line half-width is of the same order as the source-line half-width the mathematics became extremely involved[4] and are not attempted in this work.

Conclusions

The intensity expressions for I_F for resonance, stepwise and direct-line fluorescence are given in Table 4. These expressions are obtained in substituting the A_T values into equations (16) and (17).

TABLE 4

Intensity Expressions for an Isolated Atomic Fluorescence Line

Resonance Fluorescence and Simple Direct-Line Expressions ($f_z = 1$)

Absorption Line Half-Width much less than Source Line Half-Width

Low NL $$I_F = I_o f_x \Omega_a \phi_T f_z \frac{e^2 NfL}{4mc}$$

High NL $$I_F = I_o f_x \frac{\Omega_a}{4\pi} \phi_T f_z \left[\frac{2\pi e^2 fNL\, \Delta V_D{}^a}{mc\, (\ln 2)^{\frac{1}{2}}}\right]^{\frac{1}{2}}$$

Absorption Line Half-Width much greater than Source Line Half-Width

Low NL $$I_F = I_L f_x \frac{\Omega_a}{4\pi} \phi_T f_z \frac{K\, (4\pi \ln 2)^{\frac{1}{2}}\, e^2 NLf}{mc\, \Delta V_D}$$

TABLE 4 (contd.) :

High NL $I_F = I_L f_x \frac{\cap a}{4\pi} \phi_T f_z$

Stepwise- and Direct-Line Fluorescence Expressions

Absorption Line Half-Width much less than Source Line Half-Width

Low NL $I_F = \cap a \, f_z f_y \phi_t \sum_i I_{o_i} f_{x_i} \frac{e^2 N f_i L}{4mc}$

High NL $I_F = \frac{\cap a}{4\pi} f_z f_y \phi_T \sum_i I_{o_i} f_{x_i} \left[\frac{2\pi e^2 f_i N L \, \Delta V_{D_i}^{a_i}}{mc(\ln 2)^{\frac{1}{2}}} \right]^{\frac{1}{2}}$

Absorption Line Half-Width much greater than Source Line Half-Width

Low NL $I_F = \frac{\cap a}{4\pi} f_z f_y \phi_T \sum_i I_{L_i} f_{x_i} \frac{K (4\pi \ln 2)^{\frac{1}{2}} e^2 N L f_i}{mc \, \Delta V_{D_i}}$

High NL $I_F = \frac{\cap a}{4\pi} f_z f_y \phi_T \sum_i I_{L_i} f_{x_i}$

It can be seen from Table 4 that at low values of NL, the fluorescence intensity, I_F, of a spectral line should vary linearly with atomic concentration for either a continuous or a sharp-line source and this is very useful analytically. (This assumes an ideal nebuliser with complete dissociation of the element in the flame.) At high values of NL, I_F is independent of NL for a sharp-line source and proportional to $(NL)^{\frac{1}{2}}$ for a continuous source. At very high values of NL the values of f_x and f_z can fall well below unity, thus causing the I_F V N curve to fall back towards the concentration axis (i.e. I_F attains a maximum value and then decreases with further increase of concentration).

At first sight it may appear odd that the calibration curves obtained in A.F.S. with a sharp-line source are linear with respect to I_F whilst those obtained with the same source in A.A.S. are linear with respect to $\log \frac{I_o}{I}$. The reason for this can be seen by considering the fraction of the incident light absorbed (A_F) in each case. Using A.A.S. an absorbance value (A) of ca 0.5 which is often obtained at the high concentration end of a calibration curve using a 10 cm pathlength burner, is quite common. This value of the absorbance (A) corresponds to an A_F value of ca 0.7. Under similar conditions using A.F.S., assuming the average flame path (i.e. the effective flame diameter) to be ca 1 cm,

the corresponding absorbance (A) is ca O.O5 which corresponds to an A_F value of ca O.1. Remembering that in general A.F.S. is between 10-100 x more sensitive than A.A.S.,[27] then the average A_F values will be less than O.O1. Hence it can be seen that the average A_F values in A.F.S. are much lower than those in A.A.S.

Now from equation (15)

$$A_T = \int_0^\infty \frac{I_{V_o} - I_{V_t}}{I_{V_o}} \, dV$$

which for a sharp line source yields the expression:

$$A_T = \frac{I_o - I_t}{I_o} \Delta V_L \quad (\text{sec}^{-1}) \qquad (25)$$

where I_o is the measured incident radiation from the source (a.u.)

I_t is the measured transmitted radiation from the flame (a.u.)

ΔV_L is the source line width (sec^{-1})

Now $$A_F = \frac{I_o - I_t}{I_o} = \frac{A_T}{\Delta V_L} \quad (\text{no units}) \qquad (26)$$

i.e. $$A_F \propto A_T \qquad (26a)$$

Now the absorbance A is defined as:

$$A = \log_{10} \frac{I_o}{I_t} = -\log_{10}(1 - A_F)$$

$$= -0.434 \log_e(1 - A_F) \qquad (27)$$

At low values of A_F equation (27) reduces to

$$A = 0.434\ A_F \qquad (28)$$

In fact A_F (and A_T) values are almost directly proportional to absorbance values up to an absorbance of ca 0.07. A typical range of A_F values used in A.F.S. would be ca 0.05 - 0.00005. Absorbance values cannot be measured very accurately much below an equivalent A_F value of 0.01. This fact limits the range of calibration curves in A.A.S.

Comparison of A.F.S. with A.A.S. and F.E.S.

A.F.S. has certain advantages and disadvantages when compared with A.A.S. and F.E.S. and these are listed below:

Advantages of A.F.S. in relation to A.A.S.

1) A.F.S. is essentially an emission technique and the sensitivity can be increased by either increasing the source intensity or the gain of the instrument. In A.A.S. the absorbance value is a ratio ($\log \frac{I_o}{I}$), thus any increase in I_o is accompanied by a corresponding increase in I, hence the ratio $\log \frac{I_o}{I}$ remains unaltered.

2) A.F.S. requires less sophisticated apparatus and burners than A.A.S.

3) A continuous source can be used in A.F.S. with a normal monochromator, (because the detector does not 'see' the source) whilst the use of a continuous source in A.A.S. would require the use of a very high resolving power monochromator.

4) In general, for most elements, there are more fluorescence lines than absorption lines. This gives a greater choice in wavelength of measurement.

e.g. The main arsenic resonance lines lie at 1890, 1937 and 1972 Å where absorption by the air, optics and flame gases can be quite serious and also the photomultiplier response is often poor at these wavelengths. However, although these resonance lines must be used in absorption measurements, the fluorescence resulting from the absorption of these lines, can be measured at 2288 or 2350 Å.[27]

Disadvantages of A.F.S. in relation to A.A.S.

1) Atomic absorption measurements are independent of the power efficiency ϕ_T; however, fluorescence measurements are directly proportional to ϕ_T and any change in the value of ϕ_T will be reflected by a change in the value of I_F. As long as the flame temperature and composition are kept constant and the partial pressures of the nebulised species are low, (which is generally the case) interelement effects on the value of ϕ_T should be negligible. Alkemade[12] found that the quantum efficiency for the resonance fluorescence of sodium did not alter when the flame temperature of an argon/oxygen/propane flame was raised 100°C. However, changing from argon to carbon dioxide gave a six-fold decrease in the ϕ_T value.

2) The determination of refractory metals by A.F.S. using conventional nitrous-oxide and oxy-acetylene flames is difficult as A.F.S. is essentially an emission technique and larger slit-widths than commonly employed in A.A.S. are necessary at low concentrations. Although the light from the source can be modulated so that the high intensity background radiation from the flame is not amplified, this background radiation can seriously overload the photomultiplier and increases the noise level.

3) Similarly the determination of the alkali metals (with their resonance lines in the visible region) will be difficult owing to the intense emission signals which will tend to overload the photomultiplier and increase the noise level. Alkemade[12] found the D line fluorescence signal for sodium, using a sodium vapour lamp as excitation source, to be $\frac{1}{400}$ as intense as the thermal emission.

4) Scattering can become important in A.F.S. at low concentrations if a badly designed nebuliser is used. However it has been found that in general for an efficient nebulising system, scattering is generally negligible. (In the determination of bismuth[23] it is possible to excite at one line and measure at another line which is NOT present in the exciting source.)

Advantages of A.F.S. in relation to F.E.S.

1) A.F.S. depends on the absorption of radiation by ground state atoms and thus unlike F.E.S. will not be exponentially dependent on the flame temperature (see Table 2).

2) A.F.S. (like A.A.S.) is very sensitive for elements with resonance lines in the far ultraviolet (e.g. cadmium, zinc, arsenic, bismuth and antimony), whereas F.E.S. is not very sensitive in that region of the spectrum (see Table 1).

3) Relatively cool, low burning velocity flames (which give negligible thermal emission for most elements) can be used in A.F.S. for the determination of many elements.

e.g. Air-hydrogen, air-propane, nitrogen-hydrogen.

Disadvantages of A.F.S. in relation to F.E.S.

1) A.F.S. requires the use of a source, (usually a different one for each element) whilst F.E.S. does not.

2) A.F.S. is far less sensitive than F.E.S. for easily excited elements such as the alkali and alkaline earth metals which have their resonance lines in the visible region of the spectrum.

PART I

CHAPTER I

Basic Experimental Parameters of A.F.S.

1.1 Introduction

A simple A.F.S. arrangement has been shown in Fig.III. The basic units involved are: the monochromator and detector, the flame, the nebulising system and the source. These are now considered in detail.

(1) The Monochromator and Detector

Although the resolution of the monochromator used in A.F.S. is not too critical, it must be remembered that A.F.S. is essentially an emission technique and therefore the sensitivity will depend on the resolution of the monochromator to some extent. The background radiation from the flame is proportional to the square of the spectral band-pass of the monochromator[28], and the limit of detection for many A.F.S. methods is determined by noise emanating from fluctuations in the flame background. As most A.F.S. studies are performed in the medium-far U.V. region of the spectrum, a quartz prism monochromator which gives good resolution in the U.V. is a good choice. If a grating monochromator is used, it is essential that an

efficient one is chosen, as inferior gratings tend to give rather large amounts of scattered light in the far U.V. Similarly it is essential that a photomultiplier which is sensitive over the whole U.V. region is used, because the sensitivity in A.F.S. is directly dependent on the response of the photomultiplier.

In the present studies a Unicam SP900A quartz prism monochromator which gives a resolution of 4 Å/0.1 mm slit-width at 2500 Å and an EM19601B photomultiplier were used.

(2) The flame

The optimum flame in A.F.S. is a hot, low background flame. A hot flame will ensure complete atomisation of the nebulised compound to the given element and will also minimise interference from incomplete breakdown of other compounds in the flame which could prevent the complete atomisation of the desired element. Unfortunately most hot flames (e.g. nitrous oxide-acetylene and oxygen-acetylene) exhibit a very high background and have fast burning velocities. However, this is not so for the nitrous oxide-hydrogen flame (Chapter IX). In general a compromise between temperature and flame background has to be found; the lowest background flame which gives complete atomisation with a minimum of interference

from other elements is the optimum choice, e.g. for cadmium and zinc an air-hydrogen or an air-propane flame was found to be optimum.[28]

It must be realised that although the source radiation can be chopped so that the flame background is not recorded at the output of the instrument, The photomultiplier is a D.C. amplifier and will always respond to the flame background plus the fluorescence signal as well as any thermal emission of the given element. In theory only the alternating fluorescence signal should be amplified, but variations in the flame background may have a variable component over the frequency bandpass of the amplifier and in general the larger the background signal the larger the noise signal recorded at the output of the photomultiplier. With very high levels of flame background, photomultiplier fatigue can occur.

(3) The Nebulising System

An efficient nebulising system is essential in A.F.S. If it produces large droplets these will tend to pass through the flame without completely evaporating and this will give rise to scatter signals. This scattering effect has been reported in connection with the use of total consumption burners,[29,30] and this type of nebuliser is considered by the author to be inferior to an indirect nebuliser which removes the larger droplets before they reach the flame. For a complete discussion of pneumatic indirect

nebulisers the reader is referred to the work of Willis.[31]

Ultrasonic atomisers appear worthy of mention, as they produce extremely small droplets. The main drawback of ultrasonic atomisers is their relative complexity compared with conventional pneumatic nebulisers. Ultrasonic atomisers have shown great promise in plasma work[32,33] where the larger gas flow rates of pneumatic nebulisers are a great disadvantage. Hoare, Mostyn and Newland[34] have recently reported the use of an ultrasonic atomiser in A.A.S. and found the same sensitivity as given by a conventional pneumatic atomiser. There has been no reported use of ultrasonic atomisers in A.F.S.

Electrostatic nebulisers have been described[35] but their nebulising properties are rather dependent on the dielectric properties of the nebulised solution.

(4) The Source

The basic requirements of an A.F.S. source are listed below:

(1) The source should be intense at the principal resonance lines, because the intensity of atomic-fluorescence is directly proportional to the source intensity,

(2) it should emit spectral lines essentially free from self-reversal,

(3) it should be stable,

(4) it should readily be prepared for a large number of elements,

(5) it should have a long running and shelf-life and be inexpensive.

There are basically two types of sources that can be used in A.F.S. viz. line and continuous sources. The principal line sources are the hollow-cathode lamp, the vapour discharge lamp and the electrodeless discharge tube whilst the principal continuous sources are the xenon-arc and hydrogen lamps.

(a) Hollow-cathode lamps

The output from hollow-cathode lamps is generally too low to be used in A.F.S. studies. This is partly due to the low operating currents (ca 10-20 ma). At higher currents self-reversal of the resonance lines occurs and the overall useful intensity does not increase much. Also at these higher currents severe spluttering from the cathode occurs and the useful life of the lamp is drastically reduced. The demountable hot-cathode lamp has been claimed to be the most intense light source available for A.F.S. studies.[30,36] These lamps were run up to currents of 600 ma and were used to determine aluminium, titanium, zirconium and other elements by A.F.S. in and above an air-hydrogen flame maintained on a total consumption burner. It would appear that the fluorescence signals observed by these workers were mainly due to scattering of the source

radiation by water droplets and particles in the flame because the air-hydrogen flame is incapable of breaking down refractory metal oxides.[37] In addition the wavelength (3870 Å) at which the aluminium fluorescence was measured does not correspond to an aluminium (1) line, but at the band-pass of the 2.0 mm slit-width used would correspond to scatter of the 3889 Å helium line of the filler gas used. At the high operating currents used the resonance lines from these demountable lamps are almost certain to be self-reversed to a large degree.

Armentrout[38] has reported the use of a high intensity hollow-cathode lamp for the determination of nickel and obtained a limit of detection of 0.3 ppm at 2320 Å, similar to the average limit of detection at the same line using A.A.S. However, West and Williams[39] have more recently reached a limit of detection of 0.0001 ppm for aqueous solutions of silver at 3281 Å, using a high intensity lamp. This is ca 10 times lower than could be obtained by A.A.S. using the same basic instrumental arrangement.

(b) Vapour Discharge Lamps

These lamps have been successfully used as sources in A.F.S.[14,15,16,18,28] but they tend to give poor sensitivities in A.A.S.[40] This discrepancy

can be explained by the fact that at the high operating temperature of these lamps the emitted lines tend to be rather broad (possibly broader than the absorption line profile) and show some self-reversal in the central regions of the line. This demonstrates one advantage of A.F.S. over A.A.S., the fact that high sensitivity can be obtained in A.F.S. using a wide-line source. Unfortunately intense vapour discharge lamps are only manufactured for a limited number of elements, e.g. cadmium, mercury, thallium and zinc.

(c) Electrodeless Discharge Tubes

The electrodeless discharge tube normally consists of a sealed quartz tube some 2-7 cm in length and contains a few mg of a metal or a metal salt under a few Torr of an inert gas. Winefordner[15,16] and coworkers have used commercially available sealed electrodeless discharge tubes for copper, mercury, nickel and thallium fluorescence studies with rather poor results. These sources were not necessarily of a very high intensity or stability since they are marketed primarily for uses in interferometry and wavelength calibration studies. Also, they were not necessarily operated in an efficient resonant cavity.

However, this type of lamp has been found by the author to be extremely useful as a source in both A.F.S. and A.A.S. giving intense,

sharp line spectra. The preparation and behaviour of these lamps are fully discussed in the next chapter.

(d) Xenon-Arc Lamps

The xenon-arc lamp gives a continuum from the infrared to the far ultraviolet (ca 2000 Å), unfortunately the peak intensity is in the infrared and the output intensity decreases rapidly through the ultraviolet and below 2500 Å it is quite low. Even so, this lamp can be used to excite atomic-fluorescence of elements with resonance lines in the ultraviolet usually giving limits of detection about two orders of magnitude higher than those obtained using electrodeless discharge tubes.

(e) Hydrogen Lamps

Although there has been no reported use of a hydrogen lamp source in A.F.S., some cursory studies (see experimental section) indicate that a hydrogen lamp could be used as a continuous source.

EXPERIMENTAL

1.2 Apparatus (Basic Atomic-Fluorescence Arrangement)

The apparatus used in the author's studies consisted of a Unicam SP900A atomic-absorption/thermal-emission flame spectrophotometer. The stainless steel burner-heads were of the Meker type in which the fuel gas and air/sample mixture is burned above a series of concentric rings of holes giving a flame with a maximum diameter of ca 1.5 cm (see 1,3). A concentric jet nebuliser was used consisting of a metal capillary (80% Pt and 20% Ir) mounted in a Perspex cylinder. The resultant spray spins in an expansion chamber in such a manner that larger droplets are removed by centrifugal force and only a fine homogeneous mist reaches the flame. The normal EMI 9529B photomultiplier supplied with the instrument was replaced by an EMI 9601B photomultiplier which is particularly sensitive in the ultraviolet region, where most of the lines used in A.F.S. occur. Simple modification to the burner housing allowed the necessary irradiation of the flame, via an adjustable slit mechanism, from the source. The source itself was mounted so that it subtended a right angle with the entrance slit of the spectrophotometer at the flame.

With the 'emission' mode of the SP900A, light from the flame is chopped at 100 c/s after entering the monochromator and hence both the analytical signal and the background radiation are amplified by the a.c. system, and are recorded. With the absorption mode of operation, the monochromator chopper is held in the open position and the background, which is continuous, is not recorded. A 100 c.p.s. chopper is provided to give an a.c. signal from a d.c. hollow-cathode lamp used in A.A.S., but in the experiments described in this chapter this chopper assembly was not used because it would have required re-positioning of the burner. Hence a.c.-operated sources (vapour discharge lamps and a xenon-arc lamp) were used for atomic-fluorescence measurements with the 'absorption' mode of operation and with the excitation sources at the side of the flame opposite to that at which hollow-cathode lamps are normally situated for A.A.S. The analytical signal recorded under these conditions consists of the fluorescence signal, source scattering and phased fluctuations in the background radiation at the wavelength of measurement. In general, the larger the background, the larger the fluctuations. Scattering with the SP900A is kept to a minimum by the centrifugal expansion chamber which allows only the smaller droplets through to the flame.

Although the continuous flame background radiation is not recorded in the fluorescence measurements, the d.c. photomultiplier receives both the analytical signal and the background. A large background is undesirable because flooding of the photomultiplier with an 'indifferent' light signal may cause temporary fatigue of the detector, non-linear response towards the a.c. signal and will introduce a noise component into the fluorescence signal.

1.3 Types of Flame

The Unicam SP900A burner was supplied with heads and jets suitable for air-acetylene and air-propane flames. In addition to these, air-hydrogen and air-carbon monoxide flames could safely be maintained using the Unicam burner-heads and jets (see Table 5). In general it was considered dangerous to use oxygen or nitrous oxide for nebulisation because of the risk of explosive flash-back into the 1 litre glass expansion chamber of the nebuliser. This risk results from the high burning velocities of most oxygen and nitrous-oxide supported flames. However, by nebulising the test solution on nitrogen or even air, practically any gas mixture may be used without risk of explosive flashback when a third gas is introduced via a second jet in the burner base.[41] This modification of the burner

base permits the study of mixtures of two other gases with the fuel gas. Thus it has been found possible to burn over 30 different types of flame using conventional Unicam burner-heads and jets. Some of these flames are listed in Table 5.

TABLE 5

Flame Types

Group	Nebulising Gas	Fuel Gas	Additional Gas	Burner Heads[+]	General Background Intensity
a	Air	C_2H_2		1,2	High
	Air	C_3H_8		3	Low
	Air	H_2		1,2,3	Low
	Air	CO		3	High
b	N_2 or A	C_2H_2	O_2	2	Very high
	Air	C_2H_2	O_2	2	Very high
	N_2 or A	C_2H_2	N_2O	2,3	Very high
	Air	C_2H_2	N_2O	2	Very high
	N_2 or A	H_2	O_2	2	Low
	Air	H_2	O_2	2	Low
	N_2 or A	H_2	N_2O	2,3	Medium
	Air	H_2	N_2O	2,3	Medium

Continued.....

TABLE 5 (contd.)

Group	Nebulising Gas	Fuel Gas	Additional Gas	Burner Heads[+]	General Background Intensity
c	N_2O	C_3H_8*		2,3	Very high
	N_2O	H_2*		2,3	Medium
d	N_2 or A	H_2		2,4	Very low
	CO_2	H_2		2,4	Low
	N_2 or A or CO_2	C_2H_2		2,4	Low

Burner-Heads[+]

(1) Standard Unicam circular air-acetylene burner-head. This burner-head is perforated with a series of concentric rings of holes.

(2) Standard Unicam 1.8 x 7.5 cm air-acetylene emission burner-head. The steel head of this burner is perforated at one end by a 1 cm square pattern of 13 holes, and is well suited to the construction of the Unicam SP900A as it brings the flame close up to the entrance slit of the monochromator.

*Nitrous oxide could be safely used as the nebulising gas because of the low burning velocities of these two flames.

(3) Standard circular air-propane burner-head, similar to 1, except that the holes were slightly larger.

(4) Pyrex tube burner, varying in diameter from 3-10 mm.

The flames in group (a) are simple air-fuel gas flames; the air-carbon monoxide flame was found to be of little use in F.E.S. or A.F.S. owing to its low temperature,[42] high background and ability to quench fluorescence emission. The other flames in this group are described later in this chapter. The group (b) oxygen and nitrous oxide enriched flames were found (using the emission of the 589 mu sodium doublet) to be hotter and to exhibit a much higher background than group (a) flames. The air-nitrous oxide-acetylene flame was found to be quite safe with regard to flash-back and has been found[43] to reduce interelement effects in A.A.S. that have been observed in the air-acetylene flame. The group (c) flames were found to be hotter than those of group (b). The nitrous oxide-propane flame was found to have an extremely high background, but the nitrous oxide-hydrogen flame was found to have a lower background (over most regions) than the air-acetylene flame. The nitrous oxide-hydrogen flame was found by the author to be very useful in F.E.S. (Chapter IX.) and should prove useful in A.F.S. for elements that are incompletely atomised in the premixed air flames. Both flames in group (c) should prove useful in

overcoming interelement effects in A.A.S. and are safer to maintain than the nitrous oxide-acetylene flame. Group (d) flames are diffusion flames and the inner temperatures were found to be between 200-500°C depending on the burner-head. The nitrogen-hydrogen flame was found to be the most useful; this flame was completely colourless apart from occasional flashes produced by the entrance of particles of airborne dust. The hydroxyl emission at about 300-320 mu was very weak, being about 40 times less intense than in a premixed air-hydrogen flame on the same burner-head. Similarly the emission at 589 mu of a 2 ppm sodium solution was about 50 times less than in an air-hydrogen flame. When nitrogen was substituted for argon in a given flame relatively large differences in burning velocity, thermal and fluorescence emission intensities were observed. (Chapters V and VI.)

This general description of the various types of flame has had to be kept rather brief but some of the flames are more fully described later in the text. (Chapters V – IX)

The preliminary studies of atomic-fluorescence described in this Chapter utilised the air-acetylene, air-propane and air-hydrogen flames.

1.4 Flame Background Parameters

Measurements were made with the 'emission' mode of operation and with distilled water aspirating through the flame. (This slightly reduces the flame temperature.[44]) This also caused all background readings to decrease by about 15%. The flame was not irradiated in these studies.

The Unicam burner is supplied with burner-heads and jets suitable for air-acetylene and air-propane flames. In addition to these, an air-hydrogen flame was maintained using the acetylene burner-head and jet. The propane and acetylene pressures were measured on the manometer supplied, but much larger hydrogen pressure was measured on an external gauge. The air pressure used was 15 p.s.i., unless otherwise stated.

The 5 principal flame conditions used are shown in Table 6.

TABLE 6

Acetylene pressure (cm)[a]	Propane pressure (cm)[a]	Hydrogen pressure (psi)	Flame
3	7	1.0	Strikes back
4.5	10	1.5	Lean
6.7	12	2.0-2.5	Normal
8	16	3.5	Fuel Rich
10	18	5.0	Very Fuel Rich

a Manometer liquid consisted of a red dye solution in dibutyl phthallate.

a) Position of Measurement in Flame

Figure VII shows the background variation in different sections of the above three flames at 2750 Å. The distances shown are measured from the top of the burner to a position corresponding to the centre of the analysing monochromator slit.

The background radiation could be virtually eliminated in the air-propane and air-hydrogen flames by taking measurements as high as possible in the flame. However, the readings tended to fluctuate in the upper flame regions and a distance of 3cm above the burner was chosen as being the most suitable for subsequent measurements. This corresponded to a position somewhat above the primary reaction cones.

b) Fuel Gas Pressure

The background radiation was found to increase with increasing fuel gas pressure for all 3 flames (see Fig.VIII). This dependence varied with the position of measurement in the flame; for example, in the upper regions of the flame it was virtually independent of fuel gas pressure and in the primary reaction cones (when the burner was level with the bottom of the monochromator slit), the background increased drastically from that shown in Fig.VIII and this high background increased

FIG. VII

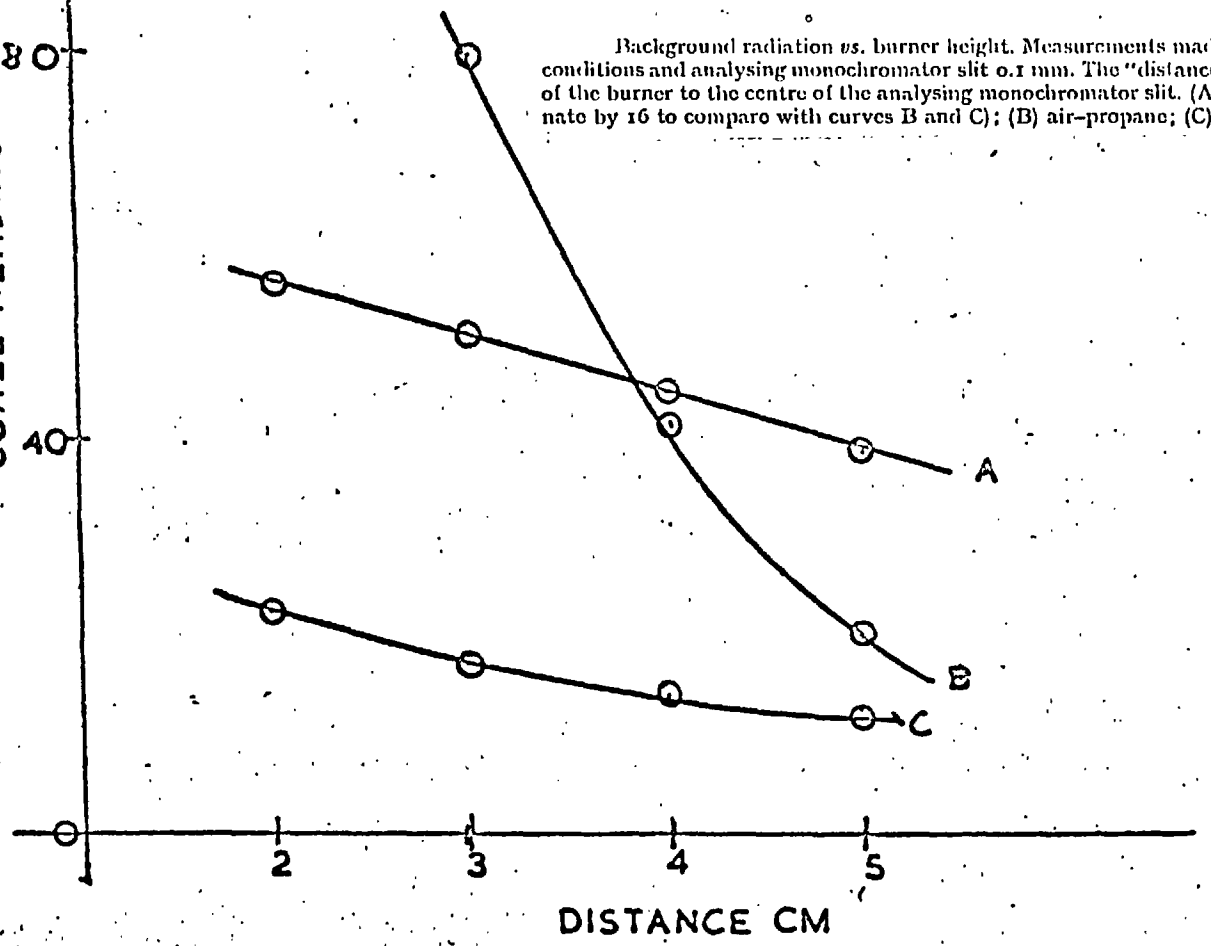

Background radiation *vs.* burner height. Measurements made at 2750 Å with normal flame conditions and analysing monochromator slit 0.1 mm. The "distances" were measured from the top of the burner to the centre of the analysing monochromator slit. (A) Air-acetylene (multiply ordinate by 16 to compare with curves B and C); (B) air–propane; (C) air–hydrogen.

FIG. VIII

Background radiation *vs.* fuel gas pressure. Measurements made at 2500 Å with analysing monochromator slit 0.2 mm and a burner height of 3 cm. Gas pressures used are shown in Table 4. (A) Air–acetylene (multiply ordinate by 5 to compare with curves B and C); (B) air–propane; (C) air–hydrogen.

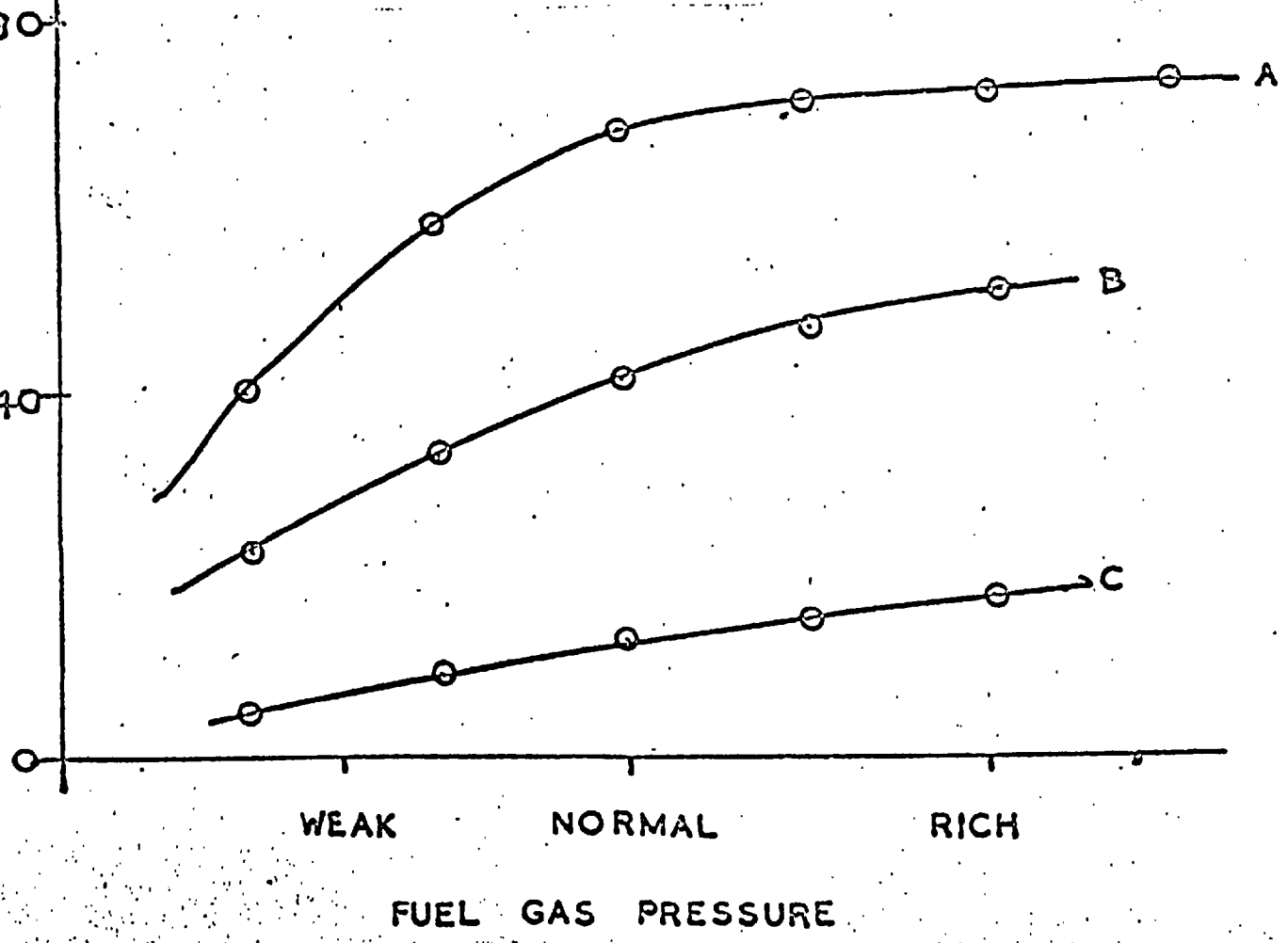

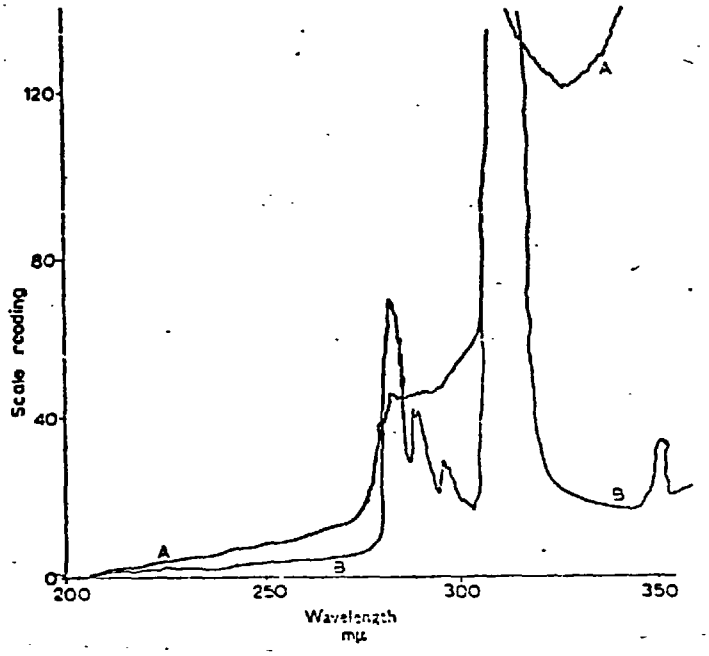

FIG IX

Background radiation *vs.* wavelength of measurement. Measurements made with normal flame conditions with an analysing monochromator slit 0.1 mm and a burner height of 3 cm. (A) Air–propane; (B) air–hydrogen.

rapidly with decreasing fuel pressure. This effect was most marked in the air-acetylene flame and least marked in the air-hydrogen flame. The primary reaction zone of any flame always exhibits a much higher background than the remainder of the flame (chemiluminescence) and is of little interest in A.F.S.

c) Wavelength of Measurement

The dependence of background upon wavelength for the air-propane and air-hydrogen flames, maintained under normal conditions (i.e. 'normal' fuel gas pressures and taking measurements 3 cm above the top of the burner), is shown in Fig. IX.

d) Analysing Monochromator Slit-Width

The background radiation from the normal air-propane and air-hydrogen flames was very dependent on the slit-width at all wavelengths. In general, doubling the slit-width quadrupled the background radiation from both flames. On the other hand, the fluorescence signal was directly proportional to the slit-width. Thus, the signal:background ratio decreased with increasing slit-width. Owing to its very high background the air-acetylene flame was not investigated.

1.5 Results and Discussion of Background Parameters

It can be concluded that chiefly because of its background emission, the air-acetylene flame is the least suitable among those examined for the measurement of atomic-fluorescence. In addition fuel rich air-acetylene flames showed some degree of scattering under irradiation from the source. The inferiority of the air-acetylene flame was verified by measuring the fluorescence signal produced by spraying cadmium solutions through the 3 different flames under irradiation from a cadmium vapour discharge lamp. At the 100 p.p.m. cadmium level, fluorescence from the cadmium intercombination line at 3261 Å could not be detected in the air-acetylene flame owing to the large noise component from the hydroxyl background at this wavelength. However a fluorescence signal at 3261 Å could easily be detected in the other two flames.

In general the air-hydrogen flame was considered to be the most suitable for fluorescence measurements, especially above ca 3200 Å . The air-propane flame background emission below 3200 Å was not excessively greater than the air-hydrogen flame and owing to the rapid rate of consumption of hydrogen, as well as the fact that air-propane mixtures gave steadier flames than those obtained with air-hydrogen mixtures, the air-propane flame was used in the next part of the study.

1.6 Atomic Fouorescence using Vapour Discharge Lamps

Because the only useful available sources at the initial stages of this work were cadmium and zinc vapour discharge lamps and a xenon-arc lamp, A.F.S. methods were developed using these sources.

(a) Zinc

Optimum operating conditions

Flame irradiation was obtained from a 20 W d.c. Osram zinc vapour discharge lamp operated at 1.5A via a ballast unit. A window was cut in the outer glass envelope to permit passage of the U.V. radiation. The source entrance-slit and analysing monochromator slit were set at 2.00 mm and 0.5 mm, respectively. The air pressure was controlled at 15 p.s.i. (4 litres/min) and the propane pressure at 12 cm, thus giving a translucent flame below the level of luminosity. Measurements were made at a position in the flame corresponding to a distance 3 cm from the top of the burner to the centre of the monochromator slit. The absorption mode of operation of the SP900A was used.

A 10^{-3}M stock solution of zinc was prepared by dissolving 0.2876 g of analytical grade $ZnSO_4.7H_2O$ in 1 litre of distilled water. 10^{-5} - 10^{-9}M solutions were prepared by appropriate dilution immediately before measurement. Because of absorption on glass surfaces, it was

considered unwise to store solutions more dilute than 10^{-4}M. The wavelength of measurement was that of the 2139 Å resonance line corresponding to the $4^1S_o \longrightarrow 5^1P_1$ transition (shown as an absorption transition). This line was found by irradiating the flame with the zinc discharge lamp (situated ca 7 cm from the burner) and, whilst aspirating a 10^{-5}M (0.65 p.p.m.) zinc solution, scanning the U.V. region of the spectrum. Fluorescence of the 3076 Å intercombination line was not observed for two reasons; firstly because it falls in the middle of the intense hydroxyl flame emission bands (cf. cadmium 3261 Å line) and secondly, according to Russell-Saunders coupling rules, the intensities of intercombination lines of light elements are extremely weak. With these settings a linear calibration curve was obtained over the range 10^{-5} - 10^{-6}M zinc solution (0.60 - 0.06 p.p.m.). For more dilute solutions, 10^{-6} - 5 x 10^{-8}M zinc solution (0.06 - 0.003 p.p.m.), the analysing slit was opened out to 1.0 mm and a linear calibration curve was again obtained.

The percentage standard deviation at both the 10^{-5}M and 10^{-6}M concentrations was obtained from the analysis of a set of 12 solutions at the given concentrations and was found to be 0.7% and 3.0% respectively.

The effects of 100-fold molar excesses of 41 cations and 18 anions over a 10^{-5}M zinc solution were examined, viz. NH_4^+, Ag, Al, As(III), Al(III), Ba, Be, Bi, Ca, Ce(IV), Co(II), Cr(III), Cu(II), Fe(II), Fe(III), Ga, Hg(II), In, K, Li, Mg, Mn(II), Mo(VI), Na, Ni, Pb, Sb(III), Sc, Se(IV), Sn(II), Sr, Te(IV), Th, Tl(I), Ti(IV), U(VI), V(V), W(VI), Y, Zn, Zr, acetate, $B_4O_7^{2-}$, Br^-, CO_3^{2-}, Cl^-, citrate, ClO_4^-, CN^-, F^-, I^-, NO_3, oxalate, PO_4^{3-}, SCN^-, SiO_3^{2-}, SO_3^{2-}, SO_4^{2-} and tartrate. Hydrolysis was prevented where necessary by the addition of sufficient acid to maintain a clear solution. None of these ions caused more than $\pm$ 5% variation in the expected fluorescence signal, thus indicating that for most practical purposes the method is free from interference. Freedom from interelement effects for cadmium and zinc has also been found by other workers.[18,45]

Extraction into Organic Solvents

The extraction of zinc diethyldithiocarbamate[46] into methyl isobutyl ketone was investigated as a means of increasing the sensitivity of determinasion by increased sample concentration and a more favourable rate of aspiration.

To 25 ml of 10^{-6}M zinc solution were added 5 ml of 20% ammonium acetate to give a near-neutral solution and 1 ml of an aqueous

1% solution of sodium diethyldithiocarbamate. The solution was then extracted with 25 ml of methyl isobutyl ketone. Both the aqueous and organic phases were then sprayed into the flame under the usual conditions. With the organic extract, the propane pressure was, however, reduced so that the usual type of non-luminous flame was obtained.

The ketone extract gave a scale reading ca 4.5 times greater than that obtained with an aqueous solution containing the same concentration of zinc. The aqueous phase remaining after the extraction gave no detectable fluorescence signal, thus indicating virtually complete extraction. A linear calibration curve was obtained over the range 10^{-5} - 10^{-6}M (0.6 - 0.06 p.p.m.), using the above procedure.

The increase in fluorescence intensity obtained on spraying the organic extract can be attributed to the enhanced rate of aspiration into the flame. The rate of aspiration for an aqueous solution under the usual conditions (i.e. air pressure of 15 p.s.i.) was found to be 2.0 ml/min. Of this, only 0.17 ml/min was found to reach the flame. The rate of aspiration with methyl isobutyl ketone was 2.5 ml/min, of which 0.85 ml/min reached the flame. Thus, the amount of ketone reaching the flame was about 5 times that obtained with an aqueous solution.

The limits of detection, corresponding to a signal to noise ratio of 1:1 were found to be ca 10^{-8}M zinc for aqueous solutions and ca 2×10^{-9}M zinc for the ketone solutions.

These sentitivities could not be improved by the use of quartz lenses to focus the light from the discharge lamp or the fluorescence from the flame. This was because the source had to be moved away from the flame, which in turn had to be moved away from the monochromator slit, in order to accommodate the lenses used which had a rather long focal length (ca 6 cm.). However, it would appear that the use of more suitable lenses of shorter focal length which do not allow the inverse square law to operate so efficiently would achieve some increase in sensitivity.

(b) Cadmium

The above procedure (except for extraction into organic solvents) was repeated for cadmium using a 20 Wdc Osram cadmium vapour discharge lamp. Instead of the Unicam SP900A, a flame spectrophotometer was built from 'spare' parts. This apparatus consisted of a Beckmann D.U. monochromator with an IP28 photomultiplier in place of the conventional photocell. The nebulising system consisted of a metal Hilger nebuliser which was fitted into an adapted Bunsen flask with a

'U tube' side arm which constituted a drain tube for the larger droplets from the nebuliser. The spray from the nebuliser was directed into the bottom of the stem of a Meker burner and propane was introduced into an adapted jet at the base of the burner. The uptake rate of the nebulising system was 1.3 ml/min of which 0.12 ml/min reached the flame. The limit of detection for cadmium was found to be 5×10^{-8}M. This demonstrates the essential simplicity of A.F.S.

Under these same conditions no mercury fluorescence (at the 100 p.p.m. level) could be observed when an Osram mercury vapour discharge lamp was used as a source. This was thought to be due to almost complete self-reversal of the mercury 2537 Å line over the complete absorption line profile. Mercury is quite volatile and at the working temperature of the lamp, the mercury pressure will exceed 1 atmosphere, thus giving severe self-reversal. Weak mercury fluorescence could be observed if a very strong blast of cooling air was directed through the base of the window in the outer glass envelope onto the mercury lamp in order to reduce the degree of self-reversal. It was concluded that the determination of mercury by A.F.S. using the above source was not feasible.

1.7 Atomic-Fluorescence using Continuous Sources

In A.F.S. the detector does not receive radiation directly from the source and the monochromator is only used to isolate the fluorescence wavelength of interest. Thus, continuous unreversed sources can be used without the need for additional instrumental modification, and such a source should permit rapid sequential elemental analyses.

(a) Xenon-Arc Lamp

Table 7 shows the limits of detection for 10 elements obtained with the Unicam SP900A in both air-propane and air-hydrogen flames with an a.c.-operated 150-Watt xenon-arc lamp as source under the usual conditions. The lamp was placed ca 15 cm from the flame and its radiation was focussed by a quartz lens to a point ca 1 cm behind the flame and ca 3 cm above the top of the burner.

TABLE 7

Atmospheric Fluorescence with a 150-W Xenon Arc Lamp

Element	Wave length (A)	Slit-width (mm)	Detection limit (p.p.m.) A.F.S.			Detection limit (p.p.m.)[c] using air-acetylene	
			Air-propane[a]	Air-hydrogen[a]	Oxy-hydrogen[b]	F.E.S.[d]	A.A.S.[e]
Zn	2139	2.0	0.6	0.6	0.6	-	0.04
Cd	2288	2.0	0.25	0.25	0.08	11	0.05
Co	2407	1.0	1.5	1.0	-	0.5	0.5
Fe	2483	0.8	5.0	5.0	-	0.4	0.5
Mn	2794	0.25	0.3	0.15	-	0.02	0.2
Pb	2833	0.3	20	10	-	12	1.0
Mg	2852	0.2	2.0	2.0	0.2	0.1	0.02
Cu	3248	0.2	1.0	0.4	0.35	0.1	0.15
Ag	3281	0.4	0.35	0.15	0.08	0.1	0.13
	3383	0.4	0.2	0.10	-	-	-
Tl	3776	0.1	1.0	0.5	0.55	0.2	5.0

a A.F.S. denotes atomic-fluorescence spectrophotometry

b Data from Winefordner et al.[29]

c Data from operating manual for SP900A (Unicam Instruments Ltd., Cambridge, England).

d F.E.S. denotes flame-emission

e A.A.S. denotes atomic-absorption.

Winefordner et al.[29] have described the use of a d.c.-operated 150-Watt xenon-arc lamp. These workers examined 13 elements with an oxy-hydrogen flame and a total consumption integral-burner. The use of this burner resulted in appreciable scattering of the source radiation. Ellis and Demers[47] have described the use of a 450-Watt xenon-arc lamp and compared the limits of detection of cobalt, magnesium, silver and zinc in the oxy-hydrogen and the hydrogen entrained air flame.

The fluorescence signals for cobalt, iron and manganese reported in Table 6 has not been reported previously. However, fluorescence signals were not obtained from aqueous solutions of aluminium, beryllium, tin(IV) and zirconium in the air-propane or the air-hydrogen flames under irradiation from the 150-Watt xenon-arc lamp. This is attributed to the fact that these elements only exist as free atoms to a very limited extent in these flames.

Table 7 also shows the limits of detection obtained with the same apparatus by F.E.S. and A.A.S. In view of the fact that the intensity of radiation from a 150-W xenon-arc lamp at any one wavelength in the U.V. region is very low, it is somewhat surprising to find such low limits of detection by A.F.S. These sensitivities are comparable with those obtained by Winefordner et al.[29] who used specially designed apparatus.

(b) Hydrogen Lamp

A rather inefficient 20 Watt hydrogen lamp from a Beckmann D.U. spectrophotometer was mounted in a similar position to the discharge lamps and weak fluorescence for cadmium and zinc was obtained. Considering the fact that the output from the lamp was reflected off a badly corroded mirror in the lamp housing, the use of a powerful hydrogen lamp as a source in A.F.S. would appear quite feasible.

CHAPTER II

THE PREPARATION AND OPERATION OF ELECTRODELESS DISCHARGE TUBES

2.1 Introduction

Hollow-cathode lamps have been used almost exclusively as spectral sources in A.A.S. since the introduction of the technique by Walsh.[5] Although they have served their purpose well, they possess a number of undesirable features. They only have a relatively short 'shelf-life', they are expensive, especially if a large number of elements are to be examined and they require a 'warm-up' period before use. Also, hollow-cathode lamps are difficult to produce for some elements, and for others the intensity is too low to give a sufficiently sensitive determination even in A.A.S., or a wide enough working range. The recent introduction of multicathode[48] and high-intensity lamps[38,49] overcomes some of these problems, but only at the expense of others; for example selective volatilisation of the more volatile elements from a multicathode lamp and the increased cost of high-intensity lamps. Lastly, the necessary equipment required to produce hollow-cathode

lamps means that the average user must rely largely on commercially available lamps.

The limited number of vapour discharge lamps limits their usefulness in A.F.S., as well as the fact that these lamps exhibit varying degrees of self-reversal.

For the purpose of A.F.S., intense sources are required because the analytical signal varies linearly with the source intensity at the wavelength of excitation. The intensity of a continuous source over an absorption line profile in the U.V. is very low, and it would require an extremely powerful continuous source to give comparable results to an intense line source, e.g. a line source can give 100 times the intensity emitted by a 150-W xenon-arc lamp over a given absorption line profile. The use of electrodeless discharge tubes (E.D.T.s) excited by microwaves, would seem to be an obvious solution to spectral source problems in both A.A.S. and A.F.S. They are known to emit very sharp and intense spectral lines, and they can be made with the minimum of equipment. The absence of electrodes leads to long life of an E.D.T. as no electrode burn-away can occur and there is no glass-electrode seal that can leak. Also contamination of the spectral output by the appearance of the electrode spectrum cannot occur.

2.2 Development of Electrodeless Discharge Tubes

The high frequency electrodeless discharge was discovered by Hittorf[50] in 1884. This was followed in 1891 when J. J. Thomson[51] published two papers entitled 'On the discharge of electricity through exhausted tubes without electrodes'. The spectra of many species were observed using a Wimshurst machine coupled to a coil of copper wire which surrounded an evacuated glass vessel. Jackson[52], in 1928, used an E.D.T. operated from a 10 Mc/sec oscillator to obtain the spectrum of caesium in order to study its hyperfine structure. Meggers et al.,[53-55] in 1948-50, described the preparation of an E.D.T. of mercury-198 and proposed it as a secondary wavelength standard, as there was no hyperfine structure owing to absence of nuclear spin and isotopic shifts. The wavelengths of the lines were quoted to 10^{-4} Å. More recently these lamps have been used to study the spectra of the lanthanides and the actinides and their isotopes[56-60] (as little as 0.1 µg of a given element was considered sufficient to produce an E.D.T.).[58] It can be seen that for radioactive elements and isotopes,[56-61] these sealed sources are much safer and more economical than the commonly employed d.c. arc. The advent of the laser caused a great deal of interest in E.D.T.'s for optical pumping studies.[62]

Radio frequency E.D.T.'s have been used as spectral sources for the alkali metals[63] and for excitation of atomic resonance fluorescence of the alkali metals.[64-65] Ham and Walsh[66] described 2450 Mc/sec powered sodium and mercury sources for use in Raman work. Microwave excited E.D.T.'s have been used to obtain continuous sources in the vacuum U.V. using argon, hydrogen, krypton and xenon as filler gases.[67-72] A microwave discharge can easily be operated at a low temperature and Vaughan[73] used a helium discharge cooled by liquid helium to obtain helium lines with an effective Doppler temperature of $10^{\circ}K$.

The preparation of metal E.D.T.'s has been described in many publications[53-61,63-66,74,75] but these sources were prepared primarily for spectral elucidation studies. Certain E.D.T's have also been proposed as spectroscopic standards where absolute cleanliness of preparation was essential.[53-55,76] However, up to the present time, there has been little work on the production of E.D.T. sources solely for use as sources in A.A.S. and A.F.S. Ivanov et al.[77,78] report the use of lamps with high frequency excitation for use as sources in A.A.S. and Goodfellow[45] has made some A.F.S. measurements using a continuous flow microwave system. This type of continuous flow system has also been proposed as

a spectroscopic source by Richards.[79] In addition Winefordner[15,16] has used some commercially available E.D.T's for fluorescence studies, with rather poor results for reasons already discussed (see 1.1). It would appear that only Dagnall, Thompson and West[80] have appreciated their real potential and have described the preparation of a large number of microwave excited electrodeless discharge tubes for use in both A.A.S. and A.F.S. (see later).

2.3 Basic Principles of Microwave Discharges

The excitation of a discharge by radio and microwave fields is very efficient, as these fields accelerate electrons over a confined region thus maintaining an emitting plasma without internal electrodes within the plasma. The electrodeless discharge is equivalent to a cold plasma owing to its non-isothermal nature.[81] This means that the effective temperature of the atoms and molecules is much less than that of the electrons. The theory of these discharges is rather complex[63] but a brief kinetic and thermodynamic description of low-pressure electrodeless discharges has been given.[81]

The frequency range mostly used has been from 10-3000 Mc/sec and a wide variety of power supplies and resonant cavities have been

described in the literature. Because of the difficulties associated with preparing two discharge tubes which give identical spectral characteristics, many of the conclusions which have been reached in the past concerning optimum preparative and excitation conditions are subject to question or modification. In general, however, microwave frequencies have been found to be more efficient than radio frequencies for converting electrical power to luminous power.[82,83] In addition, there is evidence[54,82] that the lifetime of the discharge tube is extended with increase in frequency of excitation. A recently published review[81] gives a concise account of the instrumentation required for both types of excitation.

The use of microwave frequencies (i.e. > 100 Mc/sec) for excitation is attractive not only for those reasons mentioned above, but also because of the availability of comparatively inexpensive medical diathermy units. These units supply a source of continuous microwave power at 2450 Mc/sec, usually up to ca 200 Watts, and they can be used with a wide range of different cavities and antennae. In addition, because of the thermally uniform nature of this type of discharge, the emitted radiation is comparatively free of self-reversal effects.

2.4 Preparation of Electrodeless Discharge Tubes

The discharge tubes were made from transparent quartz tubing (Jencons Limited) of 8 mm internal diameter and 1.1 mm wall thickness. (An internal diameter of 8 mm was found to be most suitable with the cavities employed.) The vacuum line used was very simple and consisted of a two-stage rotary pump, a cold-trap, a means of introducing argon from an argon cylinder, six B-10 outlets and a vacuostat (10^{-2} - 10 Torr), cf. Fig.X.

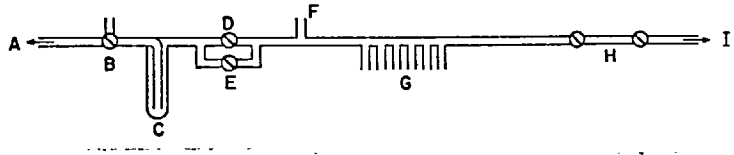

Fig.X Vacuum Line for Preparation of Electrodeless Discharge Tubes

A. Two-stage rotary pump B. Three-way tap C. Cold-trap

D. Two-way tap E. Capillary leak F. Vacuostat gauge

G. B-10 connections H. Two-way taps I. Argon cylinder.

A 15-20 cm length of quartz tubing was sealed at one end and a constriction made between 1 and 7 cm from this end to give a tube from 1 to 7 cm in length. The tubing was then connected to a B-10 glass socket with medium-pressure tubing and the whole was attached to one of the outlets on the vacuum line and pumped down to a pressure of approximately 0.1 mm Hg. Argon was then introduced into the system after which it was again pumped down to a similar pressure. The quartz tube was then heated to just below its melting point for about 5 min, during which time argon was again introduced into the system and pumped out.

This procedure was found to be adequate for degassing the quartz. Other workers[58,74] have degassed their apparatus for up to 8 hr, but this was normally for the purpose of obtaining very 'pure' spectra.

The tube was allowed to cool under vacuum and was then removed from the line. Between 5 and 20 mg of the required substance or substances were introduced into the tube which was then reconnected to the vacuum line.

The amount of substance used was found not to be critical, but too large a quantity sometimes caused plating-out during running.

The tube was evacuated as before, flushed out with argon and re-evacuated to a pressure of about O.1 mm Hg. Gentle heat, depending on the volatility of the substance, was then applied to the tube to drive off any moisture or occluded gases in the substances used. The system was flushed twice more with argon and finally a given pressure of argon, depending on the substances used, was introduced into the vacuum system and the constriction was sealed by means of an oxy-propane hand torch.

In some instances tubes were sealed under as low a pressure as could be achieved whilst being continuously pumped. The material placed in the tube must have a well defined vapour pressure of ca 1 mm at 200-400°C in order to achieve maximum stability and intensity when operated with the power unit and cavities described below. It was this property which determined whether the metal itself or the corresponding halide was employed. A table of the vapour pressures of the various elements and their halides is given in appendix (1). In general, the metal iodide was the most useful and it was normally formed in situ by addition of a few mg of iodine to the degassed metal such that the metal was present in a slight excess. This ensured complete formation of the required iodide. If an excess of iodine was present in the tube the metal spectrum was almost completely suppressed and a continuous

iodine spectrum was observed. By such techniques over 300 tubes have been prepared for over 30 elements, viz. Ag, Al, As, Bi, Co, Cr, Cu, Fe, Ga, Ge, In, Mo, Ni, Pb, Sb, Sn, Te, Ti, Tl (as metal plus iodine) and A, Br, Cd, Cl, H, He, Hg, I, Ne, N, O, P, S, Se, Xe, Zn (as the element alone).

It has been found that the chloride[84] is sometimes a more satisfactory salt than the iodide for certain elements with unstable iodides. The chloride is normally prepared by heating a small amount of the pure metal in a stream of chlorine gas. The salt is then introduced into the tube, together with a small amount of free metal in the normal way, e.g. gold and platinum.[84] The bromide has been found to be unsatisfactory mainly owing to the difficulties associated with handling and obtaining pure bromine.

Sometimes the addition of a few mg of mercury to the metal or metal iodide has been found useful. The mercury has been used as both a carrier of the initial discharge in the absence of argon and as a cleaning up agent, e.g. copper,[85] tellurium.[80] In this case care must be taken not to allow the discharge to become too hot, otherwise the mercury vapour pressure will reach such a level that only an arc type of discharge, confined to a small area of the tube, will be obtained. The size of the tube used was largely dependent on the vapour pressure

of the material used and the cavity employed. In general, for a very volatile element or compound (e.g. mercury and iodine) a rather long tube cooled by a stream of air at the lower end was found to be the optimum arrangement, whilst for an involatile substance (e.g. cadmium and zinc) efficient thermostating of the tube at the necessary high running temperature was essential.

It is not possible to give a completely uniform preparative scheme, because procedures vary from one element to another, but the preparation of a selenium tube (see Chapter 3) is general for elements and the preparation of a tellurium tube is general for metal plus iodine tubes. Normally several tubes for each element were prepared with varying lengths and argon fill pressures to establish the optimum conditions for tube preparation. If three or four tubes were prepared under exactly similar conditions (i.e. length and argon fill pressure) then they could all be guaranteed to give the required spectral output, but their overall intensities might differ somewhat.

2.5 Operation of Electrodeless Discharge Tubes

Excitation of the tubes was achieved with a 'Microtron 200' high-frequency generator in conjunction with two resonant cavities

(Electro-Medical Supplies Limited, London, W.1.). The output frequency was 2450 $\pm$ 25 Mc/sec (12.5 cm) at a power from O-25 Watts and from O-200 Watts in two ranges. A reflected power meter could be used to facilitate tuning the cavity and to ensure that the level of reflected power was not sufficient to damage the magnetron. Provided that powers not greater than ca 75 Watts were used there was little possibility of damage being caused and visual tuning to the maximum tube intensity was quite satisfactory. Initiation of the discharge, which relies on the production of free electrons, was achieved with a simple Tesla coil vacuum tester.

Two different cavities were used with the 'Microtron 200', the 210L and the 214L. The 214L cavity (Fig.XI) was the most efficient and had external dimensions of approximately 2.5 cm diameter and 6 cm length, with variable coupling at right angles to the longitudinal axis of the cavity. The coaxial input connection was integral with the cooling air inlets and the main tuning probe was in line with the axis of the cavity. The end cap of this cavity was completely removed in order to view the tube.

The 210L cavity (Fig.XII) was the least efficient (i.e. power was reflected back to the magnetron) but had the advantage of not

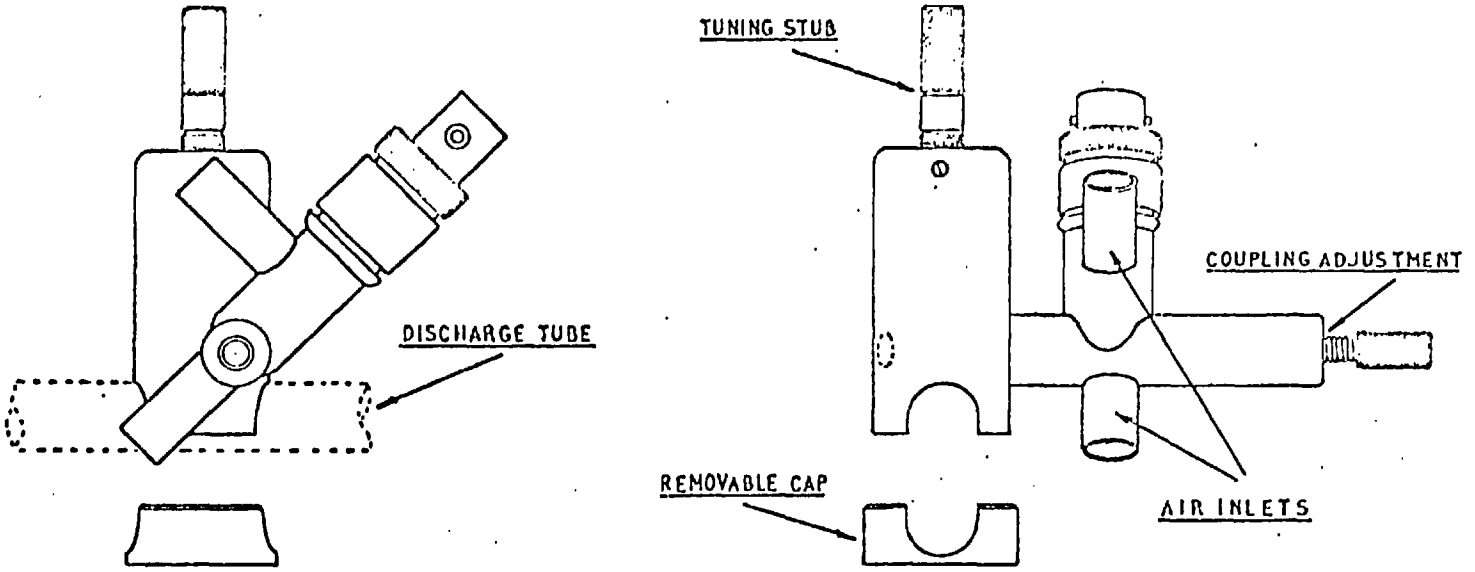

GAS DISCHARGE CAVITY No.214L

FIG.XI.

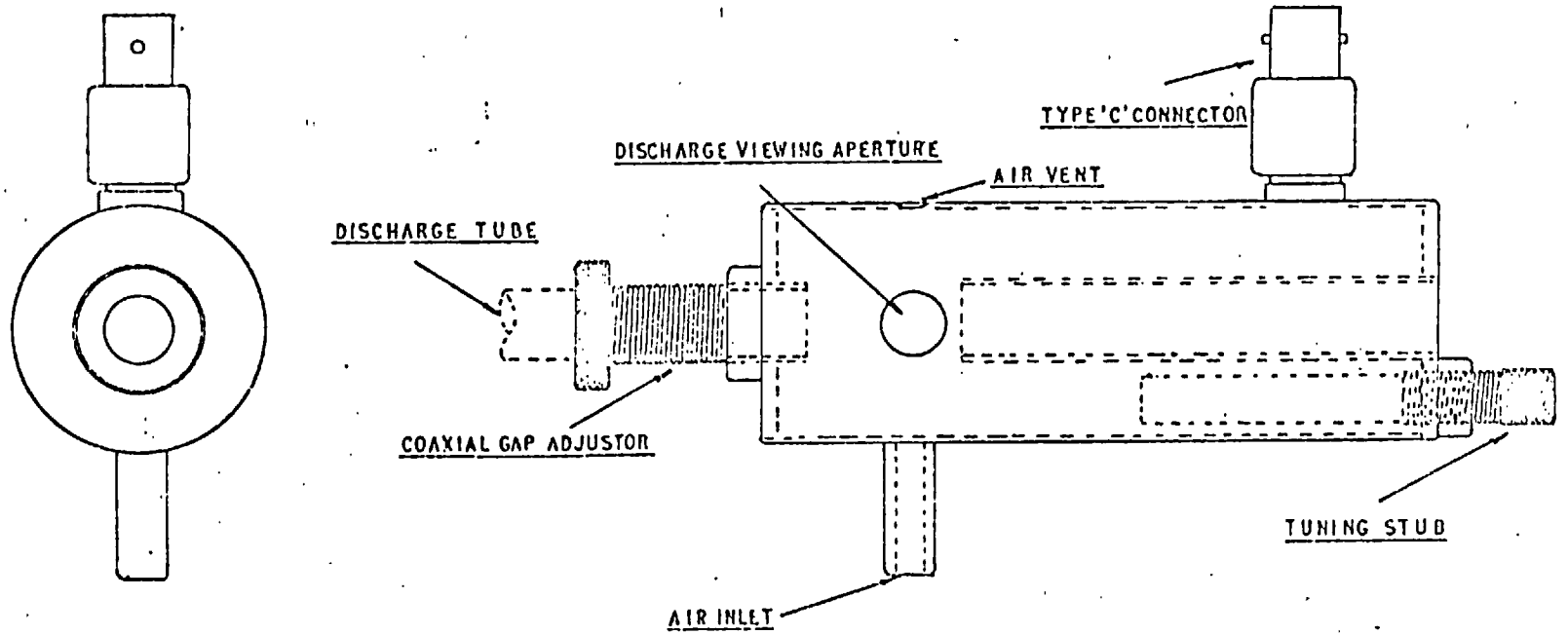

GAS DISCHARGE CAVITY (No.210L.)

FIG XII.

requiring tuning, although such means existed. The cavity was cylindrical in shape (ca 5 cm diameter and 13 cm length), had an adjustable re-entrant gap, coaxial with the discharge tube, and a tuning probe off-set and parallel to the discharge tube. The cavity could be air cooled and possessed adequate viewing apertures either at right angles or in line with the discharge tube which was completely enclosed. This cavity tended to thermostat the tube and was found to be particularly effective for relatively involatile substances (e.g. cadmium and zinc).

In general it was found that the 214L cavity gave optimum results when a low argon fill pressure was used (i.e. less than ca 3 mm) whilst the 210L cavity gave optimum results when either a high argon fill pressure (i.e. ca 10 mm) or a relatively volatile substance (i.e. TiI_4) was used. If whilst using the 214L cavity the pressure in the operating tube was gradually increased the discharge would shrink and finally only occupy a very small part of the tube in the centre of the cavity. This effect was not observed with the 210L cavity, and the discharge would normally fill the tube. This difference in behaviour was attributed to a high density of microwave radiation in the centre of the 2.5 cm diameter cavity of the 214L cavity which excited the discharge which was in turn transferred by excited atoms and electrons to the ends of the tube. This

transfer over the length of the tube would be more efficient at low pressures as the quenching collision frequency would be less at low pressures than at high pressures. The 210L cavity was thought to give an even distribution of microwaves over the whole tube length, thus the length of the discharge is independent of the fill pressure. The more efficient 214L cavity was used in all further studies, unless otherwise stated.

2.6 Spectral Characteristics of Electrodeless Discharge Tubes

All tubes required a running-in period when first prepared of up to ca 2 hours at operating powers of ca 30 watts before use. This was especially important when the metal plus iodine method of preparation was used. During this time, when the discharge characteristics could alter radically, the desired halide salt was formed in situ and the tubes reached equilibrium conditions. Once the tube reached equilibrium a warm-up period of five minutes was usually sufficient subsequently. After the running-in period there should be no observable background from the argon carrier gas or visible continuum from the iodine introduced. In all instances, however, the 2061.63 Å iodine spectral line (assuming iodine was used) was observed. Sometimes the major mercury lines were

observed; these arose from the mercury in the vacuum line. If a continuous type of spectrum was observed this was usually due to an excess of iodine (over that required to form the metal iodide) which was clearly visible if the tube was gently warmed.

The stability of the discharges was found to be comparable with that of normal hollow-cathode lamps when measured under similar conditions (e.g. $\pm$ 1% variation in response). In order to ensure good stability it is imperative that the tube be protected from draughts, and if possible cooled by a constant draught of air. An estimated life-time of the tubes cannot be given. None of the tubes, to date, have failed when they have been prepared and operated under normal conditions. Many of the tubes were prepared more than two years ago and have been used both intermittently and for long periods during the meantime. In all instances the spectral characteristics and operating conditions have not changed either.

2.7 The Effect of Pressure of Various Gases on a Microwave Discharge

If the argon pressure in a microwave discharge of argon was gradually increased (using a 214L cavity), a decrease in the length and intensity of the discharge was observed as the argon pressure was increased

from 0.02-100 mm. At pressures 100 mm - 2 Atm an arc-like discharge was obtained. It would appear that the process responsible for the production of the discharge must alter at argon pressures greater than ca 100 mm. A similar effect was observed for helium and neon. When a poly-atomic gas was used the discharge would decrease in length and intensity as the pressure was increased from 0.02 mm and would finally be extinguished. No arc-like discharge could be obtained. If even a slight trace of nitrogen or hydrogen was added to an argon discharge at atmospheric pressure the arc-like discharge was immediately extinguished. Table 8 shows the 'extinguishing pressures' of various gases at 15 and 40 Watts using the 214L cavity.

This difference in behaviour between monatomic and polyatomic gases is difficult to explain. Free electrons and ions are necessary to maintain a microwave discharge, but the ionisation potentials of the monatomic inert gases are higher than those of polyatomic gases. One possible explanation is that the mean free path of electrons and ions is very small in a polyatomic gas at the microwave powers used ($\leq$ 200 Watts) and the electrons and ions initially produced by a Tesla do not get accelerated sufficiently in the mean free path to ionise another

molecule on impact. High power microwave discharges (2 K.Watts) have been maintained in nitrogen.[86]

TABLE 8

Extinguishing Pressures of Various Gases in the 214L Cavity

Gas	Extinguishing Pressure* 15 Watts	40 Watts
Argon	1.5 atm	3 atm
Nitrogen	30 mm	80 mm
Oxygen	27	60
Air	25	70
Hydrogen	32	90
Propane	20	50
Sulphur Dioxide	20	-
Carbon Monoxide	15	35

* Average of 3 measurements.

FIG. XIII.

Elements for which Discharge Tubes have been prepared

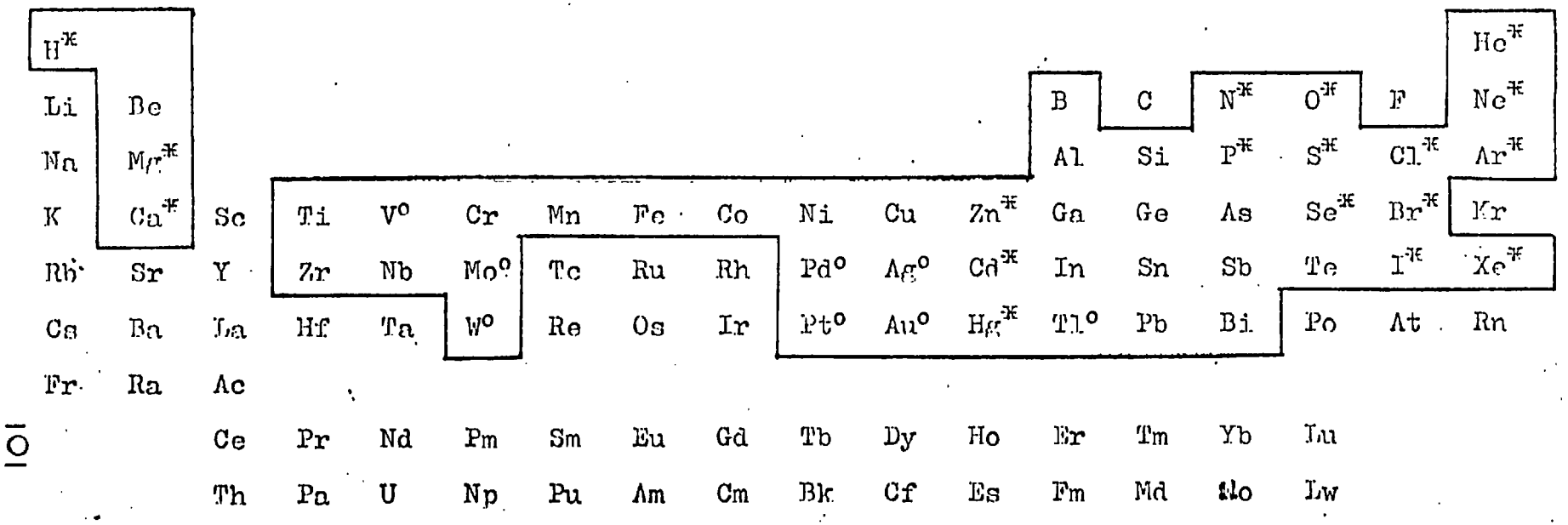

* Element.

° Element + chlorine.

□ Element + iodine.

2.8 Preparative Range

Figure XIII shows the number of elements for which satisfactory E.D.T[s]s have been prepared by the Analytical Research Department at Imperial College. The emphasis has mainly been upon those elements for which normal hollow-cathode lamps are unsatisfactory, either because of certain preparative difficulties e.g. iodine, low intensity emission e.g. arsenic and selenium, presence of interfering non-resonance lines e.g. antimony or self-reversal effects e.g. mercury. It would be reasonable to suppose that the methods of preparation could be applied to nearly all the remaining elements. The main foreseeable difficulties are the low vapour pressure of some elements and the availability of suitable compounds of these elements (e.g. the rare earths[58]), but this could be overcome by auxiliary tube heaters.

2.9 Conclusions

The application of microwave excited E.D.T[s]s in both A.F.S. and A.A.S. is at present only in its early stages and many of the experimental parameters involved in their preparation and operation have not been fully examined. However, from the results obtained it would appear there can be little doubt that they will occupy an increasingly important position in the future.

The advantages of the E.D.T's as spectral line sources in A.A.S. and A.F.S. may be summarised as follows:

1. They are simple in design, construction and operation and are inexpensive to prepare.
2. They can be prepared for nearly all elements and only require small amounts of materials.
3. They are very intense at the principal resonance lines and they are as stable as conventional hollow-cathode lamps when prepared and operated under optimised conditions.
4. They require only a relatively short warm-up period and they do not exhibit any carrier gas background; only the principal lines in the atomic spectrum are normally observed.
5. The spectral lines are very sharp, and under normal running conditions are virtually free from self-reversal.
6. Multi-element lamps can be prepared, although the single element lamps are readily interchangeable.
7. The lamps appear to have a very long running and shelf-life.

CHAPTER III

THE ATOMIC FLUORESCENCE SPECTROSCOPIC DETERMINATION OF SELENIUM AND TELLURIUM[87]

3.1 Introduction

In comparison with that for other elements, the volume of literature available on the flame-spectrophotometric determination of selenium and tellurium is relatively small. Rann and Hambly have determined selenium by atomic-absorption spectroscopy, using a hollow-cathode lamp and an electrodeless discharge tube operated at 15 Mc/s.[88] The limit of detection at 1961 Å was 1 ppm. A determination using a continuous source[89] and a medium quartz spectrograph gave limits of detection for selenium (2040 Å) and tellurium (2143 Å) of 5 and 0.5 ppm respectively.

More recently Chakrabarti[90] has determined tellurium by atomic-absorption spectroscopy using a hollow-cathode lamp (passing the light through the flame 5 times) and obtained a limit of detection at 2143 Å of 0.36 ppm. In addition to these Dean[91] has described a flame-emission method for tellurium, using an oxy-acetylene flame. The tellurium(IV)-diethyldithiocarbamate complex was extracted into carbon tetrachloride, evaporated to dryness and redissolved in methyl isobutyl

ketone to enhance the flame temperature. The limit of detection was 2 ppm.

This chapter describes the determination of selenium and tellurium by atomic-fluorescence and atomic-absorption spectroscopy under conditions which do not require a hot flame, a high-resolution monochromator or hollow-cathode lamps. The oxidation state of the selenium and tellurium is unimportant and a preliminary extraction into organic solvents is unnecessary.

3.2 Experimental

Apparatus

The apparatus used consisted of a Unicam SP900A atomic-absorption/flame-emission spectrophotometer coupled to a Honeywell Brown 0-10 mv recorder. The description of its use for atomic fluorescence measurements has been given in Chapter I. Electrodeless discharge tubes were prepared and used as sources and the discharge was maintained, with a 'Microton 200' magnetron and a model 214L discharge cavity (see Chapter II). The "emission" mode of operation of the Unicam SP900A was used for all fluorescence measurements because this pulses the fluorescence emission at 100 c/s in phase with the a.c. amplifier

of the SP9OOA. This, however, means that the detector will pick up the flame background at the fluorescence emission wavelength. For this reason it would have been better to modulate the light from the source mechanically or electronically before it entered the flame and to use the SP9OOA in its 'absorption' mode so that continuous radiation from the flame would not be recorded (the A.F.S. results obtained in Chapter I were obtained under such conditions because the a.c. discharge lamps were chopped at 1OO c/s). It was not possible to modulate the output from electrodeless discharge tubes for use with the SP9OOA and it is thought that the limits of detection by A.F.S. could be lowered by an order of magnitude if the source were modulated.

Reagents

a) Selenium solution (125O) ppm). Analytical-reagent grade selenium metal (1.25O g) was dissolved in 2O ml of a mixture of concentrated nitric and hydrochloric acids (1 + 1) and diluted to about 5OO ml with distilled water. A slight excess of ammonia was then added and the whole was diluted to 1 l.

b) Tellurium solution (125O ppm). Made up with analytical-reagent grade tellurium metal as for the selenium solution.

Both solutions were then diluted as required.

Results

3.3 Discharge Tube Parameters

a) Selenium

A range of selenium tubes was made by introducing ca 10 mg of analytical-grade selenium powder into the tubes and sealing off under various pressures of argon between 0.1 and 5.0 Torr. The selenium lines appeared to increase with decreasing argon pressure. The most intense selenium source used in this study was made by sealing whilst pumping, giving a final argon pressure of ca 0.1 Torr. If the pressure was higher than 1 Torr the selenium lines were relatively weak and often the light blue selenium discharge would change over to a purple argon discharge with considerable reduction in the selenium line intensity.

Selenium tubes were made ranging from ca 1.5 to 5.0 cm in length. The optimum length of tube for the cavity appears to be 3.5 cm. The smaller tubes were completely enclosed by the cavity and these developed hot-spots (selenium is a semiconductor) with the result that the output was neither very stable nor intense. The larger tubes did not reach a high enough running temperature to give a sufficient vapour pressure of selenium. The 3.5-cm tube was operated in such a manner

that 1 cm of the tube protruded above the cavity and the selenium was sublimed to the top of the tube before operation, by heating gently with a Bunsen burner.

The optimum tube was found to have an argon pressure of ca 0.1 Torr and was 3.5 cm long. The tubes required slight warming before initiation with the Tesla coil vacuum tester, and were initially 'run in' for about 2 hours. It is essential that all discharge tubes are 'run in' because their characteristics can alter radically during the first hour of life. The tubes required careful tuning and had to be moderately cooled to obtain a steady intense output. After continuous running of the optimum selenium tube at 40 Watts for over 2 hours, its stability was comparable with that of a hollow-cathode lamp, once the tuning and the cooling rate had been carefully adjusted.

b) Tellurium

Tubes containing only tellurium metal were found to be unsatisfactory because they had to be run at high energies (ca 75 Watts) and at relatively high temperatures owing to the involatility of tellurium (see appendix (1)). This resulted in a rather unstable output with eventual darkening of the quartz envelope.

A tube containing a trace of mercury plus tellurium gave a stable output, but of low intensity. However, a tube containing tellurium and iodine* (about 5 mg of each) which was sealed ander continuous pumping (final argon pressure ca 0.1 Torr) was found to be optimum. The argon pressure was not very critical and any argon pressure between 0.1 and 2 Torr could be used. In general it was fould that for relatively involatile substances, a low argon pressure was optimum when using the 214L cavity. The optimum tube length was found to be about 4 cm and the tube was best operated with about 1.5 cm protruding above the top of the cavity. This tube was run with slight cooling and gave a stable intense output at 30 W after an initial running-in period of 1 hour. The running-in period was necessary to allow complete reaction of the tellurium and iodine. No information regarding the life of the tubes is at present available, but both the selenium and tellurium tubes have shown no deterioration in output or stability after ca 50 hours of intermittent running.

---

*Tubes containing selenium and iodine would only give an iodine spectrum. This was thought to be due to the instability of selenium-iodine species.

3.4 Preparation of Optimum Discharge Tubes

a) Selenium

Quartz tubes ca 3.5 cm long and 8 mm i.d. were prepared as described in Chapter III. The empty tubes were degassed by heating to bright red heat by an oxy-propane blow torch and subjected to evacuation for 10 minutes. During this time, argon was periodically flushed through the system to sweep away any impurities desorbed from the walls of the tube. After cooling under vacuum, the tubes were removed from the vacuum line and a small amount (ca 10 mg) of analytical-grade selenium was added. The tubes were evacuated and the selenium was very gently heated with a microburner and periodically flushed with argon to remove any occluded gas or moisture in the selenium. After cooling, the tubes were finally sealed whilst pumping, giving an argon pressure of ca 0.1 Torr.

b) Tellurium

Quartz tubes ca 4 cm long and 8 mm in internal diameter were degassed as for selenium, then ca 5 mg of tellurium metal were added to each. The tubes were evacuated and the tellurium strongly heated with a bunsen burner and then flushed with argon to remove any occluded gases, volatile impurities or moisture in the tellurium (tellurium is very

involatile, see Appendix (1)). After cooling, ca 5 mg of iodine were introduced and the tubes were evacuated and periodically flushed with argon for about 5 minutes to remove any moisture liberated from the added iodine (heat cannot be used because of the volatility of iodine). After cooling, the tubes were finally sealed whilst pumping, giving an argon pressure of ca O.1 Torr. An excess of tellurium over that required for the formation of tellurium (II) iodide was maintained to eliminate free iodine, the intense spectrum of which would otherwise have been emitted. It is essential that an excess of metal is present in any metal-iodine tube for this reason.

3.5 Spectral Characteristics of Discharge Tubes

a) Selenium

All the expected selenium lines were observed during its operation and all of them were very sharp. The relative intensities of the ground state and intercombination lines observed, expressed as the ratio of the line intensity to that of the 1961 Å line, are shown in Table 9.

These intensities can only be taken as an approximate guide because the values given are slightly dependent on the scanning rate of the Unicam SP9OOA recorder unit. The relative intensity of the 1961 Å

line increases with cooling. This suggests that, if the tube were run at too high a temperature or at energies > 40 W, self-reversal of the resonance line might occur. On the other hand, when the tube was cooled too rapidly the discharge was extinguished. Uncooled tubes were not examined because the cavity tended to overheat. The apparently low intensity of the 1961 Å line is due to the characteristics of the 9601B photomultiplier used. This photomultiplier has a Corning U.V. glass window which has a very low transmission below 2000 Å.

TABLE 9

Emission Lines from Selenium Source

Line, Å		Relative intensity	
		Slight cooling	Moderate cooling
1961	(R)	1	1
2040	(R)	5	2.5
2063	(R)	12	2
2075	(I)	3	5.0
2165	(I)	8	2.3

R ≡ Resonance; I ≡ Intercombination

This illustrates one advantage of atomic-fluorescence measurements over atomic-absorption. Although the photomultiplier is very insensitive to the exciting radiation at 1961 Å or to emission at the same line, measurement may be made of the fluorescence at the 2040 Å "direct" line where a much increased response is given. The selenium tube also emitted the mercury spectrum because of the diffusion of mercury from the vacuostat gauge throughout the vacuum system. Although it was found virtually impossible to eliminate this contamination completely, no resulting interference was observed.

b) Tellurium

All the expected tellurium lines were observed and, as with the selenium tube, were very sharp. Table IO shows the intensities of the tellurium resonance and intercombination lines observed, relative to the intensity of the 2143 Å line. The iodine spectrum was also present in the form of a continuum with an intense line at 2062 Å.

As with selenium, the relative intensities are somewhat dependent on the rate of recorder scanning and on the cooling rate. An increase in the operating power did not increase the line intensity appreciably, but merely led to instability.

TABLE 10

Emission Lines from Tellurium Source

Line, Å		Relative intensity (slight cooling)
2143	(R)	1
2383	(R)	2.5
2386	(R)	4
2259	(I)	10
2531	(I)	1.3

3.6 Fluorescence Characteristics of Selenium and Tellurium

The resonance lines of sulphur, selenium, tellurium and polonium[92] emanate from a $^3P_2$ ground state which is part of the triplet $^3P_2$, $^3P_1$, $^3P_0$ (see Fig.XIV). The separation of these states is very small (see Table 11) and in tellurium and polonium the ^3P terms are partially inverted.

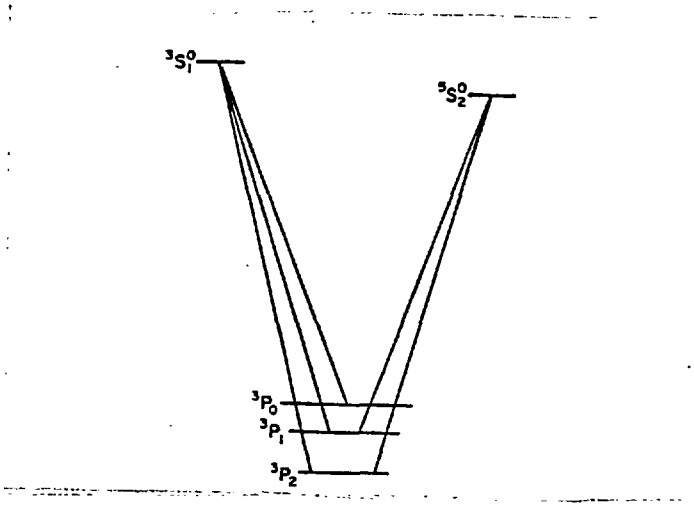

Fig. XIV Simplified Grotian diagram for S, Se, Te.

TABLE 11

Separation of Ground States

Element	Interval, cm^{-1}	
	$^3P_2 - {}^3P_1$	$^3P_1 - {}^3P_0$
S	398	174
Se	1989	545
Te	4751	-44
Po	16831	-9317

(1 eV = 8066 cm^{-1})

TABLE 12

Spectral Resonance Lines

Element	Transition, Å $^3P_2 \rightarrow {}^3S_1^O$	$^3P_1 \rightarrow {}^3S_1^O$	$^3P_O \rightarrow {}^3S_1^O$
S	1807	1820	1826
Se	1961	2040	2063
Te	2143	2386	2383
Po	2450	4170	3003

Table 12 shows the spectral resonance lines which can be used for fluorescence measurements. It was found that the intercombination lines ($^3P_2 \rightarrow {}^5S_2^O$ and $^3P_1 \rightarrow {}^5S_2^O$) gave no appreciable absorption or fluorescence for any of these elements (cf. zinc, cadmium and mercury).

The resonance lines for sulphur lie in the vacuum-ultraviolet outside the range of the monochromator of the instrument used. For this reason it was not possible to make any fluorescence or absorption measurements for sulphur in the present study. With selenium, the 1961 Å and 2040 Å lines both absorb strongly whilst the 2063 Å line absorbs only

very weakly. The 1961 Å line emanating from the ground state absorbs about 5 times as strongly as the line emanating from the $^3P_1$ state which lies O.25 eV above the ground state. For tellurium the resonance line at 2143 Å absorbs almost 10 times as strongly as the lines at 2386 and 2383 Å. The ^3P_O and $^3P_1$ states lie O.6 eV above the $^3P_2$ ground state.

Atomic-fluorescence was observed for selenium and tellurium for all three lines emanating from the $^3S_1$ state. However only very slight fluorescence was obtained for the intercombination lines for tellurium and none at all for those of selenium. The fluorescence for the transition from the $^3S_1$ excited state to the $^3P_{O,1,}$ states is probably due to direct-line fluorescence; that is, excitation with the lines at 1961 and 2143 Å for selenium and tellurium respectively, with emission of selenium lines at 2040 and 2063 Å and of tellurium lines at 2386 and 2383 Å. Resonance fluorescence (excitation and emission wavelengths the same) is a possibility since some of the atoms could be thermally excited to the metastable $^3P_1$ and ^3P_O states. However, as the resonance lines for selenium and tellurium respectively absorb 5 and 10 times as strongly as the next highest states, and the energy gaps between the ground states and the next highest states of selenium and tellurium are O.25 and O.60 eV respectively, direct-line fluorescence seems much more probable. This aspect was not examined

further because a monochromomator placed in front of the source would give a signal too weak to measure.

3.7 Atomic Fluorescence Measurements

An air-propane flame was used because of its low background emission and the discharge cavity wos placed ca 8 cm from the flome ot right-angles to the optical axis of the onalysing monochromator. Slit-widths ronging from O.5 to 2.O mm were used. The excitation sources were not chopped and so any flome background had to be subtracted arithmetically from the reodings obtoined. A slightly fuel-rich flame was used and the distonce from the top of the propane emission-burner head to the centre of the analysing monochromomator slit was co 3 cm. The atomic-fluorescence intensity was virtually independent of flame composition and position of measurement in the flame for both selenium and tellurium.

a) Selenium

The discharge tube was operated at 4O W with moderate cooling and fluorescence measurements were taken at the resonance lines (1961, 2O4O and 2O63 Å) ond the intercombination lines (2O75 and 2165 Å), with a 12.5 ppm solution of selenium. The recorder readings due to the fluorescence emission are shown in Table 13 together with the relative line intensities.

TABLE 13

Fluorescence Intensities for Selenium

Wavelength, Å	Recorder reading	Relative line intensity (source)
1961	42	1
2040	63	5
2063	33	12
2075	1	3
2165	0	8

The 1961 Å resonance line is the strongest fluorescing line, but because the photomultiplier used (EMI 9601B) is very insensitive below about 2000 Å, the 2040 Å line gives the higher readings. The latter wavelength was used for further measurements.

Linear calibration curves were obtained over the range 0.25-125 ppm of selenium, with a slit-width of $\leqslant$ 2.0 mm. More concentrated solutions were not examined. The limit of detection (signal to noise ratio unity) was 0.15 ppm and the limit of measurement was considered to be ca 0.30 ppm.

b) Tellurium

The discharge tube was run at 30 W with very slight cooling and measurements were taken (Table 14) for a 12.5 ppm solution of tellurium.

TABLE 14

Fluorescence Intensities for Tellurium.

Wavelength, Å	Recorder reading	Relative line intensity (source)
2143	44	1
2383)	60	2.5
2386)		4
2259	2.5	10
2531	0	1.3

With analysing-monochromator slit-widths ranging from 0.5 to 2.00 mm, the 2383 and 2386 Å lines could not be resolved. The relative intensity readings were taken with a slit-width of ca 0.005 mm.

The resonance line at 2143 Å was selected for further measurements because the flame background at this wavelength was much less than that

at 2383 and 2386 Å. With a photomultiplier more sensitive in the ultraviolet, the 2143 Å line would probably give increased sensitivity.

Linear calibration curves were obtained with a slit-width of $\leq$ 2.0 mm over the concentration range 0.12-125 ppm of tellurium. Again, more concentrated solutions were not examined. The limit of detection was about 0.05 ppm and the limit of determination was 0.10 ppm.

Interferences

The effect of a 100-fold molar excess of the following selected range of cations was investigated on both selenium and tellurium: Ag, Al, Co(II), Cu(II), Fe(II), Hg(II), Mg, Na, NH_4, Pb, Sb(III) and Zn. In addition, the effect of a similar excess of selenium on tellurium and vice versa was examined. All solutions were acidified with 2M nitric acid to prevent any precipitation. Sodium gave about a 20% increase in the fluorescence signal and this was found to be because of intense light emission from the flame and a slight light-leak in the monochromator. This increased signal was given at all wavelengths. All other elements produced signal differences of less than 5%.

3.8 Atomic-Absorption Measurements

The "absorption" mode of operation was now used and the electrodeless discharge tubes were placed in approximately the same position as hollow-cathode lamps would be in for absorption studies. The source was thus chopped at 100 c/s. A 7 cm long air-propane flame was used.

a) Selenium

The discharge tube was run at 30 W with moderate cooling and placed so that it was slightly out of focus at the entrance slit, in order to reduce the amount of light passing through the flame.

The 1961 Å resonance line absorbed most strongly, the 2040 Å line absorbed about a fifth as much, and the 2063 Å line absorbed still less. The intercombination lines at 2075 and 2164 Å did not absorb at all. The limit of detection (for 1% absorbance) was 1 ppm, using the 1961 Å line. Linear calibration curves were obtained from 5-100 ppm of selenium. The range could be extended beyond this if desired.

Moderate cooling of the discharge tube was found to be essential as the absorbance decreased by a factor of about 3 if the tube was not cooled, and also the calibration graph curved towards the concentration axis. Over-cooling gave a very unstable tube and the discharge tended to be extinguished.

The absorption at the 1961 Å line was similar in air-propane and air-acetylene flames. Both of these flames absorbed ca 70% of the radiation at 1961 Å. Atomic absorption occurs more strongly at 2040 Å in air-acetylene than in air-propane flames because this line does not emanate from the ground state, but a state 0.25 eV above it.

b) Tellurium

The discharge tube was run at 20 W with very slight cooling and was arranged in the same way as the selenium discharge tube.

The 2143 Å resonance line absorbed most strongly and the 2383 and 2386 Å lines absorbed only about a tenth os much. The intercombination line at 2259 Å absorbed only slightly and the other intercombination line at 2531 Å did not absorb at all.

The limit of detection (for 1% absorbance) was 1 ppm with the 2143 Å line, and linear calibration curves were obtained over the range 5-100 ppm.

3.9 Discussion

These studies show the advantages to be obtained by measuring the fluorescence emission instead of the absorption. Table 15 compares the sensitivities of the two methods, with the same instrument and the same spectral forces for selenium and tellurium.

TABLE 15

Sensitivities for Se and Te by Atomic-fluorescence and Atomic-absorption Spectroscopy

	AFS		AAS	
	Se	Te	Se	Te
Limit of determination, ppm	0.30	0.10	5	5
Limit of detection, ppm	0.15	0.05	1	1

The sensitivities of these atomic-fluorescence methods are about 10 times greater than those of the atomic-absorption methods. Improvements in the detector response would have produced a still greater increase in sensitivity e.g., a further factor of 10 is quite possible.

The examination of selected extraneous ions in the atomic-fluorescence studies also shows that the method is at least as free from inter-element effects as atomic-absorption spectroscopy.

The limits of detection in this work were calculated for a signal:noise ratio of 1:1 ; for a complete discussion on the calculation of limits of detection in A.F.S. the reader is referred to the work of Winefordner et al.[92A]

CHAPTER IV

THE FLUORESCENCE CHARACTERISTICS AND DETERMINATION OF ANTIMONY[97]

4.1 Introduction

The determination of antimony by flame emission methods presents numerous problems. The ground state atoms of antimony are difficult to excite by thermal means and the only emission studies to date[93,94] have been carried out by using the inner cone of an oxy-acetylene flame in conjunction with nebulized organic solvents. The principal resonance lines at 2068, 2176 and 2311 Å lie in the far ultraviolet and give rise to low sensitivities because of the poor response of most photomultipliers in this region. In addition, antimony hollow-cathode lamps give a low radiation output at the resonance wavelengths. In spite of this, successful atomic-absorption measurements have been made by Gatehouse and Willis, using a hollow-cathode lamp at 2311 Å.[95] The 2176 Å resonance line gave the strongest absorption, but there was less noise at the 2311 Å resonance line because of its higher intensity as detected by the photomultiplier. The limit of detection was given as 1.5 ppm. Atomic-absorption studies have also been made with a continuous source[89] and

photographic recording of line intensities. The limit of detection of this method was estimated to be 0.5 ppm.

More recently Mostyn and Cunningham[96] have determined antimony using a hollow-cathode lamp with a limit of detection at 2176 Å of 1.4 ppm.

4.2 Experimental

Apparatus

The apparatus has previously been described (see 3.2).

Reagents

Antimony solution, 10^{-3} M. 0.3249 g of potassium antimony tartrate was dissolved in distilled water and diluted to 1 litre; 1 ml ≡ 121.8 ug of Antimony.

RESULTS

4.3 Discharge Tube Parameters

Tubes containing only antimony metal were found to be unsatisfactory because they had to be run at high energies (ca 80 Watts) and at relatively high temperatures owing to the involatility of antimony (see appendix 1). This resulted in a rather unstable output with eventual darkening of the quartz envelope. In general most successful tubes were operated between 25 and 40 Watts. A tube containing ca 10 mg of antimony and iodine

was found to be optimum. The argon pressure was not critical, any pressure between 0.5 and 5 Torr being considered satisfactory. The optimum tube length was ca 3.5 cm. The tube was run with slight cooling and gave a stable intense output at 30 Watts after an initial running in period of ca 1 hour.

4.4 Preparation of Optimum Discharge Tubes

Quartz tubes 3.5 cm long and 8 mm in internal diameter were degassed as for selenium and tellurium (3.4), then ca 10 mg of electrolytic antimony were added to each. The tubes were evacuated and the antimony was heated until it just melted and then flushed with argon to remove any occluded gas, volatile impurities or moisture in the antimony. After cooling, ca 10 mg of iodine were introduced and the tubes were evacuated and periodically flushed with argon for about 5 minutes to remove any moisture liberated from the added iodine. The tubes were finally sealed with an argon pressure of ca 1.0 Torr.

4.5 Spectral Characteristics of Discharge Tubes

The ground state of the antimony atom[92] is $^4S_{1\frac{1}{2}}$ and a simplified Grotian diagram is shown in Fig.XV. All the lines shown in this diagram were observed as well as higher state lines which are accounted for by

Brode.[98] In addition, the 2062 Å iodine line was very prominent, but the continuum associated with tubes containing free iodine was absent.

The tube was run at 30 W and the resonant cavity was air-cooled by forced draught. Tuning was very critical and there were two modes of tuning . The first was obtained by screwing the larger of the two coupling probes fully into the cavity; the discharge obtained rapidly reverted to an argon discharge. The other was obtained by unscrewing the large probe about three complete turns. This gave an intense stable output. The variation in response was $\pm$ 1% over a period of 1 hr.

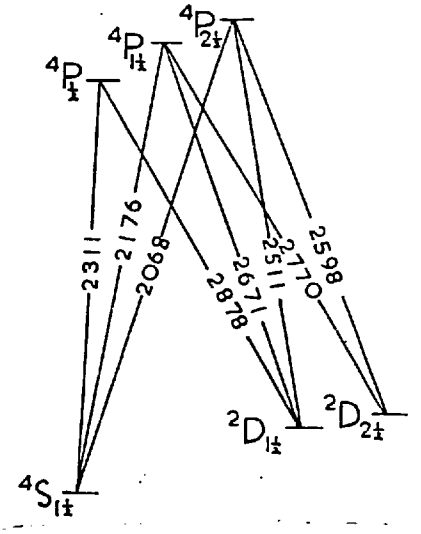

Fig.XV. Simplified Grotrian diagram for antimony.

Close to the 2176 Å resonance line there is a non-resonance line at 2179 Å which, according to Brode,[98] is slightly more intense in the spark than in the arc spectrum. The 2176 Å resonance line, however, is only an eighth as intense in the spark as in the arc spectrum. Both lines are equal in intensity in the spark spectrum and the photomultiplier response over such a small range in this region can be considered to be constant. Hence, from the relative intensities of these two lines at various operating power ratings and rates of cooling, the exact type of discharge can be evaluated.

It was found that with the microwave-excited source the ratio of the line intensities (2176:2179 Å) decreased with increasing power ratings. At 15 W the ratio was ca 3, whilst at 50 W the ratio was ca 0.7. The ratio increased rapidly with increased cooling, but the absolute line intensities decreased. At relatively high power ratings ($\geq$ 30 W), the change of intensity (I) with power (p) (i.e., dI/dp) fell to ca 0.3 for the resonance line, but was approximately unity for the non-resonance line. It would appear from this that at these higher operating powers self-reversal (and possibly self-absorption) occurs. The optimum power for operation was considered to be about 30 W for a tube containing an argon pressure of ca 1 Torr and about 35 W for a pressure of ca 5 Torr. The

argon lines were quite weak in intensity and the argon:antimony line intensity ratio decreased with increasing power ratings.

4.6 Fluorescence Characteristics of Antimony

A 10^{-3}M solution of antimony was nebulised into both air-acetylene and air-propane flames. Under optimum conditions both flames gave similar fluorescence signals, but because of its much lower background radiation the air-propane flame was selected for more detailed study (both background and fluorescence signals are recorded together under the conditions of measurements). The fluorescence readings shown in Table 16 were obtained under the optimum conditions. As can be seen the "forbidden" intercombination lines ($^4P \rightarrow {}^2D$ transitions) fluoresce relatively strongly.

TABLE 16

Atomic-fluorescence Measurements at 0.05 mm Slitwidth

Spectral line, Å	Transition	Relative fluorescence signal
2068	$^4S_{1\frac{1}{2}} \longrightarrow {}^4P_{2\frac{1}{2}}$	57
2176	$^4S_{1\frac{1}{2}} \longrightarrow {}^4P_{1\frac{1}{2}}$	80
2311	$^4S_{1\frac{1}{2}} \longrightarrow {}^4P_{\frac{1}{2}}$	108
2511	$^4P_{2\frac{1}{2}} \longrightarrow {}^2D_{1\frac{1}{2}}$	0
2598	$^4P_{2\frac{1}{2}} \longrightarrow {}^2D_{2\frac{1}{2}}$	52
2671	$^4P_{1\frac{1}{2}} \longrightarrow {}^2D_{1\frac{1}{2}}$	10
2770	$^4P_{1\frac{1}{2}} \longrightarrow {}^2D_{2\frac{1}{2}}$	25
2878	$^4P_{\frac{1}{2}} \longrightarrow {}^2D_{1\frac{1}{2}}$	35

This effect was not so marked in the previous study of selenium and tellurium, probably because with antimony the absorption process is by an

"allowed" line, but with selenium and tellurium both absorption and fluorescence are "forbidden". This type of fluorescence can be used with advantage to eliminate flame and particle light-scattering if it occurs, e.g., with a total-consumption aspirator-burner. If a filter which transmits radiation only below ca 2400 Å is placed between the source of excitation and the flame and fluorescence measurements are made at 2598, 2671, 2770, or 2878 Å, then light-scattering interference cannot occur.

The fluorescence intensity at the 2598.09 Å line ($^4P_{2\frac{1}{2}} \rightarrow {}^2D_{2\frac{1}{2}}$) is considerably greater than that at the 2671 Å ($^4P_{1\frac{1}{2}} \rightarrow {}^2D_{1\frac{1}{2}}$), 2770 Å ($^4P_{1\frac{1}{2}} \rightarrow {}^2D_{2\frac{1}{2}}$), and the 2878 Å ($^4P_{\frac{1}{2}} \rightarrow {}^4D_{1\frac{1}{2}}$) lines (cf. Table 1). This was unexpected as the wavelength for excitation, 2068 Å ($^4S_{1\frac{1}{2}} \rightarrow {}^4P_{2\frac{1}{2}}$), is not the strongest line for absorption. In addition, from Sommerfeld's intensity rule, the $^4P_{2\frac{1}{2}} \rightarrow {}^2D_{2\frac{1}{2}}$ transition intensity would be expected to be less than that of the $^4P_{1\frac{1}{2}} \rightarrow {}^2D_{2\frac{1}{2}}$ and $^4P_{\frac{1}{2}} \rightarrow {}^2D_{1\frac{1}{2}}$ transitions, and also the photomultiplier response is more sensitive at the longer wavelengths. This implies that the fluorescence signal given at 2598 Å is due to an effect other than, or in addition to, "direct-line" fluorescence. This can be explained if it is assumed that the fluorescence signal given at 2598 Å is "direct-line" fluorescence from the 2598.09 Å line ($^4P_{2\frac{1}{2}} \rightarrow {}^2D_{2\frac{1}{2}}$)

plus a fluorescence signal from the nearby, unresolved, 2598.05 Å line ($^2P_{\frac{1}{2}} \rightarrow {}^2D_{1\frac{1}{2}}$). The $^2P_{\frac{1}{2}}$ state lies only 0.13 eV above the $^4P_{1\frac{1}{2}}$ state (the $^4S_{1\frac{1}{2}} \rightarrow {}^4P_{1\frac{1}{2}}$ transition line gives the greatest absorption) and some of the excited atoms in the $^4P_{1\frac{1}{2}}$ state could be thermally excited to the $^2P_{\frac{1}{2}}$ state. This is a radiationless transition and the $^2P_{\frac{1}{2}} \rightarrow {}^2D_{1\frac{1}{2}}$ transition is a spin-allowed transition favoured by Sommerfeld's intensity rule.

Direct population of the $^2P_{\frac{1}{2}}$ state by absorption of the 2127 Å $^4S_{1\frac{1}{2}} \rightarrow {}^2P_{\frac{1}{2}}$ line is unlikely to account for the intensity of the 2598 line, as this line was found to absorb weakly (see Table 17) and was of a low intensity, thus giving a low $I_o A_T$ value.

The type of fluorescence, which can be called thermally-assisted direct-line fluorescence, does not appear to have been reported before. In this particular instance, because of the nearness of the two lines, it was not possible to come to a more definite conclusion. However, the same effect was observed in studying the fluorescence of bismuth[23] and arsenic[27] atoms and is discussed in more detail in their respective chapters.

4.7 Atomic-Fluorescence Measurements

Flame Conditions

A non-luminous fuel rich air-propane flame was used and the top

of the burner-head was set 3 cm below the monochromator slit.

Source Conditions

The antimony tube was operated at 30 Watts with a moderate degree of cooling applied by blowing compressed air through the cooling aperture. The source was placed ca 8 cm from the flame, at right angles to the line between the flame and the monochromator slit (see 1.2 and 3.7).

Calibration Curves

Linear calibration curves were obtained for aqueous solutions of antimony over the range 10^{-6} - 10^{-3}M (ca 0.1 - 120 ppm), the 2176 Å resonance line being used. The limit of detection in water (signal:noise ratio = 1) was 5×10^{-7}M (0.05 ppm). The sensitivity can be increased substantially by nebulizing with organic solvents to increase the volume of solution reaching the flame[28] (ca 5-fold increase) and by modulating the light source to eliminate all background radiation. Greater sensitivity may be obtained at 2311 Å, but this wavelength was not used in this study because of a "light leak" in the monochromator at ca 2300 Å and because it was desired to make a direct comparison with atomic-absorption measurements with the same source. The 2176 Å resonance line gives the strongest absorption signal and is the most intense resonance line[98] and in theory should, therefore, give the strongest fluorescence signal. This does not happen here

because the photomultiplier (EMI 9601B) is less sensitive at 2176 Å than at 2311 Å. The limit of detection quoted could therefore be considerably improved with better instrumentation.

Procedure for 1.2-12 ppm of Antimony

Transfer by pipette 1-10 ml portions of 10^{-3}M antimony solution into a series of 100-ml volumetric flasks and dilute to volume with distilled water. Nebulize the solutions into the air-propane flame and, using a slitwidth of 0.3 mm, a gain of 3,1, and bandwidth 3, measure the fluorescence signal at 2176 Å.

Other concentration ranges, i.e. 10^{-4} - 10^{-3}M and 10^{-6} - 10^{-5}M, may be measured by suitable dilution of the stock solution and adjustment of the slitwidth and gain controls.

Interferences

The variation in the fluorescence signal of an acidic 10^{-4}M antimony solution caused by 10^{-2}M Cd, Co(II), Cu(II), Fe(II), Hg(II), K, Mg, Mn(II), Mo(VI), Na, NH_4, Pb, Zn, arsenate, chloride, nitrate, phosphate and sulphate was less than 5%. The interference of other ions was not examined, but there is no reason to suppose that they would interfere.[18,28]

4.8 Atomic-Absorption Measurements

Flame Conditions

A non-luminous fuel-rich air-acetylene flame was obtained with the

7 cm long acetylene burner-head, and the top of the burner was set 1 mm above the bottom of the monochromator slit.

Source Conditions

The antimony tube was operated at 20 Watts with only slight cooling applied as described above. The source was placed in the usual position for atomic-absorption measurements on the SP900A, but slightly out of focus to prevent too much light reaching the photomultiplier. The SP900A was used in its absorption mode.

Calibration Curves

An air-acetylene flame was used as it gave a more stable flame than air-propane on the 7 cm burner supplied with the instrument. Also, the background is relatively unimportant in these measurements as the source is placed in the usual position for absorption on the SP900A and is therefore mechanically modulated. The source was placed slightly out of focus to prevent too much light reaching the photomultiplier. As with fluorescence measurements, the optimum flame verged on luminosity. The optimum burner height was with the top of the burner head approximately 1 mm above the bottom of the monochromator slit. Table 17 shows the absorbance measurements obtained at the three resonance lines with 10^{-3}M antimony.

TABLE 17

Atomic-Absorption Measurements at 0.005 mm Slitwidth

Spectral line, Å	Signal absorbance
2068	0.368
2176	0.515
2311	0.247
2127	0.014

The 2176 Å line gave the strongest absorption, and linear calibration curves over the range 5×10^{-5} - 10^{-3} M (6-120 ppm) antimony were obtained at this wavelength. The limit of detection (1% absorbance) was 10^{-5}M (1.2 ppm).

The non-resonance line at 2179 Å was completely resolved from the 2176 Å line at these small slitwidths and was found not to absorb. This illustrates one of the great advantages of using an electrodeless discharge tube instead of a hollow-cathode lamp. With the latter, large slitwidths must be used because of the weak intensity of the 2176 Å line, resulting

in non-resolution of the 2176 and 2179 Å lines and hence non-linear calibration curves, narrow working range, low limits of sensitivity, noise, etc. The sensitivities by A.F.S. are an order of magnitude better than those obtained by A.A.S. This was also previously observed for selenium and tellurium.

Procedure for 6-122 ppm of Antimony

Transfer by pipette 2.5-50 ml portions of 10^{-3}M antimony solution into a series of 50 ml volumetric flasks and dilute to volume with distilled water. Nebulize into the air-acetylene flame and, using a slitwidth of ca 0.01 mm, gain 2,3 and bandwidth 3, measure the absorption at 2176 Å.

CHAPTER V

THE FLUORESCENCE CHARACTERISTICS AND DETERMINATION OF BISMUTH WITH AN IODINE ELECTRODELESS DISCHARGE TUBE AS SOURCE[23]

5.1 Introduction

The determination of bismuth by flame-emission spectrophotometry is difficult because the main resonance line at 3068 Å lies in the middle of the hydroxyl band emission region and hence excessive background radiation is present. In addition, Gilbert[99] has noted absorption by bismuth atoms of the radiation from a hydroxyl band at 3068 Å in an oxy-hydrogen flame, thereby introducing more problems. The other bismuth resonance lines lie in the far ultraviolet and are in consequence difficult to excite thermally. At present, the most sensitive emission studies have been made in the inner cone of an oxy-acetylene flame in conjunction with nebulized organic solvents. Dean[94] gives a limit of detection of 6.4 ppm for bismuth under these most favourable conditions at 2231 Å.

Atomic-absorption measurements have been made at 3068 Å by Gatehouse and Willis[95] who used a hollow-cathode lamp giving a limit of detection of 2 ppm. A line at 2231 Å gives the strongest absorption but because of the close proximity of another line at 2228 Å the calibration curves tend to bend towards the concentration axis. This is a direct consequence of the low intensity output of same hollow-cathode lamps. A similar observation on the use of a conventional hollow-cathode lamp for iron has been made recently by Marshall and West.[100] Absorption studies have also been made with the continuum from a hydrogen lamp as source and with photographic recording of line intensities.[89] The integrated limits of detection in this instance were estimated to be 0.5-1.0 ppm for the 2052, 2231 and 3068 Å lines and 4.0 ppm for the 2228 Å line.

More recently Manning et al.[101] have determined bismuth using a shielded hollow-cathode lamp (which was far more intense than a conventional hollow-cathode lamp) and obtained a limit of detection at 2231 Å of 0.68 ppm.

This chapter describes the atomic-absorption and fluorescence characteristics of bismuth and also describes the use of a cool diffusion flame as an atom reservoir in atomic-fluorescence spectroscopy.

In this investigation the bismuth atoms were excited by the iodine line at 2061.63 Å (corresponding to the $5s^2 5p^4 {}^3P_2 s \rightarrow 5s^2 5p^5 {}^2P^O_{1/2}$ transition)[92] from an iodine electrodeless discharge tube. This iodine line, which coincides almost exactly with a bismuth resonance line at 2061.70 Å (corresponding to the $^4P_{2\frac{1}{2}} \longrightarrow {}^4S^O_{1\frac{1}{2}}$ transition), results from a non-ground-state transition and is hence not subject to self-reversal effects, even when the source is operated at high power ratings. In addition, an iodine discharge tube is as stable and easy to operate as that of an inert gas such as argon. Moreover, the iodine discharge tube does not emit radiation which is coincident with the direct-line fluorescence signal from the bismuth atoms at 3025 Å and so scattering from the source is completely eliminated. This latter consideration is of considerable importance because scattering is potentially one of the most serious limitations in atomic-fluorescence spectroscopy. This has not been found to be so in practice.

5.2 Experimental

Apparatus

The apparatus has previously been described (see 3.2). The Honeywell Brown recorder was replaced by a Servoscribe recorder used on the 0-10 mV range.

Reagents

Bismuth Solution, 1000 ppm. 1.000 g of bismuth metal were dissolved in 20 ml of concentrated nitric acid (analytical grade) and diluted to 1 litre.

RESULTS

5.3 Discharge Tube Parameters

a) Bismuth

Tubes containing only bismuth metal were found to be unsatisfactory owing to the involatility of bismuth (cf. antimony and tellurium) and thus they had to be run at very high energies (ca 90 watts). Tubes containing bismuth and iodine gave a stable but low intensity bismuth discharge at 40 Watts. The low intensity of the observed lines was thought to be due to the involatility of bismuth tri-iodide (m.p.409°, no vapour pressure figures available). The intensity increased at higher operating powers (60-70 Watts) and the discharge changed from a red-pink, argon, colour to a white-blue bismuth colour. An even brighter discharge was obtained without cooling, but under these conditions the tubes became overheated, with eventual loss of stability. The argon pressure was not too critical as long as it was less than 2 Torr. The optimum tube length was ca 3.5 cm. The bismuth tube was best run at 40 Watts with slight cooling.

b) Iodine

Tubes containing only iodine were found to be satisfactory. The optimum tube length was 6-7 cm. The intensity of the 2062 Å line was not very dependent on the argon pressure over the range 1-10 Torr but at argon pressures below 0.3 Torr the intensity of this line decreased considerably. This was thought to be due to the fact that the higher energy level of the 2062 Å[92] iodine line is populated by deactivation of highly excited iodine atoms by collision with argon atoms. This effect of the argon pressure on the intensity of the 2062 Å iodine line has been observed elsewhere.[102]

The iodine tubes were operated on the lower (0-25 Watts) range of the generator at 12-15 Watts with the upper portion of the tube within the cavity. The most stable and intense discharge was obtained by strongly cooling the lower portion (ca 4 cm) of the tube protruding below the cavity with a stream of air. This prevents an undue increase in the vapour pressure of iodine and consequent unstable emission. Under optimised conditions of tuning and cooling, the iodine discharge occupied about two-thirds of the tube and in a period of over an hour showed a $\pm$ 1% maximum variation in response (see Fig.XVII).

5.4 Preparation of Optimum Discharge Tubes

a) Bismuth

These tubes were prepared in a manner exactly similar to that described previously for antimony (see 4.4), i.e. with ca 10 mg each of bismuth and iodine. The tubes were 3.5 cm long and sealed with an argon pressure of ca 1 Torr.

b) Iodine

Quartz tubes 6-7 cm long and 8 mm in internal diameter were degassed as for selenium and tellurium (see 3.4), then ca 10 mg of analytical grade iodine was added to each tube. The tubes were then evacuated and as much of them as possible was immersed in a beaker of water at ca 40°C. The system was then flushed three times with argon to remove any occluded gases or moisture in the iodine. The tubes were then cooled in ice, and sealed with an argon pressure of ca 1 Torr.

5.5 Spectral Characteristics of Discharge Tubes

a) Bismuth

The ground state of the bismuth atom is $^4S_{1\frac{1}{2}}$ and a Grotian diagram[92] is shown in Fig.XVI. All the lines in this diagram were observed as well as a line at 2228 Å which is accounted for by Brode.[98] This line can be predicted from the energy difference between the $^4S_{1\frac{1}{2}}$ and $^4P_{1\frac{1}{2}}$ states.

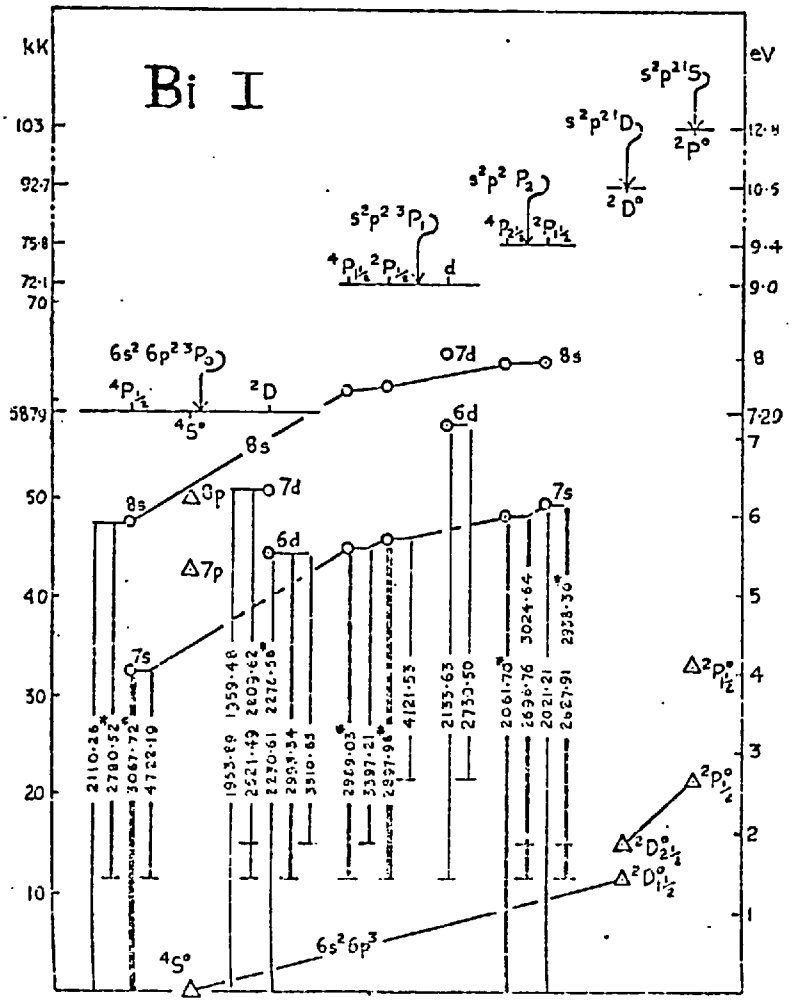

GROTIAN DIAGRAM FOR BISMUTH

FIG. XVI.

It has been used elsewhere for the atomic-absorption of bismuth.[101]

b) Iodine

The only iodine line observed was the extremely intense one due to the $5s^2 5p^4 {}^3P_2 s \longrightarrow 5s^2 5p^5 {}^2P^O_{\frac{1}{2}}$ transition at 2061.63 Å (see Fig.XVII). The remainder of the spectrum was a broad, low intensity, continuum extending from ca 2400 Å into the visible region.

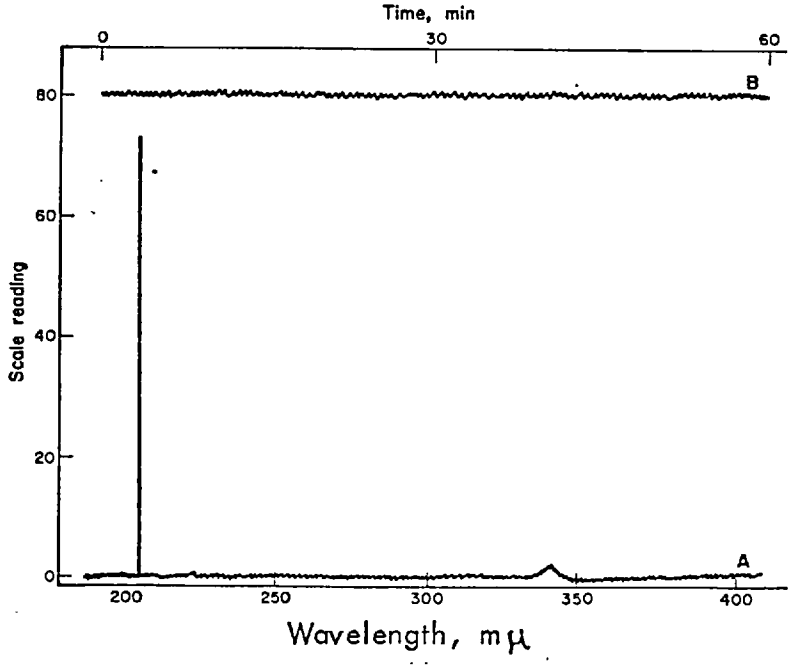

Fig.XVII. (A) Emission spectrum of iodine microwave-excited electrodeless discharge tube at 2450 Mc/s and 12 W.

(B) Stability plot of iodine tube at 2062 Å.

5.6 Fluorescence Characteristics of Bismuth

a) Source

The bismuth discharge tubes were examined as sources of excitation, but they were found to be either of rather low intensity or else somewhat unstable. Also, the most intense resonance line present in the discharge, at 3067.72 Å, coincides with a hydroxyl band emission from the flame in this region. Both the flame background and fluorescence emission signals are amplified by the a.c. detection system of the Unicam 900A because the source is not modulated. However, even with modulation it would be unwise to measure at this wavelength (i.e. 3067.72 Å) because of variations in the intense flame background.

In consequence, the iodine discharge tube was selected as the most suitable source of excitation because the extremely intense non-resonance iodine line emission at 2061.63 Å is sufficiently close to the 2061.70 Å bismuth resonance line for some absorption by bismuth atoms to occur. The cross-matching of iodine and bismuth spectra does not appear to have been reported previously in the literature, although many instances are known to exist between iron and other elements.[103]

Another unreported instance of cross-matching which has been noted in these studies is that between the non-resonance line of arsenic at 2288.12 Å

and the cadmium resonance line at 2288.02 Å. It is possible that many other instances exist which can be used with advantage, particularly in atomic-fluorescence spectroscopy, where it is not necessary to have the absorption line profile completely encompass the source line. Under these conditions absorption of the iodine line at 2062 Å would be expected with fluorescence emission from the bismuth resonance line at 2062 Å and direct-line emission at 2697 and 3025 Å.

b) Flame

Because of their low background a special type of diffusion flame, the nitrogen-hydrogen (and the argon-hydrogen) flame were used in this study. (See 1.3 and 7.2). These cool diffusion flames have several advantages over the hot premixed flames commonly used in atomic-absorption spectroscopy. For comparison, a 10^{-3}M solution of bismuth nitrate was nebulized into low background flames and the fluorescence emission was measured at 3025 Å (see below): the flames used were air-propane and air-hydrogen premixed flames and nitrogen-hydrogen and argon-hydrogen diffusion flames. The diffusion flames were obtained with the same burner-head and gas jets as used for the air-hydrogen flame, and the nitrogen or argon was used as the nebulizing gas.

The optimized fluorescence signal was exactly the same in the two premixed flames and in the nitrogen-hydrogen diffusion flame, but was twice as large in the argon-hydrogen diffusion flame. We attribute this difference to the fact that in a collisional encounter the diatomic nitrogen molecules would be expected to absorb energy from the excited bismuth atoms more efficiently than argon atoms, i.e., they would exhibit greater quenching action. The rate of sample uptake was similar ($\pm$ 1%) for all gases and was 1.72 ml/min.

Although diffusion flames are very cool[104] in comparison with the premixed flames which are normally used in thermal-emission and atomic-absorption spectroscopy, and may in consequence be more prone to show matrix effects, they also have considerable advantages. For example, the air-ground radiation propane flame back at 3025 Å is ca 100 times as high as that of the diffusion flames; that of the air-hydrogen flame is ca 25 times as high. This permits lower limits of detection and increased precision in both atomic-absorption and atomic-fluorescence spectroscopy. Because of the low temperatures of diffusion flames, thermal-emission from the alkali and alkaline earth elements is considerably reduced. In the atomic-fluorescence of bismuth no interference was observed from a 100-fold molar excess of sodium and potassium (see below) in a diffusion flame.

The transparency of these flames is also of very great significance, especially when dealing with elements which have resonance lines in the far ultraviolet region of the spectrum, e.g. arsenic.[27] This again results in a considerable lowering of detection limits and often a much wider working range becomes available. This is particularly important if an inefficient source is used, e.g., a conventional arsenic hollow-cathode lamp.

c) Wavelength of Measurement

A 200 ppm bismuth solution was nebulized with argon into an argon-hydrogen diffusion flame which was irradiated by an iodine electrodeless discharge tube. The essential optimum conditions of operation were found to be: hydrogen pressure corresponding to a reading of 16 cm on a di-n-butyl phthalate manometer gauge (flame near lift-off point); argon pressure 15 psi; top of the burner head ca 3 cm below the bottom of the analysing monochromator slit. The fluorescence response was found to be rather dependent on the hydrogen pressure and burner head height. Optimized signals were obtained with a hydrogen pressure slightly more than sufficient to prevent flame lift-off and with fluorescence measurements made half way up the flame. The most intense fluorescence signals

obtained under these conditons are shown in Table 18. A comparison is also made with the less sensitive nitrogen-hydrogen diffusion flame.

TABLE 18

Major Atomic-Fluorescence Wavelengths

Spectral line, Å	Fluorescence transition	Slitwidth mm	Relative Fluorescence signal* N_2/H_2	Ar/H_2
2062	$^4P_{2\frac{1}{2}} \rightarrow {}^4S^O_{1\frac{1}{2}}$	0.017	6.5	12
2697	$^4P_{2\frac{1}{2}} \rightarrow {}^2D^O_{1\frac{1}{2}}$	0.017	3	6
3025	$^4P_{2\frac{1}{2}} \rightarrow {}^2D^O_{2\frac{1}{2}}$	0.017	50	100
3068	$^4P_{\frac{1}{2}} \rightarrow {}^4S^O_{1\frac{1}{2}}$	0.017	38	54

*Identical gain for both flames

As expected, the three fluorescence signals were obtained from the $^4P_{2\frac{1}{2}}$ state. The additional intense signal at 3068 Å must be due to deactivation of the excited $^4P_{2\frac{1}{2}}$ state atom by radiationless transitions to the $^4P_{\frac{1}{2}}$ excited state. The high intensity of the emission at 3068 Å arises because the $^4P_{\frac{1}{2}}$ state is the lowest lying excited state and it may be populated by radiationaless transfers from other excited states. Moreover, it is the only line other than the 4722 Å ($^4P_{\frac{1}{2}} \rightarrow {}^2D^O_{1\frac{1}{2}}$ transition)

which can be emitted from this state. The analogous behaviour of the $^3P_1^O \longrightarrow {}^1S_O$, 2537 Å mercury line can be explained similarly.

In addition to the more intense fluorescence signals shown in Table 18, many unexpected and much weaker signals were recorded. These are shown in Table 19 and are compared to the weakest signal shown in Table 18 (at 2697 Å), cf. Fig.XVIII. The two lines at 2989 and 2993 Å could not be resolved at the slitwidths used. In addition to these emissions, two unidentified peaks were obtained at 2880 and 2680 Å, and with an increased gain and slitwidth a slight fluorescence signal was obtained at 2110 Å, corresponding to the $6s^26p^28s\,{}^4P_{\frac{1}{2}} \rightarrow {}^4S^O_{1\frac{1}{2}}$ transition. The 1954, 1959, 2524 and 2810 Å lines from the $6s^26p^27d\,{}^2D$ states lie ca 0.3 eV above the $^4P_{2\frac{1}{2}}$ and could not be detected. Also no fluorescence signal was observed from the 2021 Å line ($^2P_{1\frac{1}{2}} \rightarrow {}^4S_{1\frac{1}{2}}$ transition), but this is a very low intensity transition and lies at a wavelength at which the sensitivity of the photomultiplier becomes vanishingly small.

Table 18 indicates that the ground state bismuth atom can absorb energy from the iodine discharge tube at 2062 Å, be excited to the $^4P_{2\frac{1}{2}}$ state and then give rise to resonance fluorescence at 2062 Å, direct-line fluorescence at 2697 and 3025 Å and multiple stepwise-fluorescence at 3068 Å. Although the absolute intensities of these lines vary in the two

TABLE 19

Minor Atomic-Fluorescence Wavelengths

Spectral line, Å	Transition	Relative fluorescence signal N_2/H_2*	Ar/H_2**
2697	$^4P_{2\frac{1}{2}} \rightarrow {}^2D^O_{1\frac{1}{2}}$	100	100
2628	$^2P_{1\frac{1}{2}} \rightarrow {}^2D^O_{1\frac{1}{2}}$	7	12
2938	$^2P_{1\frac{1}{2}} \rightarrow {}^2D^O_{2\frac{1}{2}}$	30	47
2898	$^2P_{\frac{1}{2}} \rightarrow {}^2D^O_{1\frac{1}{2}}$	61	90
4122	$^2P_{\frac{1}{2}} \rightarrow {}^2P^O_{\frac{1}{2}}$	11	17
2228	$^4P_{1\frac{1}{2}} \rightarrow {}^4S^O_{1\frac{1}{2}}$	17	21
2989	$^4P_{1\frac{1}{2}} \rightarrow {}^2D^O_{1\frac{1}{2}}$	32	42
3397	$^4P_{1\frac{1}{2}} \rightarrow {}^2D^O_{2\frac{1}{2}}$	11	17
2231	$^2D_{2\frac{1}{2}} \rightarrow {}^4S^O_{1\frac{1}{2}}$	34	44
2277	$^2D_{1\frac{1}{2}} \rightarrow {}^4S^O_{1\frac{1}{2}}$	5.5	9
2993	$^2D_{2\frac{1}{2}} \rightarrow {}^2D^O_{1\frac{1}{2}}$	32	42
3511	$^2D_{1\frac{1}{2}} \rightarrow {}^2D^O_{2\frac{1}{2}}$	6.5	11

Contd.....

TABLE 19 (Contd.)

Spectral line, Å	Transition	Relative fluorescence signal N_2/H_2*	Ar/H_2**
4722($6s^2 6p^2 7s$)	$^4P_{\frac{1}{2}} \longrightarrow {}^2D^O_{1\frac{1}{2}}$	47	49
2781($6s^2 6p^2 8s$)	$^4P_{\frac{1}{2}} \longrightarrow {}^2D^O_{1\frac{1}{2}}$	4	6.5

* Slitwidth 0.06 mm.

**Slitwidth 0.04 mm. Gain adjusted to give 100 divisions scale reading at 2697 Å in each flame.

flames examined, their ratio is constant. This is to be expected because quenching of an excited state should not alter the ratio of line intensities emitted from that state. This effect is again observed for other states shown in Table 19.

It is apparent from Tables 18 and 19 that not only are the readings obtained in the argon-hydrogen diffusion flame greater than those in the nitrogen-hydrogen diffusion flame under similar conditions, but that the ratio of a given line intensity to the 2697 Å line in the same flame is in general 50% more in the argon-hydrogen flame, for reasons which have

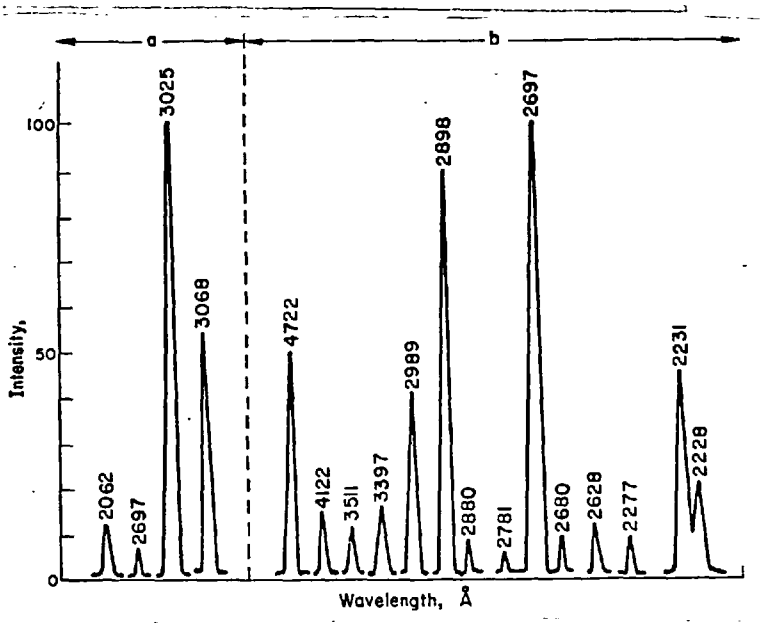

FIGURE XVIII Fluorescence Emission Spectra of Bismuth in the Argon-Hydrogen Diffusion Flame with an Iodine Discharge Tube as Source.

already been explained. The fluorescence emissions shown in Table 19 are of no real analytical significance because their intensity is rather low, but they do give a good indication of the population of the various energy levels. The fluorescence emissions at 2628 and 2938 Å which originate from the $^2P_{1\frac{1}{2}}$ state are examples of thermally assisted direct-line fluorescence, which was first postulated in the studies on the atomic-fluorescence characteristics of antimony.[97] In this instance there must be a radiationless promotion from the $^4P_{2\frac{1}{2}}$ to the $^2P_{1\frac{1}{2}}$ state (energy difference of only 0.12 eV). The other fluorescence emissions shown in Table 19 may be attributed to stepwise and/or direct-line fluorescence.

d) Mechanism of Fluorescence

All the fluorescence signals obtained can be attributed to the initial absorption of the 2061.63 Å iodine line. This was verified by the introduction of suitable filters. For example, a 10% solution of acetone in distilled water, contained in a quartz cuvette (1 cm path length) and placed between the monochromator slit and the iodine source, shows complete absorption between 2220 and 3000 Å, with 23.5% and 3% transmittance at 2062 and 3025 Å respectively. These transmission readings are uncorrected for reflection and absorption by the walls of the quartz cuvette. When this filter was interposed between the source of

excitation and the flame, the fluorescence signal at 3025 Å decreased from 100 to 24 divisions on the scale. This decrease corresponds almost exactly to the extent of the absorption of the 2061.63 Å iodine line by the acetone filter. Similarly a 0.1 M nickel chloride filter gave 6 and 80% transmittance at 2062 and 3025 Å respectively. When this filter was placed between the source and flame, the fluorescence signal at 3025 Å decreased from 100 to 6 divisions. This again corresponds to the absorption of the 2061.63 Å iodine line by the filter. Finally, a Pyrex glass filter gave 0 and 50% transmittance at 2062 and 3025 Å and when placed between source and flame produced a fluorescence signal decrease at 3025 Å from 400 divisions to 1. These results prove conclusively that the initial absorption step in the whole fluorescence process is absorption of the 2061.63 Å iodine line.

5.7 Atomic-Fluorescence Measurements

Flame Conditions

An argon-hydrogen diffusion flame was obtained with the 1.8 x 7.5 cm air-acetylene emission-head (see 1.3). The argon and hydrogen flow rates were ca 3.4 and 1 litre/min respectively, and the top of the burner-head was set 3 cm below the bottom of the monochromator slit.

Source Conditions

The iodine tube was operated at 12 Watts with 0.5 cm of the tube extending above the cavity and ca 4 cm below the cavity. A moderate degree of cooling was applied by blowing compressed air on the lower 1 cm of the tube (the cooling apertures on the cavity were not used). The source was placed ca -8 cm from the flame, at right angles to the line between the flame and the monochromator slit (see 1.2 and 3.7).

Calibration Curves

The 3025 Å line exhibits the greatest sensitivity and there is negligible scattering from the source at this wavelength. Linear calibration curves have been obtained at 3025 Å over the range from 5×10^{-7}M to 10^{-3}M solutions of bismuth (0.1-200 ppm) and the slope of the log-log curve was 0.93. The limit of detection (signal:noise ratio of 1) in aqueous solution was 2.5×10^{-7}M, i.e., 0.05 ppm of bismuth, with a slitwidth of 0.2 mm. With the aspirator-nebulizer used in this work, these sensitivity limits can be improved substantially (ca 5-fold) by nebulizing solutions containing solvents to increase the volume of liquid reaching the flame, and possibly also by modulating the radiation from the source to minimize the effects of background radiation and thus permit the use of wider slitwidths (up to 2.0 mm).

Procedure for 1-10 ppm of Bismuth

Transfer by pipette 1-10 ml of a 100 ppm bismuth solution into a series of volumetric flasks and dilute to volume with distilled water. Nebulize into the argon-hydrogen flame, use a slitwidth of 0.1 mm, gain 3,1, bandwidth 3, and measure the fluorescence at 3025 Å.

Other concentration ranges, i.e. 0.1-1 ppm and 10-200 ppm, may be measured by suitable dilution of the stock solution and adjustment of the slitwidth and gain controls.

Interferences

Salts of the following selected ions, when present in a 100-fold molar excess over a 10^{-4}M bismuth nitrate solution in 4 x 10^{-2} M nitric acid, did not produce a variation of more than 5% in the fluorescence signal; As(III), Cd, Fe(II), Fe(III), K, Na, NH_4, Sb(III) and Zn. Similarly, chloride, nitrate, phosphate, sulphate and tartrate did not interfere. Greater than a 100-fold molar excess of sulphuric acid produced a positive interference because of the strong blue S_2 emission in the diffusion flame.[104] This interference could be eliminated by bleeding a small amount of air into the flame to raise the temperature and oxidize the S_2 species. Aluminium and magnesium in a 100-fold molar excess produced, as expected, significant decreases in the fluorescence signal (40 and 20% respectively). This interference may be attributed to the

formation of oxide particles which "cage" the bismuth and which are not efficiently dissociated by the thermal energy available from the relatively cool diffusion flame. The magnesium suppression may be readily overcome by introducing a small amount of air into the diffusion flame *via* an auxiliary jet in the burner stem.[41] This results in only a slight loss in *overall* sensitivity. In the case of aluminium it was necessary to use an air-hydrogen premixed flame to overcome the interference; the overall sensitivity for bismuth was thereby reduced by *ca* 50%. Alternatively it may be possible to use an argon-oxygen-hydrogen flame in which the sensitivity loss would not be expected to be so great. There is reason to suppose that many other matrix effects may be readily overcome in the same manner. A diffusion flame burning in oxygen might be equally effective.

The interference effects in the nitrogen-hydrogen flame are very dependent on the burner design, nebuliser design, and position of measurement in the flame. The L-shaped 'holed' burner used in this study was found to give a flame with an inner temperature, 3-4 cm above the burner-head, of 400°C and an outer temperature of *ca* 1000°C (see 7.8). If this diffusion flame were maintained on a 1 cm internal diameter quartz tube, the inner temperature 3-4 cm above the burner-head was only *ca* 230°C and bad interference effects were observed using this 'tube burner'.

The Unicam SP900A nebuliser produces extremely small droplets which are easily evaporated in the flame. When an 'inefficient' nebuliser was used, it was possible to see a cone of unevaporated droplets above the burner-heads and bad interference effects would be expected to be observed, especially with the low tempeature flame of the tube burner.

5.8 Atomic Absorption Measurements

Flame Conditions

The nitrogen-hydrogen and argon-hydrogen diffusion flames gave higher (by ca 30%) absorption figures for a given concentration of bismuth than the air-propane and air-acetylene premixed flames when burning on the 7 cm long propane burner supplied with the SP900A. Since background radiation is relatively unimportant in atomic-absorption measurements because the source is modulated (the SP900A is operated in its absorption mode), the air-propane and air-acetylene flames are recommended to minimise matrix effects. The optimum position for the burner-heads was with its top level with the bottom of the monochromator slit.

Source Conditions

The low intensity bismuth electrodeless discharge tubes operated at 40 W with slight cooling were perfectly satisfactory. With the iodine

discharge as source, a detection limit of 10 ppm was obtained at 2062 Å. This is comparable to the 5.5 ppm detection limit obtained by Manning et al.[101] when using a shielded bismuth hollow cathode lamp at the same wavelength.

Comparison of Lines

Table 20 shows the absorbance measurements obtained at the five resonance lines for a 100 ppm solution of bismuth nebulized into an air-propane flame. The non-resonance line at 3025 Å is included only because of its use in atomic-fluorescence measurements.

The strongest absorption was produced at 2231 Å. At the narrow slitwidths used, this line was completely resolved from the 2228 Å line. It is relevant to note that on this occasion the strongest absorption was not obtained at the same wavelength as the strongest fluorescence signal. The detection limit for bismuth in the present study of atomic-absorbance was found to be 1 ppm and the analytical range 10-100 ppm.

TABLE 20

Atomic-Absorption Measurements (100 ppm of Bismuth)

Spectral line, Å	Slitwidth mm	Absorbance
3068	0.003	0.130
2231	0.015	0.348
2228	0.018	0.162
2277	0.020	0.025
2062*	0.001	0.028
3025	0.010	0.000

*Although a bismuth plus iodine tube was used as the source, this consists of the intense 2061.63 Å iodine line and not the relatively weak 2061.70 Å bismuth line.

5.9 Discussion

The above results have shown that an iodine source is more effective than a bismuth source for exciting atomic-fluorescence of bismuth. This is because the iodine source only emits one very intense spectral line (at 2062 Å) which overlaps the absorption profile of a bismuth resonance line.

A bismuth source only emits this line relatively weakly and thus is unsatisfactory for atomic-fluorescence measurements using this line. The major bismuth resonance line[98] (at 3068 Å) is not suitable for atomic-fluorescence measurements because it coincides with an intense hydroxyl band in the flame background.

CHAPTER VI

THE FLUORESCENCE CHARACTERISTICS AND DETERMINATION OF ARSENIC[27]

6.1 Introduction

The determination of arsenic by flame-emission spectroscopy presents many difficulties because the lowest energy resonance line requires an excitation energy of over 6 e.v. which is unobtainable with normal flames. Emission studies[94] have, however, been made recently by measuring the chemiluminescence in the reaction zone of an oxy-acetylene flame whilst aspirating with organic solvents. Under these particular conditions a limit of detection of 2.2 ppm at 2350 Å was obtained. Similarly, Gilbert[105] has observed the chemiluminescence spectrum from iso-propyl alcohol solution of arsenic in an air-hydrogen flame.

Arsenic hollow-cathode lamps give a low radiation output at the resonance wavelengths (1890, 1937 and 1972 Å) and are difficult to prepare owing to the volatility of arsenic which also causes a short operating life. In spite of these limitations, successful atomic-absorption studies have been made by Slavin, Sebens and Sprague[106] using a hollow-cathode

lamp at 1937 Å. The 1890 Å resonance line was regarded as giving the strongest absorption, but there was less noise at the 1937 Å resonance line because of its apparent higher intensity (as detected by the photo-multiplier). The limit of detection for 1% absorption was given as 2 ppm.

This chapter reports the determination of arsenic by atomic-fluorescence and atomic-absorption spectroscopy and the elucidation of fluorescence spectrum of arsenic.

6.2 Experimental

Apparatus

The apparatus was similar to that previously described (see 3.2) except that the Honeywell Brown recorder was replaced by a Servoscribe recorder used on the 0-10 mV range.

Reagents

Arsenic solution, 10^{-2}M. 0.9890 g of arsenious oxide was dissolved in distilled water and diluted to 1 litre; 1 ml ≡ 750 ug of Arsenic.

RESULTS

6.3 Discharge Tube Parameters

The preparation of a stable intense arsenic tube was found to be

rather more difficult than those previously described. Arsenic is quite volatile (see appendix 1) and it was thought that tubes containing only arsenic would be satisfactory. Quartz tubes ca 3.5 cm long containing 10 mg of arsenic metal and less than 0.5 Torr of argon gave a green coloured arsenic discharge. However, free arsenic plated out on the walls of the tube within the cavity, and the ends of the tube became quite hot during operation; this behaviour is the reverse of that normally observed. The arsenic lines were quite intense when the tube was operated at 40 watts, but the stability was very bad owing to the plating out of the arsenic. Tubes containing more than 1.0 mm pressure of argon initially gave a very intense, stable, blue arsenic discharge at 35 watts. However, after ca 2 hours of operation, the discharge transiently increased in intensity, changed to a light green colour and then abruptly to a red-violet (argon) coloured discharge. This type of discharge remained even on increasing the power to 75 watts. If the tube was now heated and again initiated with a "Tesla" coil the blue arsenic discharge was again obtained. This now only lasted for about half-an-hour before changing green and finally, as before, reverting to a normal argon discharge. The length of time that the blue discharge would remain after successive heatings became less and finally would last for no more

than one minute. This curious effect is difficult to explain, but could be connected with the amorphous arsenic used which slowly changes to a less volatile more stable allotrope under these low pressure conditions. The heating process could reveal a fresh amorphous arsenic surface as long as any remained. No evidence of arsenic attack on the quartz was observed.

Quartz tubes 3.5 cm long containing various amounts of arsenic and sulphur and 0.1 - 0.5 mm pressure of argon gave an intense arsenic discharge, but after ca 1-2 hours operation at ca 35 watts the discharge went out and could not be reinitiated. Again no evidence of attack on the quartz was observed. It is not possible to explain the failure of these particular tubes.

Quartz tubes 3.5 cm long containing hydrogen as the filler gas were also made and were operated at ca 30 Watts. When the hydrogen pressure was less than 2 mm, severe plating-out occurred after about one hour of operation. However, for hydrogen pressures > 5 mm, little plating-out occurred as long as the tube was not overcooled. Quite stable discharges were obtained at 10-15 Watts with no cooling. Although these tubes gave the arsenic spectrum, they were not very intense and were only used for some atomic-absorption measurements. Tubes

containing 5 mm pressure of hydrogen and 2 mm of argon gave more intense arsenic discharges than those tubes containing only hydrogen. The arsenic assumed a white-brown colour in the hydrogen filled tubes and a black colour in the argon filled tubes. A tube containing arsenic and mercury gave only a very weak arsenic discharge.

The best sources were made in tubes 4 cm long, using a mixture of arsenic and iodine in the weight ratio 2:1 with an argon pressure of ca. 1 mm. These tubes gave a stable intense arsenic discharge when run at ca 30 Watts with only very slight cooling or none at all. At powers > 35 Watts instability occurred because of an increase in pressure within the tube. If the iodine:arsenic ratio was increased, the tube would give a predominantly iodine type of discharge, thereby showing that the metal was not in excess.

These tubes were best operated at a power rating of 30 Watts with the upper 2 cm in the cavity and 2 cm protruding below the bottom of the cavity and with a very slight air-draught applied to the bottom of the tube from a compressed air supply. The discharge was a light blue colour under these conditions, but the cavity tuning was found to be rather critical. A spectrum obtained on a Unicam SP900A is shown in Fig.XIX. A stability plot recorded over a period of 1 hour showed a maximum $\pm$ 2%

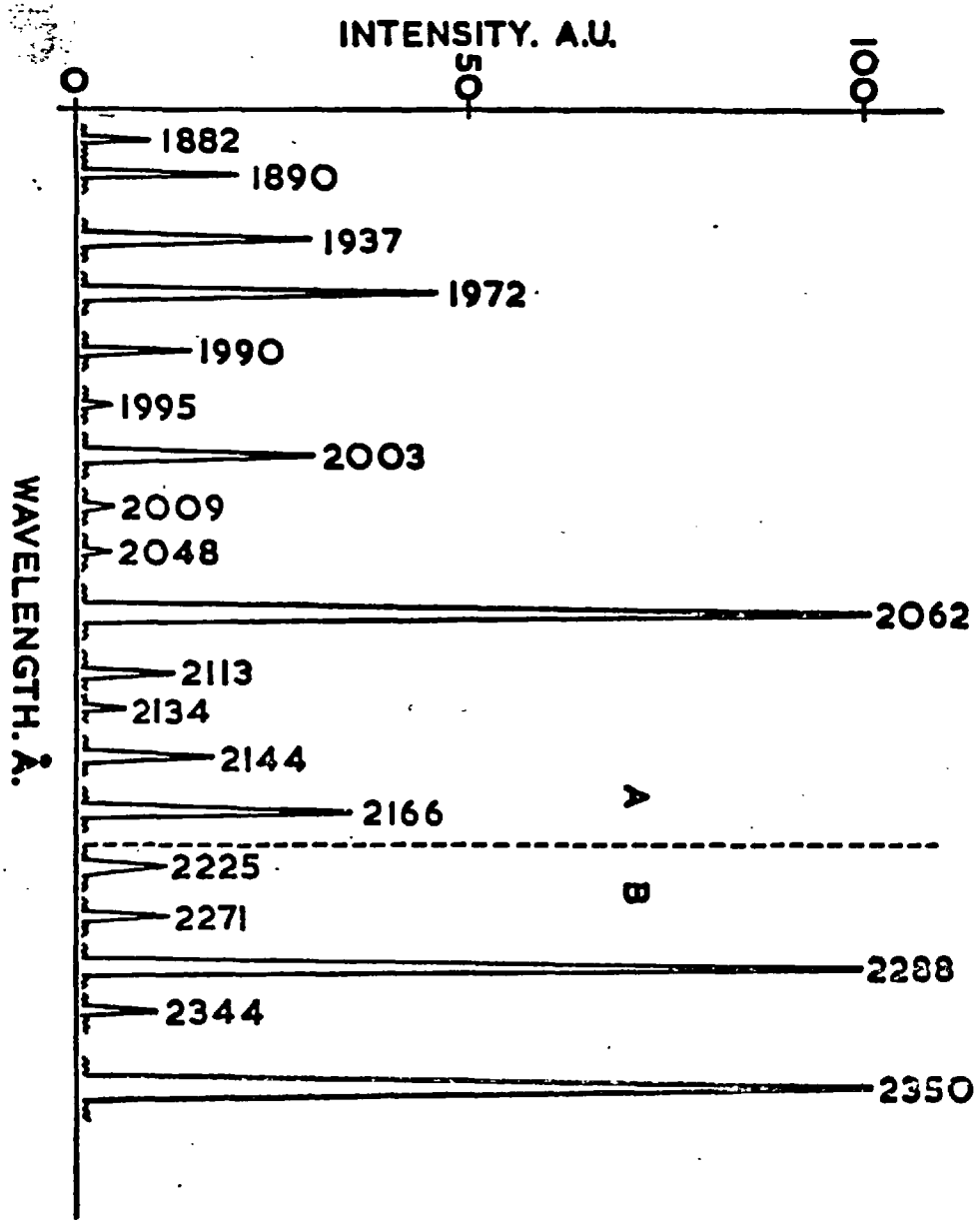

FIGURE XIX Emission Spectrum of Arsenic Discharge Tube Operated at 30 Watts.

A: slit 0.008 mm, gain 3,0

B: slit 0.003 mm, gain 3,0

variation in response. There were no sudden fluctuations and the above variation occurred in the form of gradual drifts.

6.4 Preparation of Optimum Discharge Tubes

Quartz tubes 4 cm long and 8 mm in internal diameter were degassed as for selenium and tellurium (3.4), then ca 15 mg of arsenic metal (99.999% purity) were added to each. The tubes were evacuated and flushed out with argon. A piece of wet asbestos rope was tied around the centre of the bulbs and the arsenic in the bottom of the tubes was gently heated with a microburner so that it sublimed 1-2 cm up the tubes. This process was designed to remove any occluded gases or moisture in the arsenic. After cooling to room temperature the tubes were removed from the vacuum line and ca 8 mg of iodine were added. The tubes were again connected to the vacuum line, evacuated, flushed out with argon and pumped down to a pressure of approx. 0.1 Torr. The tubes were left in this condition for some 5 minutes whilst continuously pumping, in order to allow any moisture in the iodine to volatilise. Then a pressure of 1 Torr of argon was introduced into the system and the bulb was sealed off.

6.5 Spectral Characteristics of Discharge Tubes

The ground state of the arsenic atom[92] is a $^4S_{1\frac{1}{2}}$ state and all lines (of wavelength $\geq$ 1882 Å) shown in the Grotian diagram (Fig.XX) were obtained as well as some higher state lines which are accounted for by Brode.[98] Not all the lines shown by Candler[92] are designated, but by calculating the energy differences between the various states and using Candler's table of ground state term differences, the excited state terms can be postulated. It was assumed that the excited terms are erect (normal), although there is no actual evidence for this other than the fact that the equivalent terms are shown erect (normal) for antimony. Our designations are, however, substantiated by the energy level differences given in the Tables of Spectral Line Intensities.[107] In addition to the arsenic lines the 2062 Å iodine line was quite prominent, but the continuum associated with tubes containing only free iodine was absent.

6.6 Fluorescent Characteristics of Arsenic

a) Flames

A 10^{-3}M solution (75 ppm) of arsenic was nebulised into normal air-acetylene, air-propane and air-hydrogen flames and diffusion flames of nitrogen-hydrogen and argon-hydrogen (see 1.3). Under optimum conditions these flames all gave similar responses. However, when a 10^{-3}M solution

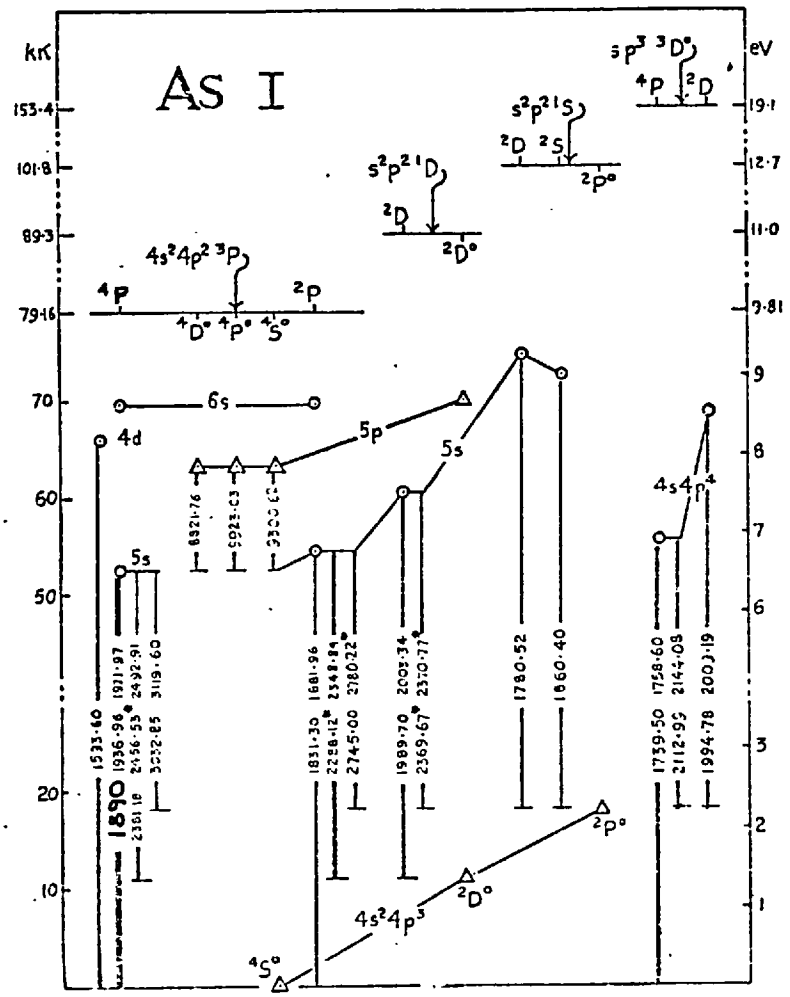

FIG.XX. GROTIAN DIAGRAM FOR ARSENIC

of potassium arsenate was nebulised, the air-acetylene* and air-hydrogen flames gave the better response. This indicates incomplete breakdown of potassium arsenate in the relatively cool diffusion flames. In consequence both the air-acetylene and the two diffusion flames were studied using solutions of arsenious oxide. The air-acetylene and the diffusion flames were obtained, using the standard acetylene jet and 1.8 x 7.0 cm acetylene emission-head supplied with the Unicam SP900A.

b) Wavelength of Measurement

Solutions of arsenic trioxide were nebulised under optimised conditions into air-acetylene and nitrogen-hydrogen flames. The intensity of the signal was found to be dependent on the type of flame, the line at which the fluorescence was measured and the arsenic concentration. The results obtained at the 1937 Å resonance line are shown in Table 21. A similar effect was observed at other resonance and some non-resonance fluorescence lines. At low concentrations (< 200 ppm) the nitrogen-hydrogen flame gave the better response, but at high concentrations

---

*The fluorescence signal was quite dependent on the acetylene pressure, increasing with the fuel richness of the flame. This suggests that incomplete breakdown of the arsenious oxide occurs even in the air-acetylene flame (cf. Tin).

TABLE 21

Relative Fluorescence Emission at 1937 Å

Flame	Relative Fluorescence Reading (a)	(b)
N_2/H_2	35	35*
Air/C_2H_2	22	40

Columns (a) and (b) are for 75 and 750 ppm arsenic respectively.

*Reading set to 35 divisions on recorder.

(> 200 ppm) the calibration curves curved towards the concentration axis. The calibration curves for the three resonance lines using the nitrogen-hydrogen flame are shown in Fig.XXI together with the calibration curve obtained at 1972 Å in the air-acetylene flame. It can be seen that in the diffusion flame at low concentrations the 1890 Å resonance line gives the best response followed by the 1937 Å line and then the 1972 Å line. However, at high concentrations the order is reversed and the 1972 Å line gives the best response. The curves at 1890 and 1937 Å rapidly deviate towards the concentration axis above 150 ppm of arsenic.

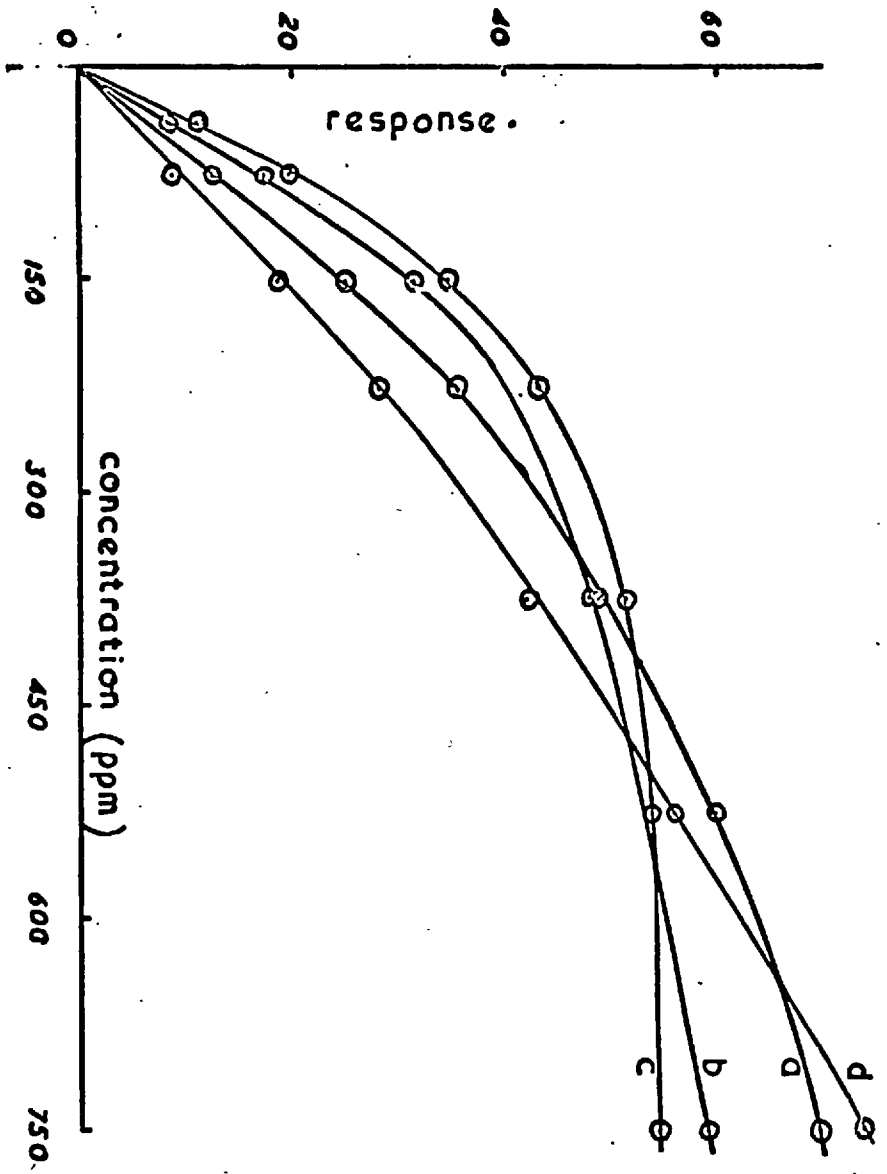

FIGURE XXI Arsenic Calibration Curves at Various Wavelengths

a) at 1972 Å in the N_2-H_2 flame, slit O.325 mm, gain 3,5

b) at 1937 Å " " " " " " "

c) at 1890 Å " " " " " " "

d) at 1972 Å in the air-C_2H_2 flame " " "

As stated previously, the air-acetylene flame gives better linearity and sensitivity at high arsenic concentrations for a given line than the diffusion flame. This can be seen for the 1972 Å line in Fig.XXI. The strongly reducing cool diffusion flame contains a higher density of arsenic atoms than the hot air-acetylene flame and this accounts for the higher resonance fluorescence intensities at low arsenic concentrations with the diffusion flame. At high arsenic concentrations this higher density of arsenic atoms causes self-absorption of the emitted resonance radiation. Hence, the diffusion flame calibration line curves more rapidly than that obtained in the air-acetylene flame.

In addition to the resonance emission at 1890, 1937 and 1972 Å, 12 non-resonance fluorescence signals were observed. The relative fluorescence readings are shown for the premixed air-acetylene and nitrogen-hydrogen diffusion flames in Table 22 whilst Fig.XXII shows the fluorescence spectrum obtained in the diffusion flame.

Toble 22 shows that there are striking differences between the relative intensities of various lines in the two flames, probably due to differences in flame absorption at the same wavelength as the exciting resonance lines. Also because of its greater atomic population there is more absorption of the resonance lines in the diffusion flame than in the

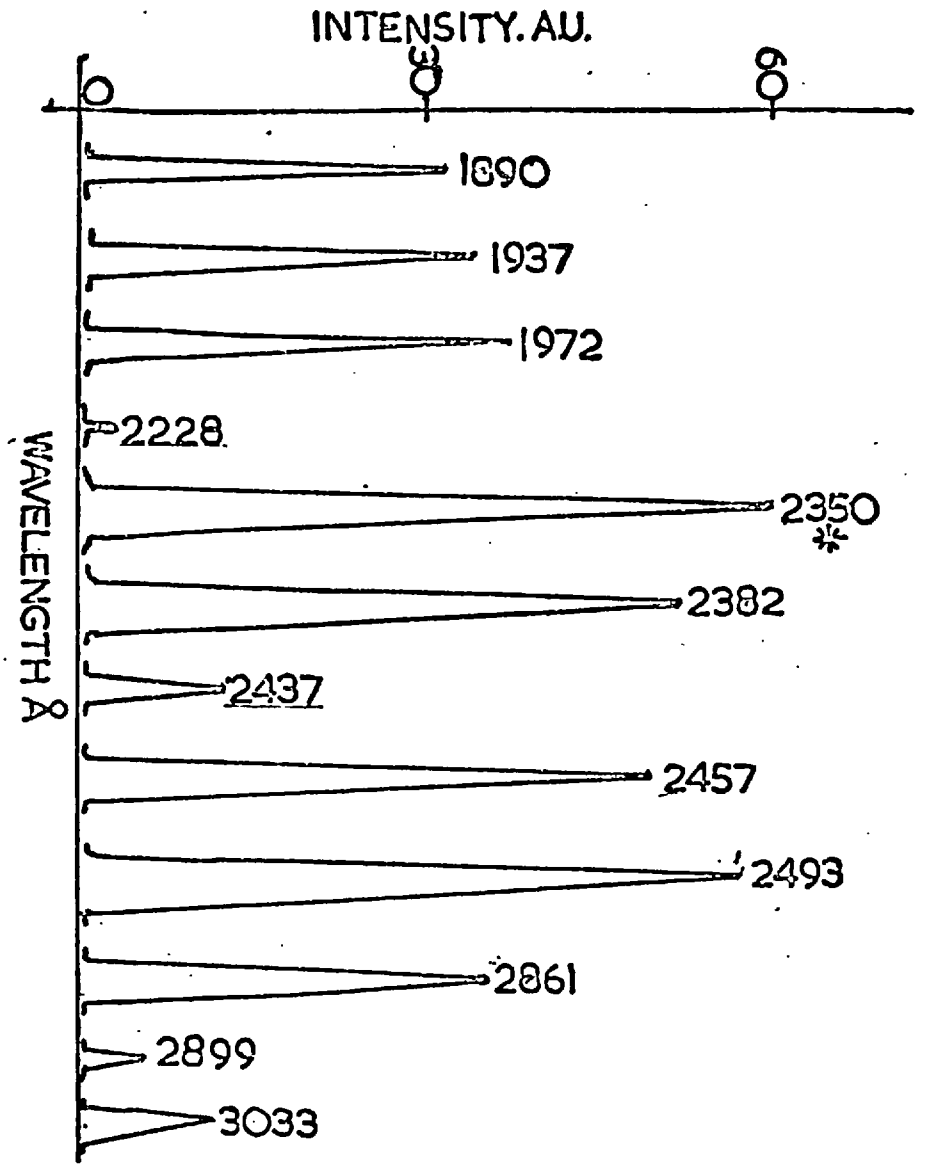

FIGURE XXII Atomic-Fluorescence Spectrum in the Nitrogen-Hydrogen Diffusion Flame

750 ppm arsenic, slit 0.1 mm, gain 3,0

*Multiply intensity scale x 2 to compare with other emission signals

TABLE 22

Relative Resonance Fluorescence Intensities

Line (Å)	Transition	Relative Fluorescence Signal[a] Air/C_2H_2	N_2/H_2
1890	$^4P_{2\frac{1}{2}} \rightarrow {}^4S^o_{1\frac{1}{2}}$	26	37
1937	$^4P_{1\frac{1}{2}} \rightarrow {}^4S^o_{1\frac{1}{2}}$	40	40
1972	$^4P_{\frac{1}{2}} \rightarrow {}^4S^o_{1\frac{1}{2}}$	40	43
2288	$^2P_{1\frac{1}{2}} \rightarrow {}^2D^o_{2\frac{1}{2}}$	58	4
2350	$^2P_{\frac{1}{2}} \rightarrow {}^2D^o_{1\frac{1}{2}}$	168	144
2382	$^4P_{2\frac{1}{2}} \rightarrow {}^2D^o_{2\frac{1}{2}}$	33	58
2437	$^4P_{1\frac{1}{2}} \rightarrow {}^2D^o_{1\frac{1}{2}}$	9	13
2457	$^4P_{1\frac{1}{2}} \rightarrow {}^2D^o_{2\frac{1}{2}}$	45	53
2493	$^4P_{\frac{1}{2}} \rightarrow {}^2D^o_{1\frac{1}{2}}$	44	61
2745	$^2P_{1\frac{1}{2}} \rightarrow {}^2P^o_{\frac{1}{2}}$	b	c
2780	$^2P_{1\frac{1}{2}} \rightarrow {}^2P^o_{1\frac{1}{2}}$	b	c
2861	$^2P_{\frac{1}{2}} \rightarrow {}^2P^o_{\frac{1}{2}}$	b	40
2899	$^2P_{\frac{1}{2}} \rightarrow {}^2P^o_{1\frac{1}{2}}$	b	6
3033	$^4P_{1\frac{1}{2}} \rightarrow {}^2P^o_{1\frac{1}{2}}$	b	13
3120	$^4P_{\frac{1}{2}} \rightarrow {}^2P^o_{1\frac{1}{2}}$	b	d

a: scale reading; 750 ppm arsenic solution used with slit widths 0.1 mm and 0.12 mm and gain 3,10.

Contd.....

b: air/C_2H_2 flame background too high to permit accurate measurements.

c: only observed with wider slit widths and higher gains.

d: measurement uncertain due to proximity of OH band emission.

air-acetylene flame. However, only measurement at a resonance line in the diffusion flame is subject to self-absorption effects of the emitted radiation. If measurement is made at a non-ground state line (direct-line fluorescence), then this radiation will not suffer any self-absorption before leaving the flame. This accounts for the relative increase in intensity of the direct-line fluorescence signals in the nitrogen-hydrogen flame as compared to the air-acetylene flame at high arsenic concentrations.

It was expected that the high rate of curvature of the calibration graphs observed for the resonance fluorescence processes would not be so marked at the corresponding direct-line or thermally assisted direct-line fluorescence processes. This was found to be so for the fluorescence emission at 2350 Å in both flames. Fluorescence readings at the 1890 Å line, which is the primary absorption line for emission at 2350 Å, gives a calibration curve that is horizontal to the concentration axis above 300 ppm of arsenic in the nitrogen-hydrogen flame (cf. Fig.XXI). However, if measurements are taken at the 2350 Å line, the curve does

not become horizontal even at 600 ppm of arsenic. The 2288 Å ($^2P_{1\frac{1}{2}} \rightarrow {}^2D^o_{2\frac{1}{2}}$), 2350 Å ($^2P_{\frac{1}{2}} \rightarrow {}^2D^o_{1\frac{1}{2}}$), 2745 Å ($^2P_{1\frac{1}{2}} \rightarrow {}^2P^o_{\frac{1}{2}}$), 2780 Å ($^2P_{1\frac{1}{2}} \rightarrow {}^2P^o_{1\frac{1}{2}}$), 2861 Å ($^2P_{\frac{1}{2}} \rightarrow {}^2P^o_{\frac{1}{2}}$) and the 2899 Å ($^2P_{\frac{1}{2}} \rightarrow {}^2P^o_{\frac{1}{2}}$) lines are all examples of thermally assisted direct-line fluorescence which has been previously observed for bismuth and postulated for antimony. The relatively high fluorescence intensity of the 2350 Å line is due to the low energy difference between the $^4P_{2\frac{1}{2}}$ and the $^2P_{\frac{1}{2}}$ states (0.027 eV) and the favoured $^2P_{\frac{1}{2}} \rightarrow {}^2D^o_{1\frac{1}{2}}$ transition. This transition is spin allowed, unlike the 2381 Å ($^4P_{2\frac{1}{2}} \rightarrow {}^2D^o_{2\frac{1}{2}}$) "direct" intercombination line. Arsenic is an atom of fairly low atomic weight that would be expected to conform to Russell Saunders coupling to some degree. Hence the relatively high intensity of the 2350 Å line compared to the three "direct" intercombination lines. It must be remembered that the $^2P_{\frac{1}{2}}$ state can only be populated from the $^4P_{2\frac{1}{2}}$ state which in turn can only be populated by absorption of the 1890 Å ($^4P_{2\frac{1}{2}} \rightarrow {}^4S^o_{1\frac{1}{2}}$) line which is not the most sensitive line for resonance fluorescence at an arsenic concentration of 750 ppm. The $^2P_{\frac{1}{2}}$ state cannot be populated by absorption of the 1882 Å ($^2P_{\frac{1}{2}} \rightarrow {}^4S^o_{1\frac{1}{2}}$) intercombination line as this line was found not to absorb. This was to be expected, because the equivalent antimony line at 2127 Å ($^2P_{\frac{1}{2}} \rightarrow {}^4S^o_{1\frac{1}{2}}$) only absorbed very weakly (see 4.8)

and antimony does not conform to the Russell Saunders coupling rules as closely as arsenic.

The thermally assisted direct-line fluorescence signals from the $^2P_{1\frac{1}{2}}$ state, which lies O.21 eV above the $^4P_{2\frac{1}{2}}$ state, were much weaker than those from the $^2P_{\frac{1}{2}}$ state (of Tables 22 and 23). These fluorescence signals (from the $^2P_{1\frac{1}{2}}$ state) were very weak in the cool diffusion flame, but were stronger in the high temperature air-acetylene flame as would be expected. The fluorescence at 2288 Å ($^2P_{1\frac{1}{2}} \rightarrow {}^2D^o_{2\frac{1}{2}}$) was 15 times stronger in the hotter premixed flame (of Table 22).

The relative quenching effects of nitrogen and argon were found by comparing the intensity of the fluorescence signals in the nitrogen-hydrogen and argon-hydrogen diffusion flames. The results shown in Table 23 indicate that the lines emanating from the $^4P_{2\frac{1}{2}}$ state are unaffected when argon is substituted for nitrogen, whilst those from the $^4P_{1\frac{1}{2}}$ state are increased ca 33%, those from the $^4P_{2\frac{1}{2}}$ state by ca 40% and those from the $^2P_{\frac{1}{2}}$ state by ca 80%. This last figure was considered to be unusual as any atoms in the $^2P_{\frac{1}{2}}$ state must have arrived in this state via a radiationless transition from the $^4P_{2\frac{1}{2}}$ state and the nitrogen molecule would be expected to favour this transfer more than the argon atom. Obviously the nitrogen molecules must quench atoms in the $^2P_{\frac{1}{2}}$ state to a greater extent than they assist the $^4P_{2\frac{1}{2}} \rightarrow {}^2P^o_{\frac{1}{2}}$ transition.

TABLE 23

Relative Quenching Effects of Nitrogen and Argon

Line	Relative Fluorescence Intensity[a]	
	N_2/H_2	Ar/H_2
1890	32	33
1937	34	46
1972	37	53
2288	3	5
2350	116	208
2382	52	56
2437	12	17
2457	48	67
2493	56	80
2745	<0.5[b]	ca 0.5[b]
2780	0.5[b]	1.0[b]
2861	34	63
2899	5	85
3033	11	15
3120	c	c

a: 750 ppm arsenic solution used with slit width 0.1 mm and gain 3,10.

Contd.....

b: observed at wider slit widths, higher gains.

c: measurement uncertain due to proximity of OH band emission.

c) Effect of Source Power

The effect of varying the source operating power is shown in Table 24. Increase in operating power appears to favour the fluorescence emission at 1972 Å whilst that at 1890 Å is decreased. This must be due to some self-reversal and pressure broadening of the 1890 Å line in the source at increased powers. Operating above ca 35 Watts caused some instability because of an increase in pressure within the tube.

TABLE 24

Effect of Source Power on Fluorescence Intensity

Power Rating (watts)	Fluorescence Signal[a]					
	75 ppm As			750 ppm As		
	1890 Å	1937 Å	1972 Å	1890 Å	1937 Å	1972 Å
30	42	35	26	24.5	26.5	29
43	50	46	36	31	34.5	39
55	54	54	43.5	32	37	47

a: The fluorescence intensity readings were obtained with a slit width of 0.5 mm and gain 3,10 for 75 ppm As and 3,0 for 750 ppm As. The discharge tube was uncooled.

6.7 Atomic Fluorescence Measurements

Flame Conditions

a) Diffusion Flames

Nitrogen (argon)-hydrogen flames were obtained with the 1.8 x 7.5. cm air-acetylene emission head (see 1.3). The nitrogen and argon pressures were set at 15 p.s.i. (corresponding to nitrogen and argon flow rates of ca 3.7 and 3.4 litres/min respectively). The hydrogen flow rate was ca 1 litre/min and the top of the burner-head was set 3 cm below the bottom of the monochromator slit.

b) Air-Acetylene

An air-acetylene flame on the verge of luminosity was obtained with the 1.8 x 7.5 cm air-acetylene emission head (the air pressure was set at 15 p.s.i.). The top of the burner-head was set 0.5 cm below the bottom of the monochromator slit.

Calibration Curves (see Fig.XX)

Calibration curves have been obtained using aqueous solutions of arsenious oxide over the range 5-750 ppm arsenic at the 1890, 1937 and 1972 Å resonance lines and at the 2350 Å thermally assisted direct-line. In the diffusion flames the 1890 Å line was the most sensitive resonance line at low concentrations, but suffered serious curvature

towards the concentration axis above 150 ppm arsenic. The 1972 Å line was the most sensitive resonance line at high concentrations of arsenic, and gave more linear calibration curves. The 1937 Å line was intermediate in behaviour as expected. The air-acetylene flame gave similar results except that the 1937 Å line gave greater sensitivity at low concentrations of arsenic, possibly due to the strong flame absorption at 1890 Å which resulted in high signal:noise ratio. . The 2350 Å thermally assisted direct-line fluorescence signal was the most sensitive, but the increased background of the air-acetylene flame was sufficient almost to offset the increased sensitivity. It was also found that the air-acetylene flame gave more linear calibration curves over a given concentration range of arsenic at a given line than the diffusion flames. At low arsenic concentrations the nitrogen-hydrogen flame was more sensitive and at high concentrations (ca 500 ppm) the air-acetylene flame was the more sensitive. This is probably because of the higher density of arsenic atoms in the more strongly reducing cooler flame which causes self-absorption of the emitted radiation at high arsenic concentrations. The limits of detection in aqueous solution are shown for the main arsenic lines in Table 25. Prior extraction of arsenic into organic solvents should considerably increase these limits as would source modulation. The limit of detection at 2350 Å using a low background air-hydrogen flame, which like the air-acetylene

flame is hot enough to give complete breakdown of all arsenic species, is O.2 ppm. The limits of detection shown in Table 25 at the three resonance lines are especially good when it is realised that the photo-multiplier used in these studies (E.M.I. 9601B) has a Corning glass window and has virtually no response below ca 2000 Å.

TABLE 25

Some Limits of Detection by Atomic-Fluorescence Spectroscopy

Line (Å)	Limit of Detection* (ppm) N_2/H_2	Slit (mm)	Air/C_2H_2	Slit (mm)
1890	O.2	2.O	1.O	2.OO
1937	O.25	2.O	1.O	1.5
1972	O.5	2.O	2.O	1.5
2350	O.15	2.O	2.O	1.O

*Signal:Noise Ratio = 1.

Interferences

With the premixed air-acetylene flame, the only interferences observed from a wide range of elements were due to intense light emission

from easily excited elements such as Na, K, Cu, etc. reaching the photomultiplier via a light leakage in the monochromator. Source modulation should also overcome this type of interferences which is not peculiar to atomic-fluorescence.

Using the diffusion flames described above, interference was observed with 10-fold molar excesses of various cations on a 75 ppm solution (10^{-3}M) of arsenic. Up to a 10% decrease in the fluorescence intensity was found with the following cations Al^{3+}, Cu^{2+}, Mg^{2+}, Zn^{2+}, Na^{+} and NH_4^{+} (decreasing order of interference). Anions such as chloride, nitrate, phosphate and sulphate had little effect. The decreases are considered to be due to the incomplete breakdown of the metal arsenite in the relatively cool diffusion flame. Passing the solutions through a cation exchange column or even burning the diffusion flame in an oxygen sheathed atmosphere to increase its temperature should overcome these matrix effects.

Possible Use of Filters

A filter interposed between the source and the flame so as to transmit radiation at 1890 Å and another filter between the diffusion flame and the photomultiplier to transmit radiation at 2350 Å [108] should lead to very considerable increased sensitivity limits. The diffusion

flame has no background at 2350 Å and this arrangement would overcome the large light losses which occur in the monochromator and also any scattering that might be observed at low arsenic concentrations. According to Jencons and White[109] a thin film of sodium metal on quartz is opaque to all wavelengths except those near 1950 Å.

6.8 Atomic-Absorption Measurements

Flames

The following flames were studied: air-acetylene, air-propane, air-hydrogen, nitrogen-hydrogen-nitrous oxide and nitrogen-hydrogen. Similar results to those quoted by Slavin, Sebens and Sprague[106] were obtained using the first three flames. Transmission signals of 18, 33.5 and 40% were obtained at 1890, 1937 and 1972 Å respectively with air-acetylene on a 7.0 cm burner. The flame absorbance for the air-acetylene flame was very dependent on flame conditions and reached a minimum for a flame on the verge of luminosity. It was at this point (which also corresponds to maximum absorbance by arsenic atoms) that atomic-absorption measurements were taken. The opacity of the nitrogen-hydrogen-nitrous oxide flame below 2000Å rendered it inferior to the air-acetylene flame and it was not used. The 7 cm nitrogen-hydrogen

diffusion flame burning on a 7 cm perforated propane burner plate showed little flame absorption at all wavelengths. The flame absorption was also not very dependent on the hydrogen pressure and transmission figures of 70, 87 and 95% at 1890, 1937 and 1972 Å respectively were obtained. Using a slot burner with less air entrainment, even higher transmission figures should be obtained. Flame absorption with the air-acetylene flame was maximal when the burner was in line with the monochromator slit, but was minimal for the nitrogen-hydrogen flame. This shows that the flame absorption is at a minimum along the centre of the diffusion flame which contains mainly non-absorbing nitrogen and hydrogen. Towards the edges of the flame air entrainment takes place, thus causing increased light absorption. This could be illustrated by slightly altering the burner position. Best results were obtained with the burner-head level with the bottom of the monochromator slit for the air-acetylene flame and ca 2 mm above it with the nitrogen-hydrogen flame. Table 26 shows the absorbance measurements obtained at the four resonance lines on nebulising a 75 ppm solution of arsenious oxide into these two flames. The arsenic electrodeless discharge tube was used as source and was placed in the usual position, but slightly out of focus to prevent too much light from reaching the detector.

Metal arsenite solutions gave higher absorbance readings in the air-acetylene flame than in the diffusion flame, thus indicating incomplete breakdown in the latter flame. This can presumably also be overcome by passing solutions through a cation exchange column.

TABLE 26

Atomic-Absorption Measurements

Line Å	Absorbance Value (75 ppm As) N_2/H_2	Air/C_2H_2
1882	0.000	0.000[ab]
1890	0.398	0.118[b]
1937	0.332	0.092[b]
1972	0.200	0.055[b]

a: zero absorbance was also given with 750 ppm arsenic

b: large noise component due to flame absorption.

6.9 Suggestions for Future Work

a) Use of Filters in Atomic-Fluorescence

The fluorescence signal from a flame passes through a monochromator, which in general has a relatively long light path and a low-effective

aperture. If, instead of the monochromator, a filter were placed between the flame and the photomultiplier a large increase in sensitivity should be obtained. With low background flames (e.g. nitrogen-hydrogen) a simple 'solid' filter with a bandpass of 200 Å or less should be adequate.[108,110,111] With high background flames interference filters with bandpasses between ca 1 and 40 Å could be used.[112,113] Ramsay and Tanaka[114] describe tuneable optical filters with bandpasses as low as 1 Å. For very low concentrations it should be possible in most cases to use direct-line fluorescence and incorporate another filter (between the flame and the source) that will transmit the exciting resonance line but absorb the 'measured' direct-line. This will overcome any scattering of the source radiation.[115] (See 4.6 and 6.7).

b) Involatile Metal Sources

It has been found[116] almost impossible to make a stable, intense and long-lived magnesium electrodeless discharge tube owing to the involatility of magnesium and its halides (see appendix 1) and to the fact that magnesium attacks quartz. The author has found that it was possible to overcome this problem by placing a piece of magnesium ribbon in an 8 mm internal diameter quartz tube which was horizontally mounted in a 214L discharge cavity (the magnesium ribbon being inside the cavity).

A very low flow of argon (at atmospheric pressure) was passed along the tube and an intense magnesium discharge could be initiated. A similar effect was observed with copper. A spluttering process (similar to that of a hollow-cathode lamp) was thought to be responsible. The discharge was most intense when viewed along the length of the tube which acted as a light guide. Unfortunately the discharge was not very stable, under the conditions used, but could easily be developed as a source for involatile metals and metals that attack quartz (e.g. Lithium, Calcium and Strontium).

c) Microwave Excitation of Emission Spectra

(i) Inorganic Excitation

Microwave plasmas have been described in the literature[86] but in general they are rather elaborate and use high power (ca 2 K.Watt) microwave generators. These high powers are necessary because nebulised water vapour tends to extinguish low power discharges. Runnels and Gibson[117] have overcome this limitation by using a simple low wattage microwave induced argon plasma and a solid sample that is slowly vaporised into the discharge. By integrating the light intensity very high sensitivities could be obtained. The above type of arrangement is rather complicated, so the author has made some preliminary studies to

develop a qualitative method of analysis of very dilute solutions. One drop of a thallium solution was added to a clean quartz bulb which was attached to a vacuum line and evaporated to dryness under vacuum. The system was flushed with argon and pumped down to ca O.1 Torr. On excitation of the bulb with a microwave discharge, the green thallium 5350 Å line, resulting from the evaporation of 1 drop of a 10^{-7}M thallium solution was clearly visible. Thus a quick qualitative analysis could rapidly be performed. Before quantitative results could be obtained, a continuous flow system with integration of the light output[117,118] would be necessary.

Rosenthal and Eyer[119] have excited a sodium 'seeded' oxy-hydrogen flame with a microwave (2450 Mc/sec) discharge. The microwave power was only ca $\frac{1}{8}$ that of thermal power of the flame, but the line emission of the sodium resonance lines was enhanced by 2 orders of magnitude.

The author has failed to excite 'seeded' air-hydrogen and air-acetylene flames using a microwave (2450 Mc/sec) discharge in conjunction with a 214L cavity, but it was found possible to excite a 'seeded' air-hydrogen flame using a 2 K.Watt, 37.5 Mc/sec, radio frequency generator. Further work is in progress on both microwave and radio frequency excited flames, the latter showing considerable promise for use in A.F.S. and F.E.S.

(ii) Organic Excitation

Gas chromatographic detectors[120,121] have been developed which are based on monitoring the intensity of electronic emission spectra of eluted organic compounds and have resulted in very high sensitivities being obtained. As gas chromatographic systems are rather elaborate it was decided to attempt to excite sealed electrodeless discharge tubes of organic compounds. The author has prepared a series of long (ca 20-30 cm) electrodeless discharge tubes which contained organic compounds. The upper part of these tubes was excited by a microwave discharge and this discharge was carried by the argon filler gas down to the organic compound in the bottom of the tube. This reduced the thermal decomposition rate. Although in general the tubes were short lived, the initial spectra of the different compounds varied considerably and this shows great promise and further work is in progress.

PART II

FLAME-EMISSION SPECTROSCOPY

Introduction

The use of flame-emission spectroscopy in analytical chemistry appears to be on the decline, mainly because of the advent of atomic-absorption spectroscopy. There are few instruments manufactured solely for flame-emission work and most modern atomic-absorption instruments have to be adapted before they can be used for flame-emission studies.

Although F.E.S. is more prone to interference effects than A.A.S. or A.F.S. (see page 10), it is essentially a more simple technique because no external source is required. Because of this, F.E.S. is more suited than A.A.S. or A.F.S. to qualitative and semi-quantitative analyses of completely unknown solutions.

The main requirements for a sensitive determination in F.E.S. are a good monochromator and a sensitive photomultiplier which most instruments that are primarily designed for A.A.S. do not have. One of the drawbacks of F.E.S. is the necessity for hot, high background flames to excite elements with refractory oxides (e.g. aluminium and beryllium) and elements

with resonance lines in the far U.V. (e.g. antimony and arsenic). These drawbacks can be overcome by either using a high resolution monochromator (see 1.4) or sheathed flames.[122,123] * It is thought that there will be a renaissance in F.E.S. in the near future.

Theory

a) Systems in Thermal Equilibrium

The flame-emission may be considered to be in thermal equilibrium when the actual occupational number of the excited state is given by the Boltzmann distribution law at the flame temperature, T. In general, most analytically used premixed flames are in thermal equilibrium above the reaction zone[12,124] where most flame emission measurements are taken. The reaction zone of a flame is not in thermal equilibrium[12,124] and the concept of temperature is not really applicable in this region (see 9.7).

---

*A sheathed flame is a flame surrounded by an atmosphere of an inert gas (e.g. nitrogen or argon). The interconal region of a sheathed flame has an extremely low background (ca 20-50 times less than that of the interconal region of the unsheathed flame), but has a similar temperature to the unsheathed flame.

Consider a small volume V of a flame region (that is in thermal equilibrium), the number of atoms per c.c., N_1 is given by the equation:

$$N_1 = N_o \frac{g_1}{g_o} \exp\left(\frac{-E_1}{kT}\right)$$

(See page 8 for definition of symbols used)

The total amount of energy radiated per sec (J) from the small volume (V) of the flame at frequency (ν) is given by the equation:

$$J = AN_1 Vh\nu \qquad (29)$$

$$(E_1 = h\nu)$$

where A is the Einstein transition probability (sec^{-1}) for the transition $(1 \rightarrow O)$. (V and N are chosen small enough to neglect self-absorption.)

Hence $$J = AVNh\nu \frac{g_1}{g_o} \exp\left(\frac{-h\nu}{kT}\right) \qquad (30)$$

Thus it can be seen that the amount of energy radiated is independent of the shape of the spectral line and is proportional to the concentration of the emitter. When self-absorption occurs the shape of the spectral line must be considered and the mathematics become rather involved. The reader is referred to several comprehensive texts on the subject.[12,125,126]

Self-absorption, (which is caused by the absorption of emitted resonance radiation by ground state atoms in the flame), causes the calibration curves to bend towards the concentration axis at high concentrations, and at very high concentrations the emission intensity is proportional to the square root of the concentration of the emitter.[12,125] Self-absorption is generally negligible for molecular emissions because the oscillator strengths of the transitions are extremely low (ca 10^{-5}),[13] thus resulting in linear calibration curves over large ranges of concentration.

b) Systems not in thermal equilibrium

Flame-emission is not a thermal equilibrium when the occupational number of the excited state is greater than that predicted by the Boltzmann distribution law.* This type of emission is termed chemiluminescence and often occurs from the primary reaction zone of a flame. The emission intensities observed from this region are often many orders of magnitude greater than that predicted by the Boltzmann distribution law. Gilbert[105] has given an extensive treatise on chemiluminescence of many elements in a variety of flames. A good example of this work was the emission of water/isopropyl alcohol solutions of tin in the primary reaction zone

---

*It is very rare for the number to be appreciably less but this case has been observed.[12]

of an air-hydrogen flame. Atomic and ion lines of tin down to ca 2000 Å were observed. Continuing this work Gibson, Grossman and Cooke[127] were unable to reverse the 2863 Å chemiluminescent tin line at the highest possible temperature of a quartz window tungsten lamp (2800°K) or even a high pressure hydrogen lamp.

These high emission intensities are thought to be the result of chemical reactions occurring within the primary reaction zone of the flame.

e.g. $M + CH + OH \longrightarrow M^* + CO + H_2$ (1)

or $MO + C \longrightarrow M^* + CO$ (2)

The three-body excitation (1) is thought to be more probable.[127] In general little chemiluminescence is observed in air or oxy-hydrogen flames,[124,128] unless some carbon containing species is nebulised into the flame. This is thought to be due to the fact that the elementary reactions in an air or oxy-hydrogen flame are not sufficiently exothermic to produce such an effect.[128]

The diffusion flame of nitrogen and hydrogen was found to give a high population of bismuth and arsenic ground state atoms (see 5.8 and 6.8) as well as high populations of selenium, tellurium and tin ground state atoms.[129] The oxides of these elements, especially arsenic and

tin (dissociation energies of 5.0 e.v. and 5.8 e.v. respectively)[130] are relatively stable and the inner temperature of the diffusion flame (see 7.8) is insufficient to account for this breakdown of the oxide to the metal which therefore must be a chemical reduction.

i.e. $M - O + H_2 \longrightarrow M + H_2O$.

Work performed by the author[131,132] (see 8.6) further substantiates this theory (i.e. a high ground state population only occurs for elements with oxides that can be reduced by hydrogen under the flame conditions).

In general there is insufficient energy to produce excited atoms from this type of reduction and no atomic emission was observed from even large concentrations of tin[132] in the diffusion flame. But if some isopropyl alcohol were added to the tin solution, strong chemiluminescent emission (extending to ca 2000 Å) was observed throughout the diffusion flame. This gives further support to the theory that the tin is primarily broken down to tin atoms and then is excited by a three-body excitation mechanism.

Molecular emission was observed from quite a few species in the diffusion flame[104,131,132] (all nebulised in aqueous solution) and in these cases (see 7.4, 8.4 and 8.8) the reduction energy of the reaction

between the nebulised compound and hydrogen must be sufficient to produce excited molecules.

Part II of this work consists of three Chapters; the first two concern the behaviour and determination of sulphur and phosphorus species in the nitrogen-hydrogen flame (system not in thermal equilibrium), whilst the third concerns the analytical uses of the nitrous oxide-hydrogen flame (system thought to be in thermal equilibrium) and some suggestions for future work.

CHAPTER VII

THE BEHAVIOUR OF SULPHUR SPECIES IN A NITROGEN-HYDROGEN DIFFUSION FLAME AND IN A SHIELDED (SEPARATED) AIR-HYDROGEN FLAME[104]

7.1 Introduction

A.F.S. and A.A.S. are extremely versatile techniques and can be used for the determination of traces of many metals, however, both these techniques depend on the absorption of resonance radiation by discrete atoms. The principal resonance lines of sulphur are in the vacuum ultra-violet region of the spectrum (1807, 1820 and 1826 Å) where the background absorption of the oxygen in the atmosphere and also of the burning flame gases is excessively high, thus making any A.A.S. or A.F.S. measurements extremely difficult.

By utilising certain hydrogen containing flames it was found possible to determine sulphur by measuring the emission of the S_2 species.

Emission of the S_2 species has previously been reported by Crider[133] who used a shielded air-hydrogen flame to determine sulphur dioxide and sulphuric acid aerosols in certain atmospheres. Brody and Chaney[134] have

reported the measurement of S_2 emission. In this instance, organic vapours leaving a gas chromatographic column with nitrogen as carrier gas were mixed with a volume of oxygen to give the same nitrogen:oxygen ratio as occurs in air. This mixture was then burnt with hydrogen as fuel gas in a specially designed flame photometer burner. The use of narrow band-pass interference filters and a photomultiplier resulted in a very sensitive and selective detector for sulphur compounds. The limit of detection at 394 mu was O.6 ppm of sulphur. Unfortunately it is applicable only to organic sulphur compounds which can be handled directly by gas phase chromatography.

7.2 Experimental

Apparatus

A Unicam SP900A flame-emission-absorption spectrophotometer, fitted with standard air-acetylene (rectangular) and air-propane (circular) burner heads, was used. Flame shielding for the pre-mixed flame was as described in the text.

Fuel Gas: Hydrogen, from a cylinder.

Diluent gas: Nitrogen, from a cylinder.

Supporting gas: Air, from a compressor unit.

Reagents

Sulphuric Acid, 10^{-1}F - Prepared by diluting analytical-reagent grade sulphuric acid, standardising and subsequently adjusting the solution to exactly 10^{-1}F.

1 ml of 10^{-1}F sulphuric acid ≡ 3200 ug of sulphur.

Sulphur Dioxide solution, 10^{-2}F - Prepared by passing gaseous sulphur dioxide into deaerated distilled water. A sample of this stock solution was oxidised by hydrogen peroxide (neutralised) and standardised alkalimetrically. An aliquot of the stock solution was then diluted with deaerated distilled water to be exactly 10^{-2}F in sulphur dioxide.

1 ml of 10^{-2}F sulphur dioxide ≡ 320 ug of sulphur.

7.3 The Nitrogen-Hydrogen Flame

This flame was maintained on the standard 1.8 x 7.5 cm air-acetylene emission burner-head.

Nitrogen was used as the nebulising gas at an optimised pressure of 15 p.s.i. by using the conventional SP900A nebulising system, and hydrogen was introduced at the base of the burner in the usual way at a pressure sufficient to prevent the flame from lifting off. These optimised values were obtained by monitoring the emission at 384 mu of a solution of sulphur

dioxide sprayed into the flame. The flame itself is completely colourless, apart from occasional flashes produced by the entrance of particles of air-borne dust. With these settings of gas pressure, the hydroxyl emission at about 300 to 320 mu was very weak, being about 40 times less intense than in a pre-mixed air-hydrogen flame on the same burner head. Similarly, the emission at 589 mu of a 2 ppm sodium solution was about 50 times less than in an air-hydrogen flame.

The effect of introducing air into the flame through a third jet[41] was to increase the flame temperature, and the emissions from sodium and the hydroxyl band, while drastically decreasing the S_2 emission at 384 mu. With nitrous oxide, no emission at 384 mu could be detected.

These large decreases in the S_2 emission on adding even a trace of air or nitrous oxide are probably due to the increase in the temperature of the central regions of the flame and to the presence of oxygen containing species in the central regions of the flame, both these effects could inhibit the formation of S_2.

The emitting S_2 species are congregated in the cool inner regions of the flame, and it was observed that a dark blue emission was most marked about 3 cm above the burner top for $\leq 10^{-2}$F sulphur dioxide solution and

spread down to the top of the burner head for stronger solutions. Subsequent experiments revealed that the temperatures in the outer regions of the flame were much higher than those in the sharply defined blue-emitting zone, while those immediately above the burner head were too low to produce appreciable concentrations of the S_2 species (see 7.8).

A total consumption burner only gave weak S_2 emission. This was thought to be due to the turbulent nature of this type of flame, thus causing an ingress of air with a subsequent rise in temperature.

7.4 Identity of Nebulised Species

All of the inorganic sulphur-containing species examined showed varying degrees of the characteristic blue emission at 384 mu. These were sulphuric acid, ammonium sulphate, sodium and potassium sulphite, potassium metabisulphite, sodium thiosulphate, ammonium thiocyanate, sodium dithionite, sulphur dioxide, hydrogen sulphide and also thioglycollic acid. The maximum response per mole of sulphur present was obtained from sulphur dioxide and hydrogen sulphide solutions. The order of emissive response in unbuffered solutions was found to be sulphide > sulphite > thiosulphate >> ammonium sulphate $\simeq$ sulphuric acid >> alkali-metal sulphates. The emission from alkali sulphites and sulphides was found to increase about 100-fold upon acidification, presumably because of the release of sulphur

dioxide and hydrogen sulphide. Thiosulphates did not show the same marked increase, however, because of their tendency to deposit sulphur before entry into the flame. Sulphates do not give increased response upon acidification and the emission of sulphuric acid is about 600 times less than that of an equimolar solution of sulphur dioxide. Further, the optimum height for emission from sulphates is higher up in the flame, about 4 cm above the burner head, thus indicating that they require a higher temperature for the production of S_2 species. On the other hand, these species are not produced in any appreciable concentration, even from sulphates, in the hotter pre-mixed air-hydrogen flame. This is most probably due to dissociation and perhaps oxidation of the S_2 molecules to sulphur monoxide in such a milieu. A compromise between the requirements of higher temperature and the breakdown of the S_2 species was subsequently obtained by shielding a pre-mixed hydrogen-air flame with a cooled borosilicate glass or quartz sheath. This device and the results obtained are described subsequently.

In the unshielded diffusion flame, however, a spectral scan of the emission obtained by spraying a 5×10^{-3} F aqueous sulphur dioxide solution with a 0.018 mm slit-width yielded the results shown in Fig.XXIII.

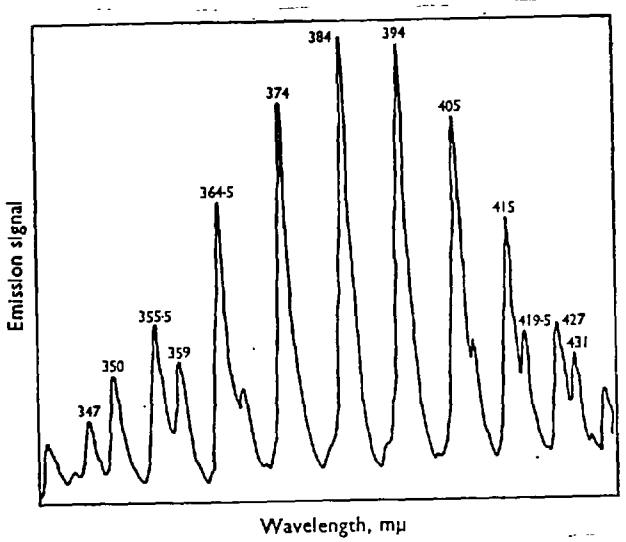

FIG. XXIII.

Emission spectrum of S_2 species obtained by nebulising a 5×10^{-3} M aqueous solution of sulphur dioxide into a hydrogen - nitrogen diffusion flame and measuring with a Unicam SP900A spectrophotometer under the following conditions: slit-width, 0·018 mm; gain, 2·0; band-width, 1; hydrogen-pressure reading, 10 cm on a butyl phthalate filled manometer; nitrogen pressure, 15 p.s.i.; and top of burner head, 3 cm below centre of analysing monochromator slit

The only emission due to sulphur corresponds to the S_2 species.[135] On increasing the gain of the instrument further weak S_2 emission bands were observed down to ca 260 mu. The main S_2 bands and their relative intensities are listed in Table 27.

TABLE 27

Main S_2 Emission Bands

Wavelength mu	Relative Intensity	Upper Vibrational Level	Lower Vibrational Level
431	3	1	13
427	4	0	12
419.5	4	1	12
415	6	0	11
405	9	0	10
394	10	0	9
384	10	0	8
374	9	0	7
364.5	7	0	6
359	3	1	6
355.5	4	0	5
350	3	1	5
347	2	0	4
342	1	1	4
337	0.5	0	3

The relative intensities of these lines are not corrected for variations in the spectral response of the monochromator and photomultiplier.

Other possible species such as SO, which has a band peaking at 320 mu and SH with two bands at 324 and 328 mu, were not detected. Similar results were obtained with an argon-hydrogen flame.

The intensity of the emission does not exhibit a linear response with the concentration of sulphur dioxide in the nebulised solution. This was first of all suspected to be because of the ease of oxidation of sulphur dioxide in aqueous solution, but careful control of conditions to eliminate this possibility, up to the point of entry into the flame, revealed that while oxidation could lead to appreciable diminutions in signal, the non-linear response was inherent in the system, and investigation showed that the signal was, in fact, proportional to the square of the concentration. The signal was also found to vary linearly with the square of the monochromator slit-width. In this latter respect, the behaviour strongly resembles that observed in the measurement of flame background.

The relatively high energies required to excite the S_2 emission down to 260 mu must be of a chemiluminescent origin because the thermal energy of the flame is insufficient to account for this emission. The fact that the S_2 emission is proportional to the square of the sulphur concentration

suggests that the production of the S_2 species is kinetically controlled by a two stage reaction:

e.g. First Reaction

$$SO_2 \xrightarrow{H_2} S - H$$
$$SO_2 \xrightarrow{H_2} S - O$$

Second Reaction

$$S - H + S - H \longrightarrow S_2^* + H_2$$
$$S - H + S - O \longrightarrow S_2^* + OH$$

The above scheme is only a possible outline of the type of process responsible, but any similar mechanism to the above would account for the chemiluminescent origin and the square law calibration curve of the S_2 species.

The S_2 spectrum was emitted by a sulphur electrodeless discharge tube operating at 30 Watts. The main flame-emission bands were observed at 384 mu (0.8) and 394 mu (0.9) and these transitions occur from the lowest vibrational level of the excited state to high vibrational levels of the ground state and thus would not be expected to be observed in absorption. No absorption of the 303.3 mu (3.0), 299.7 mu (4.0) bands[135] or any ground state band emitted from a sulphur discharge tube was observed in the diffusion flame even when nebulising high concentrations (ca 0.1 M) of sulphur dioxide solution. This is to be expected for two reasons, firstly,

as the S_2 emission is chemiluminescent, the ground state population of the S_2 species will be low, and secondly the oscillator strength for molecular transitions are very low.[13]

7.5 Calibration Curves for Sulphur Dioxide

Linear calibration curves were obtained over the range 10^{-4} - 10^{-2}F solution of sulphur dioxide, i.e. 3.2 to 320 ppm, by using the dependence of signal on the square of the concentration. A limit of detection of 5×10^{-5}F (1.6 ppm), i.e. corresponding to signal to noise ratio of 1:1, was observed. Special care must be taken to prevent oxidative degradation of the very dilute solutions of sulphur dioxide. This can be done by thoroughly degassing the distilled water, used to make up the solutions, with nitrogen. Solutions containing less than 10 ppm of sulphur dioxide were found to be very unstable and they were always made up prior to measurement.

7.6 Determination of Sulphates by S_2 Emission

Because it is difficult to convert most sulphur-containing species quantitatively into sulphites and to stabilise the sulphite ion, but relatively easy to convert them into sulphates which are very stable, an effort was made to improve the production of S_2 species from sulphate ion by using the flame-shielding arrangement described briefly above.

A borosilicate-glass tube, 15 cm long by 2.4 cm i.d., was placed over the 1.75 cm diameter burner stem of a conventional (circular) Unicam propane-emission burner-head and attached at the lower end by a rubber stopper. By systematic variation of conditions it was found that optimum stability and sensitivity for S_2 emission from sulphate solutions was obtained, as before, when the nebulising gas pressure was 15 p.s.i. and the hydrogen flow-rate slightly more than sufficient to prevent strike-back. When the shielded flame is lit, a penetrating whine is heard that dies out after about 1 minute when the shield has warmed up and condensation has ceased. If the hydrogen pressure is too high the whine will persist. These experiments also revealed that the tube must be vertical to allow even diffusion and removal of water vapour, and that the best results were obtained with the glass tube projecting about 10 cm above the burner-head, with the latter situated about 0.5 cm above the bottom of the entrance slit of the monochromator. Because of the higher temperature of this flame only low emission was observed from S_2 species, but when the outer surface of the screening tube was cooled by a current of cold air from a piece of pressure tubing (0.65 cm bore) placed about 1 cm away from the wall of the tube, level with the entrance slit of the monochromator, and at right angles to the line between the slit and the tube, good S_2

emission signals were obtained. The screening tube should be allowed to warm up for 1 minute before switching on the cooling air, as this minimises problems that may arise otherwise from condensation of water vapour. The glass slide placed over the entrance slit prevents dust being blown into the monochromator. With the arrangement described, condensation was observed only on cooling very strongly, and even then only in the lower regions of the tube below the burner-head.

The above flame is colourless inside the protective tube, but is shown up as a separated flame upon spraying a sodium solution into it. Within the tube the signal obtained from a 2 ppm solution of sodium was about 15 times less than that for an unprotected pre-mixed hydrogen-air flame and about three times greater than that of the nitrogen-hydrogen diffusion flame. The signal obtained from an ammonium sulphate solution in this flame was about 30 times greater than in the nitrogen-hydrogen diffusion flame, while the emission from a sulphur dioxide solution was virtually identical. The ratio for the S_2 signals from ammonium sulphate and sulphur dioxide of the same sulphur content is about 1:20 far the protected flame and about 1:600 for the diffusion flame. Varying signals are obtained for different salts. Thus, where a standard solution of sulphuric acid gave an S_2 emission at 384 mu, corresponding to 21 scale-

divisions, equimolar solutions of ammonium sulphate, sodium sulphate and potassium sulphate gave 23, 12 and 12, respectively. This problem of differing response with different accompanying cations may be readily resolved, however, by passing these salts over a cation-exchange resin in the hydrogen-ion form, so that all forms of sulphate are converted into sulphuric acid. In this way the ease with which most inorganic sulphur species may be converted into sulphate, and also organic compounds via the oxygen flask (or some other simple combustion process), may provide a simple and reasonably sensitive procedure for the determination of all sulphur species.

Interferences

Interference studies were carried out with a 5×10^{-3}F solution of sulphuric acid and optimised flame conditions, with the shielded air-hydrogen flame. The following did not interfere when present in 10-fold molar excess (i.e. concentrations of 5×10^{-2}F), hydrochloric, perchloric, boric, acetic, oxalic, hydrobromic, nitric and orthophosphoric acids, and hydrogen peroxide. In addition, 40-fold excesses of hydrochloric and perchloric acids, and hydrogen peroxide (i.e. 1×10^{-1}F concentrations) could be tolerated. Above 10-fold excess, orthophosphoric, nitric and hydrobromic acids caused a decrease in the S_2 signal, while acetic and oxalic acids caused an increase in signal. These effects are probably caused by

viscosity and surface tension, respectively,which modify the nebuliser efficiency. In all instances, however, good calibration graphs for sulphur may be obtained in the presence of any of these acids. The enhancing or depressive action of individual acids may, therefore, be accaunted for by dilution or by making up to a pre-determined strength. Cationic interferences were not investigated because the method proposed here wauld operate best following ion-exchange separation of the sulphuric acid.

7.7 Calibratian Curves for Sulphuric Acid

As before, the method shows a linear dependence of signal upon the square of the concentration of the sulphate ion. The detection limit (signal-to-noise ratio = 1) for sulphuric acid corresponded to 10^{-4}F (about 3 ppm of sulphur) and linear calibratian graphs were obtained over the range 6.4 to 500 ppm. For cancentrations of sulphur greater than 100 ppm the diffusion flame gives adequate sensitivity and is simpler to use than the shielded flame.

7.8 Flame Temperatures

Whereas the temperatures of most flames can only be determined satisfactorily by spectroscopic techniques such as line reversal, the diluted diffusion flame and the caoled, separated flame used in these experiments give temperatures of only a few hundred degrees centrigrade, and they can

thus be measured fairly reliably by inserting a calibrated thermocouple probe into the flame. In these studies, the end of the ceramic cover of an industrial pyrometer was removed so that the small area of the exposed thermocouple junction did not greatly affect the flow of the flame gases. While it was recognised that the presence of hydrogen might give rise to catalytic effects that could cause spuriously high temperatures, the temperatures at the centre of the flame were found to be only about 300° to 400°C, and no catalytic glow could be detected. The thermocouple was calibrated in a heating-bath up to 360°C by using a standardised 0° to 360°C thermometer. It will be seen from Table 28 that the temperature varies from top to bottom of the hydrogen-nitrogen diffusion flame and from the inner to the outer regions of the flame. The temperatures recorded at the centre of the flame are minimum temperatures obtained by lateral movement of the probe at a constant height, while those recorded at the outer edge are maximum temperatures similarly obtained. The flame conditions used to obtain the temperatures recorded in Table 28 were those used under the conditions recommended for the determination of sulphur dioxide, with distilled water aspirating through the flame. The temperature at the centre of the flame, at the position most favourable for analysis, corresponds to 390°C. These temperatures are recorded only to the nearest 10°C because of the temperature gradient across the flame.

TABLE 28

Approximate Flame Temperatures in the Hydrogen-Nitrogen Diffusion Flame during Aspiration of Distilled Water

Distance above burner head cm	Temperature, °C: Centre of flame (minimum)	Edge of flame (maximum)
1	280	810
2	330	830
3	370	840
4	410	850
5	450	850
6	480	850

Without water aspirating through the flame the centre temperatures at about 3 cm above the burner head increased by 30°C, while the outside temperatures increased by only 5°C. Aspiration of acetone and methanol caused a slight temperature decrease in the centre of the flame and a more marked temperature increase at the outer edge of the flame.

Temperature measurements were made in the hydrogen-air shielded flame by exposing a further length of the probe from its ceramic sheath and

inserting it into the flame from the base of the tube via a slit cut in the rubber bung. Temperature measurements were made with the probe situated mid-way between the edge of the burner-head and the flame shield. The flame conditions were those used for the sulphuric acid determination, with distilled water spraying through the flame. In this instance, the temperature measurements recorded in Table 29 were obtained with, and without, air cooling of the outer sheath. Without water aspirating in

TABLE 29

Approximate Flame Temperatures in the Lower Part of the Shielded Air-Hydrogen Flame during Aspiration of Distilled Water

Distance above burner head cm	Temperature at outer edge of flame, °C	
	Cooled sheath	Uncooled Sheath
0.1	280	420
0.3	320	440
1.0	360	520

Temperatures at centre of flame > 1400°C.

this type of flame the temperature increased by 10° to 20°C. When the wires leading to the thermocouple were bent so that the thermocouple junction was over the centre of the burner-head, inner flame temperatures in excess of 1400°C were reached. As the thermocouple was uncalibrated in this region, this latter temperature can only be regarded as approximate.

7.9 Procedures

a) Calibration Curve for Sulphuric Acid (32 to 160 ppm of Sulphur) in the Air-Hydrogen Flame

Transfer by pipette 1 to 5 ml aliquots of 10^{-1}F sulphuric acid into a series of 100 ml standard flasks and dilute to volume with distilled water. Assemble the sheathed burner unit, as described previously, and arrange it so that the burner-head is opposite and projecting 0.5 cm above the level of the bottom of the entrance slit of the monochromator, and in such a position that a stream of cooling air may be directed on the glass shielding tube at right angles to the plane it subtends with the slit, and at the same level.

Set the air pressure at 15 psi and the hydrogen flow-rate to about 16 cm on the butyl phthalate filled manometer of the fuel-meter, and light the flame. Allow the shield to warm up for 1 minute before switching on the cooling air. Set the monochromator at 384 mu, select the emission

mode of the flame spectrophotometer and select the band-width setting No.3. Spray the calibration solution into the flame, allowing sufficient time for equilibrium to be reached and record the emission intensity at 384 mu. The background signal, which is very low (about 1.5 divisions, with a slit of 0.05 mm and an instrumental gain of 3.3) should be deducted from the observed signal. The calibration graph, prepared by plotting emission intensity against the square of the sulphur concentration, is virtually linear in this range. For higher concentrations (above 100 ppm of sulphur) of sulphuric acid the procedure with the hydrogen-nitrogen diffusion flame is simpler to operate and possesses adequate sensitivity.

b) Calibration Curve for Sulphurous Acid (3.2 to 16 ppm of Sulphur) in the Nitrogen-Hydrogen Diffusion Flame

Transfer by pipette 1 to 5 ml aliquots of the freshly prepared 10^{-2}F sulphur dioxide solution into a series of 100 ml standard flasks and dilute to volume with freshly de-aerated water. Set up the air-acetylene burner-head so that the headplate is about 3 cm below the centre of the entrance slit of the monochromator. Set the nitrogen pressure to 15 p.s.i. and the hydrogen flow-rate to about 10 cm on the manometer, and light the flame. Clean the spray unit and burner-head by aspirating distilled water through it and by using the same optical settings on the instrument as above,

nebulise the sulphur dioxide solutions as expeditiously as possible to avoid aerial oxidation of the dissolved sulphur dioxide. Prepare calibration graphs of signal against the square of sulphur concentration, as before.

Calibration graphs can be conveniently prepared only over a 5-fold concentration range because of the square law relationship. When sulphuric acid solutions containing more than 100 ppm of sulphur are being sprayed into the nitrogen-hydrogen diffusion flame, the burner-head should be situated about 4 cm below the centre of the slit to allow for the maximum S_2 signal being obtained higher up in the flame for sulphuric acid than for sulphurous acid. A convenient working range for sulphuric acid in the diffusion flame corresponds to 160 to 500 ppm of sulphur.

7.10 Discussion

The above experiments show how useful progress may be made in molecular-emission studies in relatively cool flames, despite the steady trend in atomic-absorption spectroscopy and flame-emission spectroscopy for hotter flames to be used to produce greater populations of refractory metal atoms and thus to improve signals. The behaviour of sulphur species in hydrogen flames has been discussed in this Chapter and it has been shown how an analytical method for sulphur may be devised, irrespective of the original

species, by oxidation to sulphate, conversion to sulphuric acid and measurement of S_2 emission in a hydrogen-nitrogen diffusion flame or, more sensitively in a shielded pre-mixed hydrogen-air flame, in which the sheath is cooled to prevent dissociation of the S_2 species produced in the hot lower region of the enclosed flame. The sensitivity of the method for sulphur dioxide is considerably greater than that for sulphuric acid in either flame, and shows greater and more extensive emission than that observed by Crider[133] in a shielded air-hydrogen pre-mixed flame without cooling.

The method proposed here appears to have considerable promise in relation to previously described flame (atomic)-emission methods that have depended on depressive effects on the emission of elements such as barium[136] or strontium,[137] or on indirect methods involving the precipitation of barium sulphate[138] and determination of the excess of barium. Because of the square law dependence on sulphate-ion concentrations, the method suggested here is most attractive for a narrow range of sulphur concentrations. Work is now in progress on the application and adaptation of the principle of the procedure to the analysis of technical materials. Meanwhile, it is apparent that the sulphur content of most organosulphur compounds could be readily obtained directly by the above procedure, following rapid

decomposition by an oxygen-flask[139] technique. Although the method based on sulphite is considerably more sensitive than that based on sulphate, the ease with which most organic and inorganic sulphur species may be oxidised quantitatively to sulphate, and when necessary converted into sulphuric acid by ion exchange, suggests that the sulphuric acid procedure may be generally more useful for most analytical problems.

CHAPTER VIII

THE BEHAVIOUR OF PHOSPHORUS SPECIES IN A NITROGEN-HYDROGEN DIFFUSION FLAME[131]

8.1 Introduction

Like sulphur, phosphorus has its principal atomic resonance lines in the vacuum ultraviolet region of the spectrum (1775, 1783 and 1788 Å) thus making any A.A.S. or A.F.S. measurements extremely difficult (see 7.1).

The more usual methods of determining phosphorus by emission spectroscopic techniques involve indirect procedures such as the depressive effect of phosphate on the emission of calcium and magnesium.[140] However, only a somewhat limited range of phosphate concentrations can be examined using a given concentration of calcium. In addition, the method is not very sensitive; using a 100 ppm calcium solution the estimated limit of detection is ca 30 ppm of phosphorus.

A direct method with a limit of detection of 3 ppm has been described by Brite[141] who measured the emission from the continuum at 540 mu obtained using an oxy-hydrogen total consumption burner and organic solvents.

Davis and co-workers[142] also used an oxy-hydrogen turbulent flow burner to obtain a limit of detection in aqueous solution of 8 ppm at a slit-width of 2.0 mm. Wide slits are necessary to gather sufficient energy from the continuum. The use of organic solvents unfortunately leads to high background emission which must be subtracted from the phosphorus emission. Another method,[134] which is also concerned with the determination of phosphorus in organic compounds, involves the measurement of the emission from the H-P-O species. In this instance, organic vapours leaving a gas chromatographic column with nitrogen as carrier gas were mixed with a volume of oxygen to give the same nitrogen:oxygen ratio as occurs in air. This mixture is then burnt with hydrogen as fuel gas in a flame photometer burner. The use of narrow band-pass interference filters and a photomultiplier resulted in a very sensitive and selective detector for sulphur and phosphorus compounds. The limit of detection at 526 mu is 0.0063 ppm of phosphorus. However, it is applicable only to organic phosphorus compounds and in this instance only to those which can be handled directly by gas phase chromatography.

The atomic spectrum of phosphorus has been excited in an oxy-acetylene flame supported by an organic solvent.[143] The limit of detection (in absolute ethanol) at the 2536 Å non-resonance line, was 400 ppm.

By utilising the nitrogen-hydrogen flame it was found possible to determine phosphorus by measuring the emission of the H-P-O species.

8.2 Experimental

Apparatus

As previously described (see 7.2).

Reagents

Phosphoric acid, 10^{-2}M. Prepared by dilution of A.R. syrupy phosphoric acid, standardisation and subsequent adjustment to be exactly 10^{-2}M.

1 ml 10^{-2}M H_3PO_4 ≡ 310.2 ug.P.

8.3 The Emission of Phosphorus in the Nitrogen-Hydrogen Flame

The green phosphorus emission which is at a maximum at 528 mu is easily obtained by nebulising a solution of phosphoric acid into the nitrogen-hydrogen diffusion flame. As with sulphur it was observed that the signal was drastically decreased by the addition of small amounts of air or nitrous oxide through a third jet in the base of the burner.[41] Temperature measurements show that this is due to the increase in flame temperature obtained through the addition of oxygen. The green colour was noted to be particularly prominent in the cool (ca 350°C) inner regions of the diffusion flame, and was most marked about 1 cm above the burner

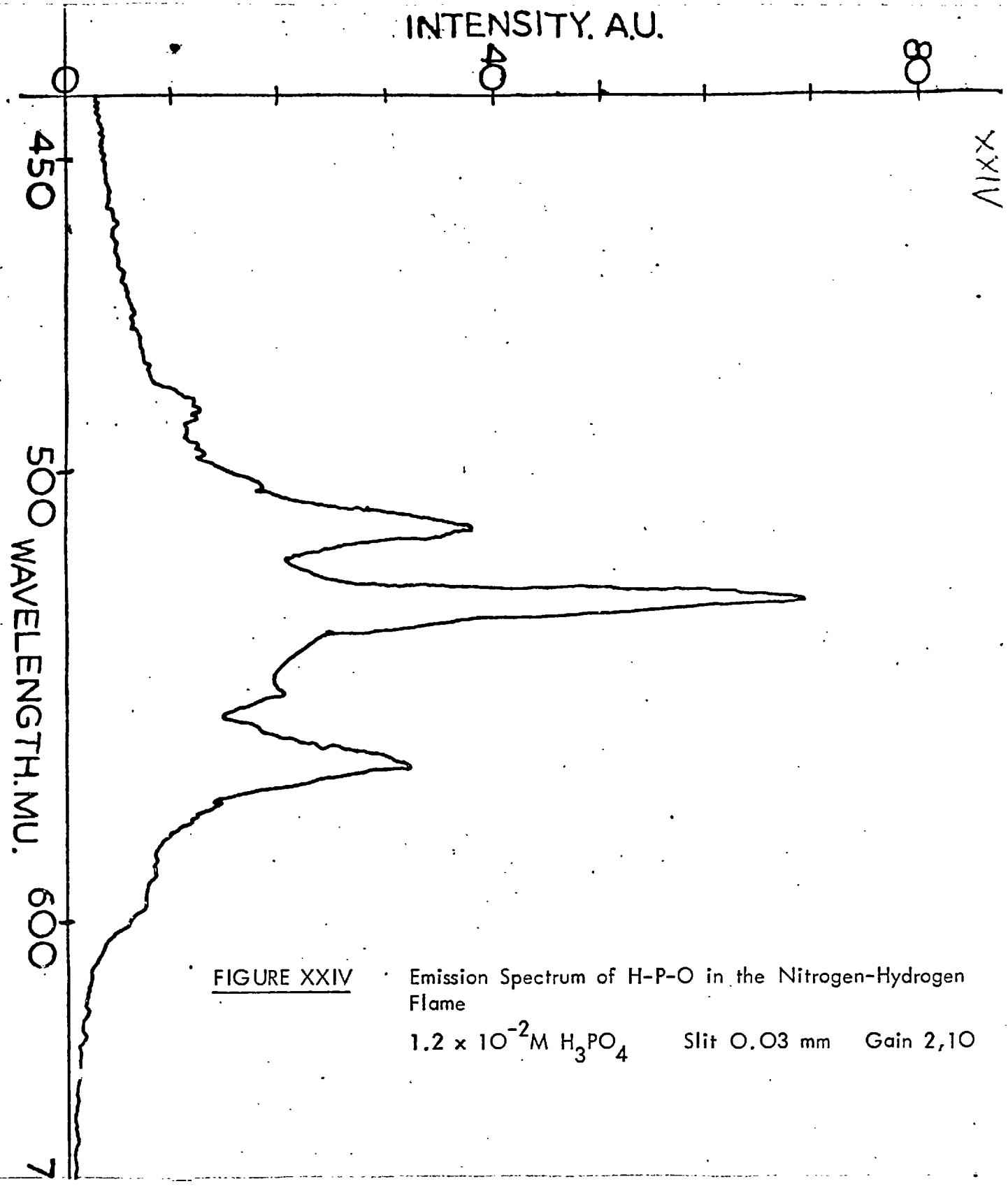

FIGURE XXIV · Emission Spectrum of H-P-O in the Nitrogen-Hydrogen Flame

1.2×10^{-2}M H_3PO_4 Slit 0.03 mm Gain 2,10

top (280°C) - cf Fig.XXIV.

A total consumption burner gave very weak emission, probably because the turbulent nature of the flame causes considerable entrainment of air and hence gives rise to a much hotter flame than that obtained with the simple diffusion flame. The separated air-hydrogen flame, previously designed to aid the breakdown of sulphates, etc. and so give a more uniform sulphur emission, (see 7.6), was also investigated. The experimental arrangement was exactly as used for the sulphur studies, i.e. a premixed air-hydrogen flame with a cooled borosilicate glass or quartz sheath, but it was found not to be particularly advantageous in this instance. The green colour persisted for a long time after nebulisation had been terminated. This was thought to be due to condensation of phosphoric acid or phosphorus pentoxide onto the walls of the glass sheath and subsequent slow evaporation. The emission occurred mainly around the cool walls of the sheath, just above the burner (ca 350°C) and was only slightly more intense (ca 20%) than in the normal diffusion flame.

8.4 Identity of Nebulised Species

The green emission was most marked in the nitrogen-hydrogen diffusion flame on nebulising phosphoric acid. Metallic phosphates gave only a very weak signal, due to lack of dissociation in the relatively cool flame

(see 8.6). A spectral scan of the emission obtained whilst spraying a 1.2×10^{-2}M aqueous solution of phosphoric acid using a slit width of 0.03 mm is shown in Fig.XXIV. The air-hydrogen flame yielded an exactly similar spectrum, but was at least 5 times less intense and there was much more of a continuum. Also, the comparatively large background emission of the air-hydrogen detracts from the sensitivity towards dilute phosphoric acid solutions. In all cases, emission corresponds only to the H-P-O species.[135]

The intensity of the emission at 528 mu in the diffusion flame exhibits a linear response with phosphoric acid solutions over the range 0.2-500 ppm phosphorus. Larger amounts of phosphorus were not examined.

The fact that the H-P-O emission is proportional to the phosphorus concentration suggests that the H-P-O species is produced by direct reduction of phosphoric acid molecules by hydrogen.

8.5 Calibration Curves for Phosphoric Acid

Linear calibration curves were obtained over the range 0.2-500 ppm of phosphorus. A limit of detection (signal:noise = 1) of 0.1 ppm of phosphorus was obtained using a slit-width of 0.17 mm. (At higher slit-widths, light leakage occurred.) The use of filters and a more sensitive photomultiplier (EMI 9601B used in these studies) would give considerably

lower limits. There is also little doubt that the use of a simple filter system to isolate the desired radiation around 528 mμ would improve the sensitivity considerably.

The emission at 528 mu was not very dependent upon the hydrogen pressure or the height of measurement in the flame, since the emission extends uniformly over most of the inner flame regions. Measurements were optimised with the hydrogen pressure somewhat above that necessary to prevent flame lift-off and with the top of the burner 1 cm below the bottom of the monochromator slit.

8.6 Interference Studies

a) Response towards various phosphorus containing compounds

Table 30 shows the emission signals obtained for 2×10^{-3}M solutions of various phosphorus containing compounds commonly encountered. The readings were obtained by taking the peak (at 528 mu) to trough (at 515 mu) height from a recorded spectrum. This was considered to be more accurate than an emission signal reading at 528 mu because it eliminates any errors due to a slight sodium continuum at 528 mu. The peak to trough height was found to vary almost linearly with phosphoric acid concentration.

TABLE 30

Emission Intensities of Various Phosphorus Compounds in the Nitrogen-Hydrogen Diffusion Flame

Compound (2×10^{-3}M)	Emission Reading (Peak to Trough Height)
H_3PO_4	48
NaH_2PO_4	15
Na_2HPO_4	6
Na_2HPO_3	5.5
$Na_4P_2O_7$	5
$CaHPO_4$	12

All readings were obtained with a slit width of 0.05 mm and a gain of 3,10.

The sodium:phosphorus ratio has a critical effect on the emission signal; as the ratio increases the emission signal decreases.

The addition of hydrochloric acid (up to 1 M concentrations) to the solution of disodium hydrogen phosphate or an increased hydrogen flow to the diffusion flame did not produce any increased response.

b) Effect of extraneous ions

Interference studies (Table 31) were carried out with a 5.6×10^{-3}M solution of phosphoric acid and optimised diffusion flame conditions. Following the addition of the extraneous ion all solutions were made O.2M with respect to hydrochloric acid. As before, all readings are peak (at 528 mu) to trough (515 mu) heights to eliminate any light leaks in the monochromator, etc. In this instance the slit width was O.O3 mm and the gain was 3,9.

The only increased response is caused by copper and arises from the very strong Cu-Cl and Cu-H band emission in the same region as the phosphorus emission.

It would appear from Table 31 that the degree of the depressive effects are not related to the volatility or stability of the various metal phosphate species produced in the flame. However, there is some correlation between these effects, and the ease with which the species may be reduced by hydrogen. This may be illustrated with reference to lead phosphate ($Pb_3(PO_4)_2$) which has a higher melting point than either lithium phosphate (Li_3PO_4) or sodium pyrophosphate ($Na_4P_2O_7$). Also iron(III) forms a more stable phosphate species than sodium or lithium but gives less interference.

These effects could be explained if cool diffusion flames unlike normal premixed flames are assumed to produce atoms from nebulised metal salt solutions by reduction as well as by thermal breakdown. In a normal premixed flame no interference due to compound formation is observed with sodium because its salts are thermally unstable at temperatures of about 2000°C. Phosphate compounds of elements such as cadmium, cobalt, lead and iron are much more likely to be reduced by hydrogen at temperatures of about 400°C than aluminium, lithium, sodium and magnesium.

The depressive effect increases with increasing concentrations of sodium and lithium. This appears to be a mass action effect because increasing the metal chloride concentration must increase the free metal concentration in the flame and, as the chlorides would be expected to be thermally less stable than the corresponding phosphates, the dissociation of the metal phosphate would be depressed. The effect is not so marked with increasing concentrations of cadmium, lead and iron suggesting that the breakdown process is not entirely thermal, but a reduction process which is not very dependent on metal ion concentration.

The effect of varying concentrations of sodium, lithium and calcium on a solution 5×10^{-3}M in phosphoric acid and O.2M in hydrochloric acid

TABLE 31

Effect of some Extraneous Ions on the H-P-O Emission in the Diffusion Flame

Interference	Concentration (M)	Emission Reading (peak to trough)
-	(5.6×10^{-3}M) in H_3PO_4	54
$AlCl_3$	1×10^{-2}	0
NH_4Cl	1×10^{-2}	55
$NH_4Fe(SO_4)_2$	1×10^{-2}	22
	5×10^{-2}	17
$(NH_4)_2Fe(SO_4)_2$	1×10^{-2}	21
$CdCl_2$	1×10^{-2}	21
	5×10^{-2}	13
$CaCl_2$	1×10^{-2}	4
$CoCl_2$	3×10^{-2}	22
$CuCl_2$	3×10^{-2}	>100
$Pb(NO_3)_2$	1×10^{-2}	32
	5×10^{-2}	23
LiCl	1×10^{-2}	18
	3×10^{-2}	2
NaCl	1×10^{-2}	6
	2×10^{-2}	3
$MgCl_2$	1×10^{-2}	2

is shown in Fig.XXV. It can be seen that the sodium and calcium curves show a pronounced change of slope at a metal concentration equivalent to that of the phosphorus, corresponding to the formation of NaH_2PO_4 $CaHPO_4$. Lithium does not show such a change until the metal concentration is twice that of phosphorus, i.e. corresponding to the formation of Li_2HPO_4. The curve then levels off until the metal: phosphorus ratio (3:1) corresponds to the formation of Li_3PO_4. A gradual decrease is then observed with further increase in lithium concentration. Thus it would appear that the lithium dihydrogen phosphate is not as stable as the diffusion flame as the dilithium hydrogen phosphate. The following reaction presumably occurs:

$$2LiH_2PO_4 \longrightarrow Li_2HPO_4 + H_3PO_4$$

It is a well known fact that lithium salts differ in behaviour from the corresponding sodium and potassium salts.

At low calcium:phosphorus ratios (< O.5) the calcium curve is linear and when extrapolated gives a ratio of 1:1. As this ratio increases above O.5, the curve becomes rounded and extrapolation tends to give a calcium: phosphorus ratio of 1.5:1. Thus it would appear that in solutions containing a two or more fold molar excess of phosphoric acid over calcium,

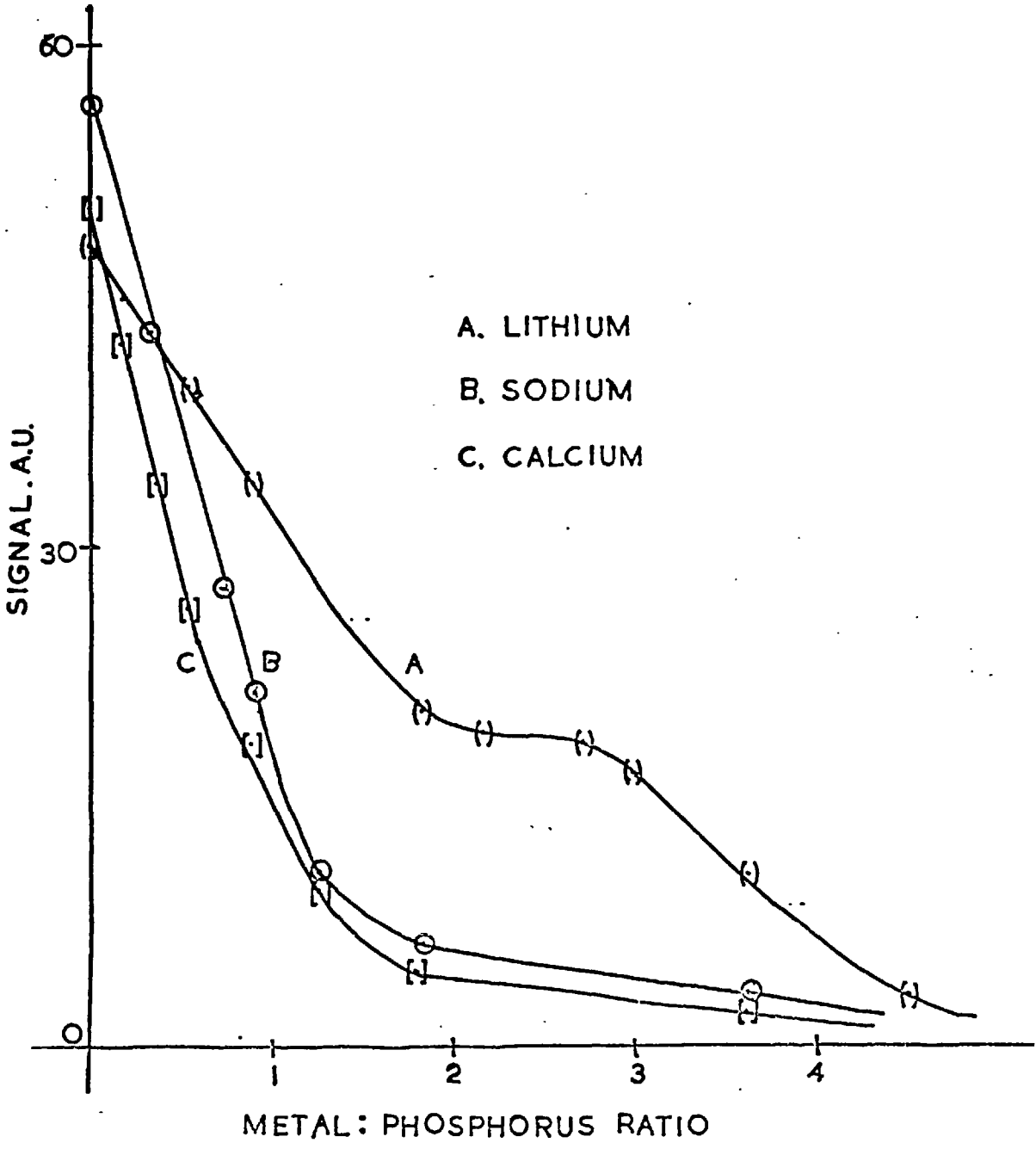

FIG.XXV.

Effect of Lithium, Sodium and Calcium on the H-P-O Emission.

then calcium hydrogen phosphate ($CaHPO_4$) is formed, but in solutions containing greater amounts of calcium, calcium phosphate is formed ($Ca_3(PO_4)_2$).

However, the following acids when present in a 50-fold molar excess over a 7×10^{-4}M H_3PO_4 solution produced no variation in response $\geq \pm$ 5%:acetic acid, hydrobromic acid, hydrochloric acid, nitric acid, oxalic acid, sulphuric acid and tartaric acid.

The present of a 100-fold molar excess of the above, except for sulphuric acid, produced ca 10% decrease in signal, due to the increased viscosity and attendant depression of nebulisation. Strong solutions of sulphuric acid produced an increase of signal, due to the intense blue S_2 emission.

The presence of 10% $^v/_v$ of organic solvents miscible with water all produced ca 85% decrease in signal. This was almost identical to the effects which they produced with the S_2 emission. The reason is not known at present but is most probably due to the quenching action of CH, CHO radicals etc. Temperature measurements proved that the decrease in signal is not due to any increase of temperature.

c) Removal of cationic interferences

It was considered that cationic interferences could generally be overcome by removal on a cation exchange resin in its hydrogen form.

According to Samuelson[144] phosphate can be quantitatively separated on such a resin from the following cations: Li^+, Na^+, K^+, NH_4^+, Rb^+, Cs^+, Mg^{2+}, Ca^{2+}, Sr^{2+}, Ba^{2+}, Zn^{2+}, Mn^{2+}, Co^{2+}, Ni^{2+}, Cd^{2+}, Al^{3+} and Fe^{3+}.

Alternatively, it should also be possible to remove phosphate on an anion exchange resin and then regenerate it as phosphoric acid. Using such a method it might be possible to obtain a concentration step.

Some preliminary measurements have been carried out using the cation exchange resin Zeo-Carb 225.

It was found that aluminium, calcium, iron and magnesium could be removed quantitatively simply by shaking a few grams of the washed Zeo-Carb resin in the hydrogen form with about 30 ml of solution containing phosphoric acid plus a 10-fold molar excess of the interfering ion. The interference caused by sodium and potassium was reduced by about 95%, but this is presumably because Zeo-Carb 225 is not a very efficient resin for monovalent cations neither is the batch-method of exchange.

There is no reason to assume that most other cationic interferences cannot be removed by such methods.

The separated air-hydrogen flame was also investigated, but did not show any advantage in minimising interferences. In fact the results

tended to be inferior, owing to the higher temperature and the increased emission signals from easily excited elements. Elements and compounds with emission bands and lines close to 528 mu gave large apparent increases in signal.

8.7 Procedure

Calibration Curve for 3.1-31 ppm P.

Pipette 1-10 ml of 10^{-2}M phosphoric acid into a series of 100 ml volumetric flasks and dilute to volume with distilled water. Nebulise into the nitrogen-hydrogen diffusion flame under the following experimental conditions: nitrogen pressure 15 p.s.i., hydrogen flow rate ca 15 cm on the di-n-butylphthate filled manometer, top of burner-head 1 cm below bottom of monochromator slit, slit width 0.06 mm, gain 3,10 and bandwidth 3. Measure the emission in the usual way at 528 mu and plot signal against concentration of phosphorus. Other concentration ranges (between 0.3 and 310 ppm) can be prepared by suitable dilution.

Linear calibration curves over the ranges 3.1-31 ppm and 31-620 ppm of phosphorus have also been prepared in a similar manner, but in the presence of 0.1M concentrations of hydrochloric acid. In these instances slit-widths of 0.06 mm and 0.02 mm and gains of 3,10 and 3,5 respectively were used.

8.8 Other Species Observed in the Nitrogen-Hydrogen Diffusion Flame

a) Tin[132]

If a solution of stannous chloride is nebulised into the nitrogen-hydrogen diffusion flame, red Sn-H emission can be observed in the inner regions of the flame. This emission is directly proportional to the tin concentration. On adding hydrochloric acid to the tin solution, blue SnCl emission (as well as the red Sn-H emission) can be observed in the centre of the flame just above the burner-head. With hydrobromic acid green SnBr emission is observed.

The effect of adding a trace of air to the diffusion flame whilst nebulising stannous chloride solution, is to replace the red Sn-H emission by a blue emission due to Sn-O. The principal spectral characteristics of the above species are listed in Table 32.

b) Indium

If a solution of indium nitrate is nebulised into the diffusion flame, In_2, In-O and In-H emission can be observed. On adding chloride ions to the indium solution, intense In-Cl bands are emitted, similarly In-Br and In-I bands can be obtained (no In-F spectrum was observed). Using the indium halide band systems it is possible to determine the halide ions (e.g. bromide can be determined in a thousand-fold excess of chloride). The principal spectral characteristics of these species are listed in Table 32.

TABLE 32

Spectral Characteristics of Tin and Indium Species in the Nitrogen-Hydrogen Flame

Species	Type of Spectrum	Main Band or Continuum Range (mu)	Approximate Limit of Detection ppm
Sn-H	Sharp Band	609.5	2
Sn-Cl	Continuum	490 - 390	-
Sn-Br	Continuum	540 - 400	-
Sn-O	Banded Continuum	560 - 360	5
In_2	Banded Continuum	400 - 360	-
In-O	Continuum	450 - 410	-
In-H	Bands	591	-
In-Cl	Sharp Bands	360	1
In-Br	Sharp Bands	376	1
In-I	Sharp Bands	410	1

CHAPTER IX

THE NITROUS OXIDE-HYDROGEN FLAME IN SPECTROSCOPIC ANALYSIS

9.1 Introduction

Recent trends in spectroscopic analysis have been directed towards producing premixed high temperature flames. These have the effect of increasing sensitivity in thermal-emission studies and of eliminating the depressive matrix effects produced by elements which form refractory oxides in atomic-absorption spectroscopy. To this end the nitrous oxide-acetylene flame is finding considerable application in the latter technique[37] whilst oxy-acetylene is perhaps one of the most versatile flames in emission spectroscopy.[35,145]

One of the biggest general disadvantages of these flames is that they are nearly all accompanied by a high background emission (the oxy-hydrogen flame being an exception except over the OH band region). This is not usually very stable and hence leads to less precision and high limits of detection in both emission and absorption measurements, regardless of the method of amplifying the photomultiplier signal. In addition to this general disadvantage most high temperature flames present other problems,

e.g. the high burning velocity of the nitrous oxide-acetylene flame makes burner design difficult and the explosive nature of some mixtures such as oxy-cyanogen and oxy-acetylene renders them unsatisfactory for routine use. An equally important consideration is the anomalously high electronic excitation (chemiluminescence) which occurs in some premixed flames when metal salts are present.[124] This phenomenon is particularly strong in the reaction zone of premixed flames of hydrocarbons with air or oxygen and especially with acetylene. The oxy- and air-hydrogen flames which have very favourable background radiations unfortunately seem to be completely free from this anomalous behaviour. Hence there appears to be no one flame at present which is completely acceptable as an atom reservoir for either thermal-emission or atomic-absorption studies. The present interest in atomic-fluorescence spectroscopy makes the need for alternative high temperature, low background flames even more pressing.

It is the purpose of this Chapter to illustrate some of the advantages to be gained from the use of a premixed nitrous oxide-hydrogen flame in the above areas. Firstly this flame has a low burning velocity, unlike oxy-acetylene or oxy-hydrogen, and thus the burner design and gas mixtures are not critical. In fact it has been found that this flame can be burned on practically any commercially available burner-head whether it be designed for emission or absorption measurements. In addition the risk of an

explosion is no greater with this flame than with any other commonly in use.

The background radiation is also very much lower in the nitrous oxide-hydrogen flame than in any other hydrocarbon flame because there is no possibility of emission from carbon species. The only background emission obtained under normal operating conditions results from OH bands at ca 3000-3200Å (present in all flames), the NH band at ca 3360 Å and from the NH_2 radical or the reaction between O and NO in the visible region.[124] Inspite of this the temperature of this flame is not thought to be any lower than the usually recognised high temperature flames such as nitrous oxide-acetylene, oxy-hydrogen, etc.

In theory it would seem that this flame is well suited to the requirements of thermal-emission, atomic-absorption and atomic-fluorescence measurements.

At this time evidence is presented to support its use in thermal-emission studies.

9.2 Experimental

a) Apparatus

A Unicam SP900A flame-emission absorption spectrophotometer was used.

Fuel Gases - Hydrogen, from a cylinder.

Acetylene, from a cylinder.

Supporting Gases - Nitrous oxide, from a cylinder.

Air, from a compressor.

Diluent Gas - Nitrogen, from a cylinder.

b) Burner Design

Initially the flame was burned on the 7 x 1.5 cm long air-acetylene emission burner-head supplied as standard with the Unicam SP900A thermal-emission/atomic-absorption flame spectrophotometer. This burner has a 1 cm square series of 13 holes near one end and is particularly suitable for use with this instrument. A steady flame condition could be maintained by nebulising on 15 p.s.i. of nitrous oxide and supplying between 1.5 and 2.5 p.s.i. of hydrogen. The nitrous oxide was supplied to the burner via the normal instrumental nebulising system, but the hydrogen was supplied via an external gauge and was led into the burner through the jet fitted in the base of the burner stem.

Below 1.5 p.s.i. of hydrogen, the flame struck back and above 2.5 p.s.i. the primary reaction cones became unstable. This flame gave good emission signals from zinc (2139 Å) and cadmium (2288 Å) solutions, but relatively poor signals for aluminium (3944 and 3962 Å) which required a more fuel rich flame (ca 3 p.s.i.). Very good aluminium emission

signals were obtained using the circular air-propane burner head also supplied as standard for use with the Unicam SP900A. In the instance steady flame conditions were achieved with 15 p.s.i. of nitrous oxide and between 2.5 and 3.5 p.s.i.of hydrogen.

In the early stages of this work the flame was lit with a small volume of nitrogen flowing through an auxiliary jet in the burner base[41] to eliminate any danger of flashback. When the required pressures of nitrous oxide and hydrogen had been supplied, the nitrogen flow was turned off. The reverse procedure was carried out when the flame was extinguished. This precaution is not essential, however, as only a comparatively weak "pop" is experienced when a flashback occurs.

c) Reagents

Aluminium solution, 1000 ppm:- 1 g of aluminium foil was dissolved in 40 ml of 1:1 analytical grade hydrochloric acid and diluted to 1 litre with distilled water. 1 ml ≡ 1000 ug Al.

9.3 Spectrum of the Nitrous Oxide-Hydrogen Flame

The flame background of the nitrous oxide-hydrogen flame burning on the circular air-propane Unicam emission head only showed above the yellow primary cones strong OH band emission between ca 3000-3200 Å, weak NH band at ca 3370 Å and a steady continuum from 3500-6000 Å

which is partly due to the reaction between NO and O . The primary cones, in addition, exhibit in the visible region the ammonia a- band system which is now known to be due to the NH_2 radical.[124]

The air-acetylene flame background, measured under as similar conditions as possible and also above the primary cones, was ca 4-5 times greater than the nitrous oxide-hydrogen flame at ca 4000 Å. Measurements in the primary cones showed an even greater difference in background radiation.

9.4 Applications to Thermal Emission of Aluminium

Thermal emission from aqueous solutions of aluminium at the resonance lines 3944 and 3962 Å was observed throughout the length of the nitrous oxide-hydrogen flame, but reached a maximum about 3-4 cm above the top of the burner-head. Optimum emission was obtained using the Unicam circular air-acetylene burner-head with a slightly fuel rich flame. A typical spectral plot is shown in Fig.XXVI. In agreement with other workers[44] using different flames the emission at 3962 Å is about twice that at 3944 Å .

The limit of detection (signal:noise of 1) measured at 3962 Å with a slit width of 0.015 mm was ca 4 ppm aluminium. Calibration curves were plotted over the range 20-500 ppm. Between 20-200 ppm they

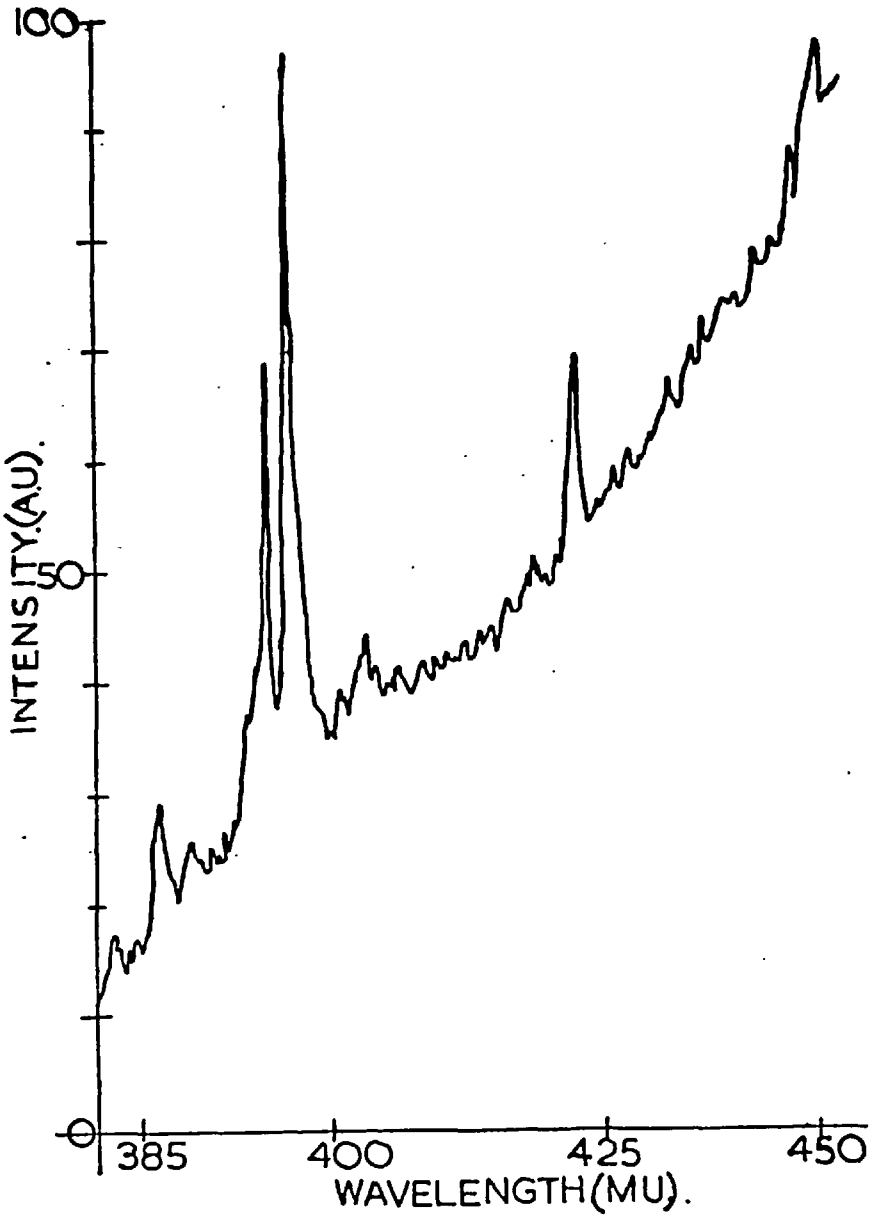

FIGURE XXVI Spectrum of 1000 ppm Aluminium Solution in the Nitrous Oxide-Hydrogen Flame

Slit 0.008 mm Gain 3,5

were linear, but above this a slight curvature developed. Above 1000 ppm aluminium the log-log slope was ca 0.56, indicating appreciable self-absorption.

The above limit of detection could be lowered by diluting the aqueous phase with organic solvents. For example, a solution 20% in iso-propyl alcohol doubled the response of an equivalent concentration of aluminium in aqueous solution. This illustrates further advantages of this flame, that is, the ability to handle solutions containing high concentrations of inflammable organic solvents without risk or modifying the operating conditions.

A solution containing 10 and 20% of glycerol on the other hand caused a signal decrease of 12 and 21% respectively. The differences in the nebulisation rates largely account for these effects.

9.5 Procedure for 20-2000 ppm Aluminium

Pipette 2 - 20 ml of the standard aluminium solution into 100 ml calibrated flasks and dilute to volume with distilled water. Nebulise aliquots of the solutions using 15 p.s.i. nitrous oxide and measure the emission at 3962 Å with a hydrogen pressure of 3.5 p.s.i., slit width 0.015 mm, gain 3,10, bandwidth 3 and with the top of the burner-head 3-4 cm below the centre of the monochromator slit.

9.6 Other Emitting Species

Preliminary measurements indicate that this flame may be used with advantage in thermal-emission studies of elements other than refractory oxide producers such as aluminium. For example, zinc, cadmium and lead which normally show negligible emission characteristics in air-hydrogen flames[44] are readily excited in the nitrous oxide-hydrogen flame. The emission from these elements extends throughout the flame and is usually strongest some 2 cm above the top of the burner-head. Comparable emission signals for zinc and cadmium in an air-acetylene flame can only be obtained by taking measurements from the primary reaction zone about 2 mm above the top of the burner-head. The emission from lead atoms in the nitrous oxide-hydrogen flame is about twice that obtained in the primary reaction zone of an air-acetylene flame.

Easily excited elements such as calcium can also be measured with advantage in the nitrous oxide-hydrogen flame. The ionic calcium doublet at 3934 and 3968 Å are quite strong and exhibit an intensity ratio of 2:1. Emission signals at these lines cannot normally be obtained either in air-hydrogen or air-acetylene flames. Table 33 shows a comparison of the emission signals of the above elements in normal nitrous oxide-hydrogen, air-hydrogen and air-acetylene flames on the Unicam SP900A spectrophotometer. Measurements were made in the primary reaction zone and

TABLE 33

Thermal-Emission Studies in the Nitrous Oxide-Hydrogen Flame

Element	Concentration ppm	Wavelength Å	Slit-width mm	Gain	Emission Signals: air-hydrogen a	air-hydrogen b	air-acetylene a	air-acetylene b	nitrous oxide-hydrogen a	nitrous oxide-hydrogen b
Zn	2000	2139	0.1	3,10	0	0	28	0	25	17
Cd	1000	2288	0,05	3,10	4	0	168	3	92	60
Pb	200	4057	0.01	3,5	4	0	42	23	62	78
Ca	40	3934	0.01	2,0	0	0	background	0	86	20
	40	3968	0.01	2,0	0	0	too high	0	46	10
Al	1000	3962	0.012	3,5	0	0	0	0	45	90

a corresponds to emission in primary reaction zone

b corresponds to emission 3 cm above top of burner head

3 cm above the top of the burner-head.

The calcium emission from the ionic doublet at 3934 and 3968 Å was quite strong and at low calcium concentrations (< 0.05 ppm) was more intense than that from the 4227 Å resonance line. Table 34 shows that the 4227 : 3934 Å intensity ratio for various concentrations.

TABLE 34

Calcium Intensity Ratio Measurements

Calcium Concentration ppm	Emission Intensity Ratio 4227 : 3934 Å
40	29
16	21
4	8
2	5
0.4	3.3
0.1	1.4
0.05	1

Hence at low calcium concentrations appreciable ionization must occur in this flame. This extent of the ionization at these wavelengths is known to be very sensitive to traces of the other easily ionised elements, e.g. K, Rb, Cs, etc., and hence emission at these wavelengths is not

normally used analytically. However, in their absence, e.g. in distilled water, a more sensitive determination of calcium becomes possible in the nitrous oxide-hydrogen flame.

9.7 Suggestions for Future Work

a) Chemiluminescent Studies

Chemiluminescence generally occurs from the primary reaction zone of a flame where non-equilibrium conditions exist. This region is, in general, quite small in normal flames and can be increased in size by either burning the flame at greatly reduced pressure[42] which requires rather complex apparatus or by efficient burner design. The author has found that it is possible to enlarge the primary reaction zone of normal flames by maintaining the flame on a quartz tube instead of a conventional burner-head. An air-acetylene flame maintained on a 3 mm internal diameter quartz tube gave a flame with a 2 cm long primary reaction zone. This type of burner gave ca 3 times greater chemiluminescent emission intensities than the conventional Unicam air-acetylene burner (the cones of this last flame were ca 5 mm long). Another useful asset of the 'tube' burners is that chemiluminescence generally reaches a maximum intensity for relatively fuel lean flames and conventional metal burner-heads tend to overheat unlike simple quartz tube burners.

Strong chemiluminescent emission of antimony, arsenic, bismuth, cadmium, mercury and tellurium was observed from the primary reaction zone of an air-acetylene burner maintained on a 3 mm internal diameter quartz tube. Estimated limits of detection were between 2 and 10 ppm. A nitrous oxide-acetylene flame was maintained on a 2 mm internal diameter quartz tube, quite safely, and a 2-3 cm long, red primary reaction zone was observed. Emission studies, using this flame, are in progress at the present time. Chemiluminescence is a potentially sensitive and very rapid, qualitative and semi-quantitative method of analysis that does not require the use of complex instrumentation, elaborate burners or sources, and should prove quite useful analytically.

b) Augmented Flames

It is possible to augment a flame with an electrical discharge (microwave and R.F. augmented flames have already been mentioned (see 6.9)). The atomic hydrogen torch[146,147,148] is a good example of an augmented flame and consists of an electrical discharge between tungsten electrodes (about 2 mm apart) in a hydrogen diffusion flame. The discharge produces atomic hydrogen which exothermically recombines about 1-2 cm above the arc giving a high temperature low background region. Tungsten wire can be melted in this arc and lower melting point metals (e.g. iron) are rapidly vaporised. The author[148] has made some

preliminary emission studies of the atomic hydrogen torch by nebulising various species into the arc and promising results have been obtained. This system should prove useful for both F.E.S. and A.F.S. where hot low background flames are required.

It is possible to augment a nitrogen-hydrogen diffusion flame by placing carbon or tungsten electrodes in the flame (about 1.5 cm apart) just above the burner-top and connecting the electrodes to a 15,000 Volt (20 m.a.) transformer. A diffuse discharge is produced and this discharge has been found to raise the temperature of the useful, oxygen-free inner regions of the diffusion flame considerably without increasing the background. With further development it should be possible to obtain low background, oxygen-free flames with temperatures comparable to normal premixed flames.

c) Emission of Organic Compounds

The analytical aspects of flame emission from organic compounds have only been recently reported.[149,150] These studies have used air and oxy-hydrogen flames to obtain the spectra of various diatomic species (e.g. C_2, CH, CN and NH). In addition the determination of certain hydrocarbons dissolved in methanol[150] was described using the measurements of C_2 emission at 516 mu.

The author has observed strong emission from various methanolic solutions of organic compounds using the nitrogen-hydrogen flame and the enlarged primary reaction zone of an air-hydrogen flame maintained on a 5 mm internal diameter quartz tube. In addition to the species mentioned above, bands of the following species have been observed: CCl, NO and NH_2. The C_2:CH emission intensity ratio appears to bear some relationship to the actual C:H ratio of the compound. The CN:NH:NO emission intensity ratio is dependent on the form of the nitrogen present (e.g. -CN, $-NH_2$, > NH, ⩾ N, $-NO_2$).

A further aspect of 'organic emission' under study, is that produced by passing helium or argon (at atmospheric pressure) through a microwave discharge and then passing the excited helium or argon atoms into a nitrogen-hydrogen flame that contains nebulised organic compounds. Thus it should be possible to produce highly excited organic species at a low temperature. Alternatively a high voltage diffuse discharge (see above) can also be used to excite organic species in the nitrogen-hydrogen flame.

REFERENCES

1. G. Kirchhoff, Pogg.Ann., 1860, 109, 275.
2. G. Kirchhoff and R. Bunsen, Pogg.Ann., 1860, 110, 161.
3. H. Lundegårdh, 'Die quantitative Spektralanalyse der Elemente', Fischer, Jena; Part I, 1929; Part II, 1934.
4. A.C.G. Mitchell and M.W. Zemansky, 'Resonance Radiation and Excited Atoms', University Press, Cambridge, 1961.
5. A. Walsh, Australian Patent No.23041/53, 1953 (Spectrochim.Acta, 1955, 7, 108).
6. C.T.J. Alkemade and J.M.W. Milatz, J.Opt.Soc.Amer., 1955, 45, 583.
7. R.W. Wood, Phil.Mag., 1905, 10, 513.
8. E.L. Nichols and H.L. Howes, Phys.Rev., 1923, 22, 425, and 1924, 23, 472.
9. R.M.Badger, Z.f.Phys., 1929, 55, 56.
10. R. Mannkopff, Verhandl.d.Deutsch Phys.Ges., 1933, 14, 16.
11. J.W. Robinson, Anal.Chim.Acta, 1961, 24, 254.
12. C.T.J. Alkemade, Proc.Xth Colloquium Spectroscopium Internationale (1962), Spartan Books, Washington, D.C., 1963, p.143.

13. J.D. Winefordner and T.J. Vickers, Anal.Chem., 1964, 36, 161.

14. J. D. Winefordner and R.A. Staab, Anal.Chem., 1964, 36, 165.

15. J.D. Winefordner and R.A. Staab, Anal.Chem., 1964, 36, 1367.

16. J.D. Winefordner, J.M. Mansfield and C. Veillon, Anal.Chem., 1965, 37, 1049.

17. T.S. West, Lecture to Society for Analytical Chemistry, Burlington House, London, 6th October, 1965. cf. Analyst, 1966, 91, 69.

18. R.M.Dagnall, T.S. West and P. Young, Talanta, 1966, 13, 803.

19. L. De Galan, W.W. McGee and J.D. Winefordner, Anal.Chim.Acta, 1967, 37, 436.

20. K. Yasuda, Anal.Chem., 1966, 38, 592.

21. M. L. Parsons, W.J. McCarthy and J.D. Winefordner, Appl.Spec., 1966, 20, 223.

22. P. P. Pringsheim, 'Fluorescence and Phosphorescence', Interscience, New York, 1949.

23. R.M. Dagnall, K.C. Thompson and T.S. West, Talanta, 1967, 14, 1467.

24. J.D. Winefordner, M.L. Parsons, J.M. Mansfield, and W.J. McCarthy, Spectrochim.Acta, 1967, 23B, 37.

25. D.R. Jenkins, Spectrochim.Acta, 1967, 23B, 167.

26. J.D. Winefordner, W.J. McCarthy and M.L. Parsons, Spectrochim.Acta, 1967, 23B, 25.

27. R.M. Dagnall, K.C. Thompson and T.S. West, Talanta, 1968, 15, In Press.

28. R.M. Dagnall, K.C. Thompson and T.S. West, Anal.Chim.Acta, 1966, 36, 269.

29. C. Veillon, J.M. Mansfield, M.L. Parsons and J.D. Winefordner, Anal.Chem., 1966, 38, 204.

30. J.I. Dinnin, Anal.Chem., 1967, 39, 1491.

31. J.B. Willis, Spectrochim.Acta, 1967, 23A, 811.

32. C.D. West and D.N. Hume, Anal.Chem., 1964, 36, 412.

33. H.C. Hoare and R.A. Mostyn, Anal.Chem., 1967, 10, 1153.

34. H.C. Hoare, R.A. Mostyn and B.T.N. Newland, Anal.Chim.Acta, 1968, 40, 181.

35. R. Hermann and C.T.J. Alkemade, 'Chemical Analysis by Flame Photometry', Interscience, New York, London, 1963.

36. J.I.Dinnin and A.W. Helz, Anal.Chem., 1967, 39, 1489.

37. M.D. Amos and J.B. Willis, Spectrochim.Acta, 1966, 22, 1325.

38. D.N. Armentrout, Anal.Chem., 1966, 38, 1235.

39. T.S. West and X.A. Williams, Anal.Chem., 1968, In Press.

40. W.T. Elwell and J.A.F. Gidley, 'Atomic Absorption Spectrophotometry', 1st Ed. Pergamon, Oxford, 1961, p.9.

41. R. Mackison, Analyst, 1964, 89, 745.

42. A.G. Gaydon and H.G. Wolfhard, 'Flames, Their Structure, Radiation and Temperature', Chapman and Hall, London, 1960.

43. H.D. Fleming, Spectrochim.Acta, 1967, 23B, 207.

44. J.A. Dean, 'Flame Photometry', McGraw Hill, New York, London, 1960.

45. G.I. Goodfellow, Anal.Chim.Acta, 1966, 36, 132.

46. G.H. Morrison and H. Freiser, 'Solvent Extraction in Analytical Chemistry', J. Wiley, London, 1957.

47. D.W. Ellis and D.R. Demers, Anal.Chem., 1966, 38, 1943.

48. L.R.P. Butler and A. Strasheim, Pittsburg Conference on Anal.Chem. and Appl.Spec., March, 1964.

49. J.V. Sullivan and A. Walsh, Spectrochim.Acta, 1965, 21, 721.

50. C. Ellis, A.A. Wells and F.F. Heyroth, 'The Chemical Action of U.V. Rays', Reinhold Publishing Corp., U.S.A., 1941, p.36. (W.Hittorf, Wiedermann's Annalen XXI, p.138.)

51. J.J. Thomson, Phil.Mag., 1891, 32, 321 and 445.

52. D.A. Jackson, Proc.Roy.Soc., 1928, A121, 432.

53. W.F. Meggers, J.Opt.Soc.Amer., 1948, 38, 7.

54. W.F. Meggers and F.O. Westfall, J.Res.Nat.Bur.Std., 1950, 44, 447.

55. W.F. Meggers and K.G. Kessler, J.Opt.Soc.Amer., 1950, 40, 737.

56. L. Bovey and H. Wise, AERE-R, 1959, 2976.

57. C.H. Corliss, W.R. Bozmann, and F.O. Westfall, J.Opt.Soc.Amer., 1953, 43, 398.

58. F.S. Tomkins and M. Fred, J.Opt.Soc.Amer., 1957, 47, 1087.

59. E.F. Warden, R.G. Gutmacher and J.G. Conway, Appl.Opt., 1963, 2, 707.

60. D.J. Hunt and G. Pish, J.Opt.Soc.Amer., 1956, 46, 87.

61. R.J. Hull and H.H. Stroke, J.Opt.Soc.Amer., 1961, 51, 1203.

62. B. Budick, R. Novick, and A. Lurio, Appl.Opt., 1965, 4, 229.

63. W.E. Bell, A.L. Bloom and J. Lynch, Rev.Sci.Instr., 1961, 32, 688.

64. R.T. Atkinson, G.D. Chapman and L. Krause, J.Opt.Soc.Amer., 1965, 55, 1269.

65. D.H. Burling, V. Czajkowski and L. Krause, J.Opt.Soc.Amer., 1967, 57, 1162.

66. N.S. Ham and A. Walsh, Spectrochim.Acta, 1958, 88, 12.

67. P. Warneck, Appl.Opt., 1962, 1, 721.

68. Y. Tanaka and P.G. Wilkinson, J.Opt.Soc.Amer., 1955, 45, 1044.

69. H. Okabe, J.Opt.Soc.Amer., 1964, 54, 478.

70. E.W. Schlag and F.J. Comes, J.Opt.Soc.Amer., 1960, 50, 866.

71. P.G. Wilkinson and E.T. Byram, Appl.Opt., 1965, 4, 581.

72. Y. Tanaka and M. Zelikoff, J.Opt.Soc.Amer., 1954, 44, 254.

73. Vaughan, J.M., J.Opt.Soc.Amer., 1964, 54, 318.

74. M. Zelikoff, H. Wyckoff, M. Aschenbrand and R. Loomis, J.Opt.Soc.Amer., 1952, 42, 818.

75. A. Davison, A. Giacchetti and R.W. Stanley, J.Opt.Soc.Amer., 1962, 52, 447,

76. E.B.M. Steers, Proc.Soc.Anal.Chem., 1965, 2 (No.107), 108.

77. N.P. Ivanov, L.V. Minervina and S.V. Boranov, Tr.Vses.Nauchn-Issled.Inst.Khim.Reactivov.i.Osobo.Chistykh.Khim.Veshchestr., 1965, No.27, 276.

78. N.P. Ivanov, L.V. Minervina, S.V. Boranov and L.G. Pofralidi, Zh.Analit.Khim., 1966, 21, 1129.

79. E.W. Richards, Spectrochim.Acta, 1966, 22, 158.

80. R.M. Dagnall, K.C. Thompson and T.S. West, Talanta, 1967, 14, 551.

81. J.R. Hollahan, J.Chem.Ed., 1966, 43, A401 and 43, A497.

82. E. Jacobsen and G.R. Harrison, J.Opt.Soc.Amer., 1949, 39, 1054.

83. A.T. Forrester, R.A. Gudmundsen, and P.O. Johnson, J.Opt.Soc.Amer., 1956, 46, 339.

84. K.M. Aldous, R.M. Dagnall and T.S. West, Analyst, 1968, Submitted for publication.

85. M.J. Al Ani, R.M. Dagnall and T.S. West, Analyst, 1967, 92, 597.

86. R. Mavrodineanu, and R.C. Hughes, Spectrochim.Acta, 1963, 19, 1309.

87. R.M. Dagnall, K.C. Thompson and T.S. West, Talanta, 1967, 14, 557.

88. C.S. Rann and A.W. Hambly, Anal.Chim.Acta, 1965, 32, 346.

89. J.E. Allan, Spectrochim.Acta, 1962, 18, 259.

90. Chakrabarti, Anal.Chim.Acta, 1967, 39, 293.

91. J.A. Dean and J.G. Simms, Anal.Chem., 1963, 35, 699.

92. C. Candler, 'Atomic Spectra', Hilger and Watts, London, 1964.

92A. J.D. Winefordner, M.L. Parsons, J.M. Mansfield, and W.J. McCarthy, Anal.Chem., 1967, 39, 436.

93. J.A. Dean and J.E. Adkins Jr., Analyst, 1966, 91, 709.

94. J. A. Dean and W.J. Carnes, Analyst, 1962, 87, 743.

95. B.M. Gatehouse and J.B. Willis, Spectrochim.Acta, 1961, 17, 710.

96. R.A. Mostyn and A.F. Cunningham, Anal.Chem., 1967, 39, 433.

97. R.M. Dagnall, K.C. Thompson and T.S. West, Talanta, 1967, 14, 1151.

98. W.R. Brode, 'Chemical Spectroscopy', Wiley, London, 1943.

99. P.T. Gilbert, Anal.Chem., 1962, 34, 211R.

100. G.B. Marshall and T.S. West, Talanta, 1967, 14, 823.

101. D.C. Manning, J. Volmer, and F. Fernandez, Atomic Absorption Newsletter (Perkin-Elmer), 1967, 6, (No.1), 17.

102. A.G. Leiga and J.A. McInally, J.Opt.Soc.Amer., 1967, 57, 317.

103. C.W. Frank, W.G. Schrenk and C.E. Meloan, Anal.Chem., 1966, 38, 1005.

104. R.M. Dagnall, K.C. Thompson ond T.S. West, Analyst, 1967, 92, 506.

105. P. T. Gilbert Jr., Proc.Xth Colloquium Spectroscopium Internationale, Spartan, Washington, D.C., 1963, p171.

106. W. Slavin, C. Sebens and S. Sprague, Atomic Absorption Newsletter, 1965, 4, 341.

107. W.F. Meggers, C.H. Corliss and B.F. Scribner, Tables of Spectral Line Intensities, Part I, National Bureau of Standards, Monograph 32, 1961.

108. S.F. Pellicori, C.A. Johnson and F.T. King, Appl.Opt., 1966, 5, 1916.

109. F.A. Jenkins and H.E. White, Fundamentals of Optics, McGraw-Hill, London, 1957, p.522.

110. S.F. Pellicori, Appl.Optics, 1964, 3, 361.

111. C.W. Sill, Anal.Chem., 1961, 33, 1584.

112. G. Honcia and K. Krebs, Optik, 1962, 19, 156.

113. K.M. Greenland, Endeavour, 1952, 11, 143.

114. J.V. Ramsay and Y. Tanaka, J.Sci.Instr., 1965, 42, 334.

115. R.M. Dagnall, K.C. Thompson and T.S. West, XXIst I.U.P.A.C. Congress, Prague, 1967.

116. R.S. Hobbs, Personal Communication.

117. J.H. Runnels, and J.H. Gibson, Anal.Chem., 1967, 39, 1398.

118. G.G. Vurek, Anal.Chem., 1967, 39, 1599.

119. J.E. Rosenthal and C.F. Eyer, J.Electrochem.Soc., 1965, 112, 68.

120. A.J. McCormack, S.C. Tong and W.D. Cooke, Anal.Chem., 1965, 37, 1470.

121. H. A. Moye, Anal.Chem., 1967, 39, 1441,

122. K.C. Thompson, Unpublished Studies.

123. R.S. Hobbs, G.F. Kirkbright, M. Sargent and T.S. West, Anal.Chim.Acta, 1968, Submitted for Publication.

124. A.G.Gaydon, 'The Spectroscopy of Flames', Chapman and Hall, London, 1957.

125. J.D. Winefordner, W.W. McGee, J.M. Mansfield, M.L. Parsons and K.E.Zacha, Anal.Chim.Acta, 1966, 36, 25.

126. R. Mavrodineanu and H. Boiteux, 'Flame Spectroscopy', John Wiley and Sons Inc., New York, London, Sydney, 1965.

127. J.H. Gibson, W.E.L. Grossman and W.D. Cooke, Anal.Chem., 1963, 35, 266.

128. R. Mavrodineanu, Spectrochim.Acta, 1961, 17, 1016.

129. K.C. Thompson, Unpublished Studies.

130. V.I. Vedeneyev, L.V. Gurvich, V.N. Kondrat'yev, V.A. Medvedev and Ye.L. Frankevich, Bond Energies, Ionisation Potentials and Electron Affinities, Edward Arnold Ltd., London, 1966.

131. R.M. Dagnall, K.C. Thompson and T.S. West, Analyst, 1968, In Press.

132. R.M. Dagnall, K.C. Thompson and T.W. West, Analyst, 1968, submitted for publication.

133. W.L. Crider, Anal.Chem., 1965, 37, 1770.

134. S.S. Brody and J.E. Chaney, J.of Gas Chromatography, 1966, February, p.42.

135. A.G. Gaydon and R.W.B. Pearse, The Identification of Molecular Spectra, Chapman and Hall, London, 3rd Ed., 1965.

136. W.M. Shaw, Anal.Chem., 1958, 30, 1682.

137. S. Ikeda, Sci.Rep.Res.Inst. Tôhoku Univ., 1957, 9A, 16.

138. R.D. Strickland and C.D. Maloney, Amer.J.Clin.Path., 1954, 24, 1100.

139. A.M.G. MacDonald, Analyst, 1961, 86, 3.

140. W.A. Dippel, C.E. Bricker and N.H. Furman, Anal.Chem., 1954, 26, 553.

141. D.W. Brite, Anal.Chem., 1955, 27, 1815.

142. A. Davis, F.J. Dinan, E.J. Lobbett, J.D. Chazin and L.E. Tufts, Anal.Chem., 1964, 36, 1066.

143. R.K. Skogerboe, A.S. Gravatt, and G.H. Morrison, Anal.Chem., 1967, 39, 1602.

144. O. Samuelson, 'Ion Exchange in Analytical Chemistry', J. Wiley and Sons Inc., New York, 1953, p.124.

145. V.A. Fassel and D.W. Golightly, Anal.Chem., 1967, 39, 466.

146. I. Langmuir, Ind. and Eng.Chem., 1927, 19, 667.

147. H.J. Van Den Bold, and J.A. Smit, Physica, 1946, 12, 475.

148. R.M. Dagnall, K.C. Thompson and T.S. West, Anal.Chim.Acta, 1968, In Press.

149. J.W. Robinson and V. Smith, Anal.Chem.Acta, 1966, 36, 489.

150. P.F. McCrea and T.S. Light, Anal.Chem., 1967, 39, 1731.

151. Handbook of Chemistry and Physics, 48th Edition, Chemical Rubber Publishing Co., Cleveland, Ohio, U.S.A., 1967.

PUBLICATIONS

Analytical Applications of Metal-Acetylacetonate Complexes in Toluene.

Talanta, 1967, 14, 715.

An Investigation of some Experimental Parameters in Atomic-Fluorescence Spectroscopy.

Anal.Chim.Acta, 1966, 36, 269.

Microwave-Excited Electrodeless Discharge Tubes as Spectral Sources for Atomic-Fluorescence and Atomic-Absorption Spectroscopy.

Talanta, 1967, 14, 551.

The Atomic-Fluorescence Spectroscopic Determination of Selenium and Tellurium.

Talanta, 1967, 14, 557.

The Fluorescence Characteristics and Determination of Antimony.

Talanta, 1967, 14, 1151.

The Fluorescence Characteristics and Analytical Determination of Bismuth with an Iodine Electrodeless Discharge Tube as Source.

Talanta, 1967, 14, 1467.

The Fluorescence and Analytical Characteristics of Arsenic using a Microwave-Excited Electrodeless Discharge Tube as Source.

Talanta, 1968, 15, In Press.

The Behaviour of Sulphur Species in a Nitrogen-Hydrogen Diffusion Flame and in a Shielded Air-Hydrogen Flame.

Analyst, 1967, 92, 506.

The Behaviour of Phosphorus Species in a Nitrogen-Hydrogen Flame.

Analyst, 1968, 93, In Press.

The Use of Electrodeless Discharge Tubes as Spectral Sources in Atomic-Absorption Spectroscopy.

Atomic-Absorption Newsletter (Perkin-Elmer), 1967, Nov.-Dec., 117.

The Thermal and Atomic-Fluorescence Emission of Germanium in a Nitrogen-Oxygen-Acetylene Flame.

Anal.Chim.Acta, 1968, 40, In Press.

Some Preliminary Studies of the Analytical Potentialities of the Atomic Hydrogen Plasma Torch.

Anal.Chim.Acta, 1968, 40, In Press.

APPENDIX 1

Table of Vapour Pressures[151]

Name	Formula	Temperature °C 1 mm	10 mm
Aluminium	Al	1284	1487
Aluminium Iodide	AlI_3	178s	226
Antimony	Sb	886	1033
Antimony Tri-iodide	SbI_3	164	224
Arsenic (metallic)	As	372s	437s
Arsenic Tri-bromide	$AsBr_3$	41.8	85.2
Arsenic Tri-iodide	AsI_3	No Figures available	
Bismuth	Bi	1021	1136
Bismuth Tri-chloride	$BiCl_3$	s	264
Bismuth Tri-iodide	BiI_3	No Figures available	
Cadmium	Cd	394	484
Cadmium Iodide	CdI_2	416	512
Copper	Cu	1628	1879
Cuprous Chloride	Cu_2Cl_2	546	702

Contd.....

Table of Vapour Pressures[151] (contd.)

Name	Formula	Temperature °C 1 mm	10 mm
Iodine	I_2	38.7s	73.2s
Magnesium	Mg	621s	743
Magnesium Chloride	$MgCl_2$	778	930
Mercury	Hg	126	184
Selenium	Se	356	442
Silver	Ag	1357	1575
Silver Chloride	AgCl	912	1074
Tellurium	Te	520	650
Tellurium Iodide	TeI_2 or TeI_4	No Figures available	
Thallium	Tl	825	983
Thallous Iodide	TlI	440	531
Zinc	Zn	487	593

s = sublimes